Pliocene – Early Pleistocene Arvicolids of North China: Taxonomy, Phylogeny, and Biochronology

（中国北部における鮮新世・前期更新世のハタネズミ類
—その分類，系統および生物年代学）

Yingqi ZHANG
（張　穎奇）

Pliocene – Early Pleistocene Arvicolids of North China: Taxonomy, Phylogeny, and Biochronology

（中国北部における鮮新世・前期更新世のハタネズミ類
—その分類，系統および生物年代学）

理学研究科
生物地球系専攻

平成１９年度

Yingqi ZHANG
（張　穎奇）

CONTENTS

FIGURES

TABLES

PLATES

ABSTRACT

Thirteen arvicolid forms belonging to four known genera (*Mimomys*, *Villanyia*, *Allophaiomys*, *Borsodia*, and *Proedromys*), one new species belonging to a new genus (*Omniprocessimys parallelus* gen. et sp. nov.), one new species without specific specification (*Villanyia* sp. nov.), and one species without specific and generic specification (Arvicolinae gen. et sp. indet.) are systematically described in the present study. The six Pliocene ~ Early Pleistocene localities, where these arvicolid species were unearthed, include 93001 and 72074(4) of Lingtai, Gansu, Renzidong, Anhui, culture layer of Xiaochangliang, Nihewan, Bilike, Inner Mongolia, Gaotege, Inner Mongolia. Three of these localities, 93001 of Lingtai, Gansu, Gaotege, Inner Mongolia and Xiaochangliang, Nihewan, have magnetostratigraphic external age controls, but only the magnetostratigraphic study results of the latter two localities are adopted, because there is considerable disagreement between the paleomagnetic correlation and the stage of evolution of the fossil arvicolids on 93001 section of Lingtai, Gansu. Four arvicolid lineages during Pliocene ~ Early Pleistocene are revealed based on the morphological study of these species and other arvicolid species involved in the comprehensive review on Chinese *Mimomys* contributed by ZHENG AND LI (1986). Among the four lineages revealed here, the *Mimomys bilikeensis - M. teilhardi - M. orientalis - M. youhenicus - M. gansunicus - Allophaiomys deucalion* lineage is the one best demonstrated by the "stage of evolution" or the evolutionary gradualism, and the only one spanning the entire geological time interval of Pliocene ~ Early Pleistocene mainly taken into account in this dissertation. Another lineage, the *Omniprocessimys peii - O. parallelus* lineage, probably represents a very special domestic lineage with distinctive pattern of sinuous line surviving in China from Middle Pliocene to at least Late Pliocene. In addition, two less confident cementless lineages supported by insufficient materials, the *Villanyia* sp. nov. - *Villanyia* sp. 1 - *V. fanchangensis* lineage spreading over about the whole Pliocene and the *Villanyia* sp. 2 - *Borsodia chinensis* lineage lasting from around Middle Pliocene to at least Early Pleistocene, are also proposed. These two lineages can probably indicate that the *Borsodia* lineage stemmed out from the *Villanyia* lineage during Middle Pliocene and evolved in a different direction from the *Villanyia* lineage since then.

On the basises of the arvicolid lineages revealed here by us, the magnetostratigraphic study results of Gaotege section and Xiaochangliang section, and referring to the composite magnetostratigraphy and lithostratigraphy section of Yushe Basin with the stratigraphic positions of fossil arvicolids discovered therein (ZHANXIANG QIU, personal

communication), five arvicolid biochronological zones are preliminarily proposed. All these zones are just loosely defined at present because of insufficient external age control data, and only the typical arvicolid species surviving the time interval of each zone are assigned to each zone, and most boundaries are left undetermined. The *Promimomys asiaticus* -?> *Mimomys bilikeensis* -> *M. teilhardi* zone represents the time interval between the first appearance of *Promimomys asiaticus* and the last appearance of *Mimomys teilhardi*, which can be correlated to the early stage of the Gaozhuangian (NMU12) of DENG (2006) or MN14 of the European Mammal Neogene zones. The first appearance datum of *Promimomys asiaticus* only has a early Early Pliocene faunal age assignment. But the last appearance datum of *Mimomys teilhardi* on Gaotege section was magnetostratigraphically dated as 4.15 Ma. This age is taken as the upper boundary for this zone and the lower boundary for the next zone. And this is also the only clearly defined boundary. The next zone, the *Mimomys orientalis* zone, is characterized by the typical arvicolid species *Mimomys orientalis*, which can probably be correlated to the late stage of the Gaozhuangian (NMU12) of DENG (2006) or MN15 of the European Mammal Neogene zones. No data is available for the determination of the upper boundary for this zone. The *Mimomys youhenicus* -> *Omniprocessimys peii* zone is represented by the two typical arvicolid sepcies. And *Mimomys youhenicus* is probably older than *Omniprocessimys peii* in time. No boundary determination can be made for this zone at present. This zone can be correlated to the Mazegouan (NMU13) of DENG (2006) or MN16 of the European Mammal Neogene zones. The next zone, the *Mimomys gansunicus - Villanyia fanchangensis - Omniprocessimys parallelus* zone, is characterized by the co-occurrence of these species in China. The geological time of the boundary between WL7 and WL6 on 93001 section of Lingtai, where is the highest stratigraphic datum of *Mimomys gansunicus* and also its last appearance datum, is preferable to define the upper boundary for this zone and the lower boundary for the next younger zone. As for the lower boundary for this zone, the first appearance of *Mimomys gansunicus* is preferable to define it, but it seems clear that the first appearance of *Mimomys gansunicus* is not recorded on 93001 section of Lingtai, and it is still necessary to find a suitable section where it is recorded. Presently, this boundary will be left undetermined. This zone can be thought as the equivalent to Nihewanian (strict sense) of Chinese Neogene mammal ages or MN17. The last zone proposed here, the *Allophaiomys deucalion - Borsodia chinensis* zone, is characterized by the co-occurrence of these two species. The upper boundary determination for this zone can not be made based on the knowledge up to now. This zone can be correlated to MQ1 in the sense of AGUSTÍ ET AL. (2001).

I. Introduction

The study of fossil arvicolids in China can be considered to start from that KORMOS (1934) named a right mandible with $M_{1\sim3}$ (TEILHARD DE CHARDIN and PIVETEAU, 1930, p. 123, text-fig. 40) from Xiashagou, Nihewan as *Mimomys chinensis*. Arvicolid fossils from scattered localities have greatly increased thereafter (YOUNG, 1935; PEI, 1939; ZHENG, 1976; XUE, 1981; ZHENG ET AL., 1985; ZONG ET AL, 1982; ZONG, 1987, and so on). Most of these localities have just a single fossil-bearing layer, and almost all of them have no external age controls. The most recent comprehensive reviews on Chinese fossil arvicolids so far were carried out by ZHENG AND LI (1986, 1990), in which they established the initial arvicolid biochronological framework based on the materials obtained previous to 1980s. Since then, numerous new arvicolid-bearing fossil localities from the Pliocene ~ Early Pleistocene of China have been discovered, such as Bilike, Inner Mongolia (QIU AND STORCH, 2000), Gaotege, Inner Mongolia (LI ET AL., 2003; LI, 2006), Yushe, Shanxi (TEDFORD, 1991; FLYNN ET AL., 1997), Lingtai, Gansu (ZHENG AND ZHANG, 2000, 2001; ZHANG AND ZHENG, 2000, 2001), Renzidong, Anhui (JIN ET AL., 2000), and so on, some of which are continuous sections even with multiple arvicolid-bearing layers and paleomagnetic age controls. Hence a new comprehensive review on the phylogeny and biochronology of Chinese fossil arvicolids has become achievable and in anticipation.

Besides the attempt to discuss the phylogeny of the fossil arvicolids from Pliocene ~ Early Pleistocene of North China, owing to the fact that studies on fossil arvicolids are particularly beneficial to biochronology of late Cenozoic, another main purpose of this dissertation is to provide an update on the Chinese arvicolid biochronological framework established by ZHENG AND LI (1986, 1990). But it is absolutely necessary to go through the related concepts and their histories before the discussion. For that reason, the history of the term "biochronology" and the development of mammal chronology in North America, Europe, and China is introduced as background knowledge. In addition, some brief historical remarks on the geology, chronology and fauna of the direct involved localities, research methods, classification, and so on will be addressed. The localities that are going to be directly involved here are: 93001 and 72074(4) of Lingtai, Gansu, Renzidong, Anhui, Xiaochangliang, Nihewan, Bilike, Inner Mongolia, and Gaotege, Inner Mongolia (Figure 1). Thirteen arvicolid species belonging to four known genera (*Mimomys*, *Villnayia*, *Allophaiomys*, *Borsodia*, and *Proedromys*), one new sepcies belonging to a new genus (*Omniprocessimys parallelus* gen. et sp. nov.), one new species without specific specification (*Villanyia* sp. nov.), and one species without both generic and specific

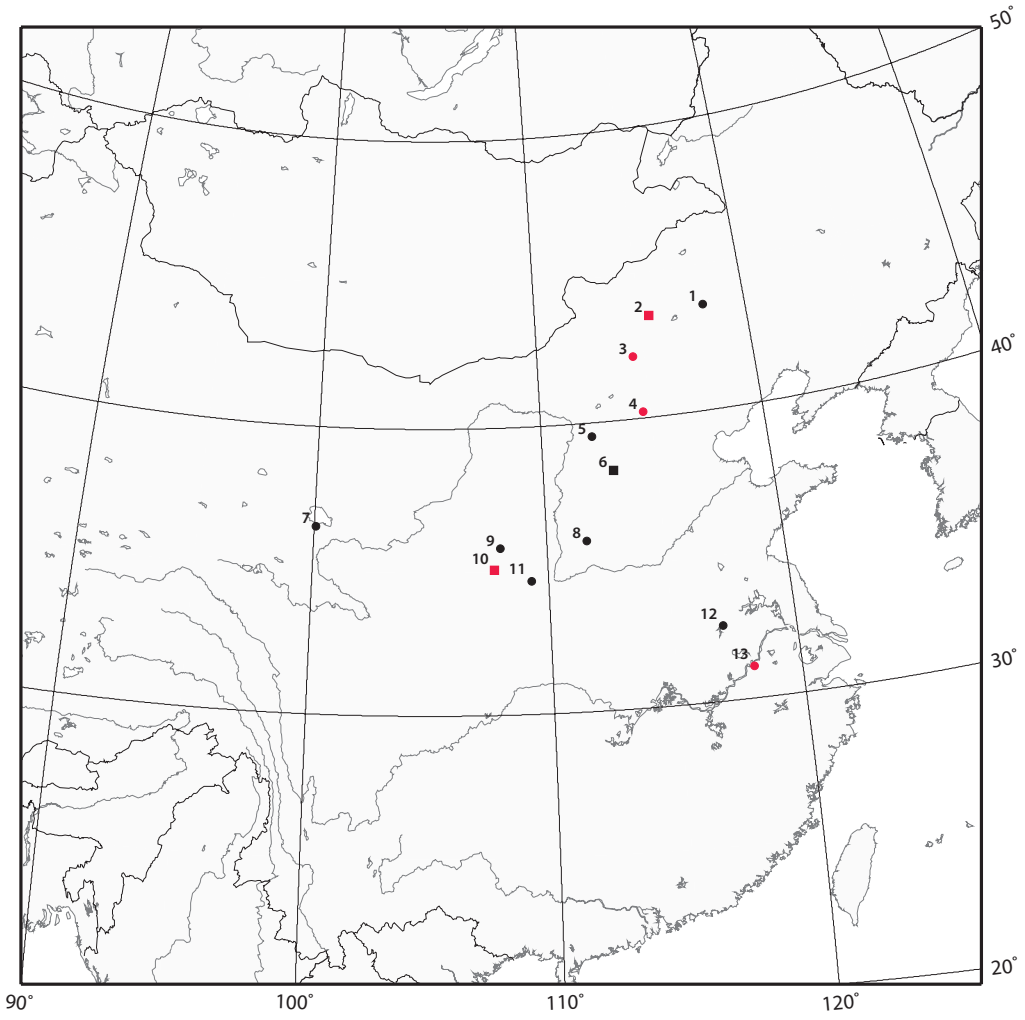

Figure 1. Pliocene~Early Pleistocene arvicolid fossil localities involved in this study

1. Linxi, Inner Mongolia (ZHENG AND LI, 1986): *Borsoida chinensis*; **2. Gaotege, Inner Mongolia** (LI ET AL., 2003; XU ET AL., 2007): *Mimomys* cf. *M. bilikeensis*, *Mimomys* cf. *M. orientalis*, *Borsodia* sp.; **3. Bilike, Inner Mongolia** (QIU AND STORCH, 2000): *Mimomys bilikeensis*; **4. Xiaochangliang, Nihewan, Hebei** (ZHANG ET AL., 2008, in press): *Borsodia chinensis*, *Allophaiomys deucalion*; **5. Dongyan, Huixing, Pinglu, Shanxi** (ZHENG AND LI, 1986): *Mimomys orientalis*; **6. Yushe, Shanxi** (FLYNN ET AL., 1997): **(1) Upper Gaozhuang Formation**: *Mimomys* sp.; **(2) Mazegou Formation**: *Mimomys irtyshensis*; **(3) Haiyan Formation**: *Borsodia chinensis*, *Mimomys gansunicus*, ?*Villanyia* sp. (the opinion of the present author); **7. Gonghe, Qinghai** (ZHENG AND LI, 1986): *Borsodia chinensis*; **8. Dacai, Xiangfen, Shanxi** (ZHENG AND LI, 1986): *Mimomys peii*; **9. Heshui, Gansu** (ZHENG AND LI, 1986): **(1) Jingou**: *Mimomys gansunicus*; **(2) Langgou, Bangiao**: *Mimomys banchiaonicus*; **10. Lingtai, Gansu** (ZHENG AND ZHANG, 2001): **(1) 93001**: *Mimomys gansunicus*, *Borsodia* sp. nov., *Allophaiomys terrae-rubrae*, *Allophaiomys pliocaenicus*, *Proedromys* sp., *Hyperacrius yenshanensis*; **(2) 72074(4)**: *Mimomys bilikeensis*, *Mimomys gansunicus*; **11. Youhe, Weinan, Shaanxi** (ZHENG AND LI, 1986): *Mimomys youhenicus*, *Mimomys orientalis*; **12. Xindong, Huainan, Anhui** (JIN AND ZHANG, 2005): *Promimomys asiaticus*; **13. Renzidong, Anhui** (JIN ET AL., 2000; ZHANG ET AL., in press): *Villanyia fanchangensis* sp. nov., *Mimomys gansunicus*; *Mimomys* cf. *M. peii*.

■: Localities with magnetostratigraphic age control; ●: Localities with only faunal age control; greyed: Localities studied or restudied in this dissertation.

specification (Arvicolinae gen. et sp. indet.) unearthed from these localities are going to be

described systematically in this dissertation. The phylogenetic method is formally employed to accomplish the reconstruction of their phylogenetic relationships. Based on an intuitively acceptable phylogenetic tree constructed here, four arvicolid lineages during Pliocene ~ Early Pleistocene are preliminarily revealed. Furthermore, on the basises of these arvicolid lineages and the magnetostratigraphic study results of Gaotege section and Xiaochangliang section, and referring to the composite magnetostratigraphy and lithostratigraphy section of Yushe Basin with the stratigraphic positions of fossil arvicolids discovered therein (ZHANXIANG QIU, IVPP, personal communication), five loosely defined arvicolid biochronological zones are going to be demonstrated as an update to the framework of ZHENG AND LI (1986, 1990). But even updated here, it is still in its infancy due to insufficient external age control data.

II. Significance of Arvicolid Research

The word "arvicolid" was used as an informal name to represent a polyphyletic group of rodents with distinctly hyposodont, triangularly prismatic cusps on their cheek teeth including five lineages derived from different cricetid rodents with low-crowned cusps on their molars and treated as five subfamilies of the family Cricetidae, such as Arvicolinae, Lemminae, Prometheomyinae, Ondatrinae, and Dicrostonychinae by REPENNING ET AL. (1990). However, here it is used as a general name to represent the species of the subfamily Arvicolinae in the sense of REPENNING ET AL. (1990). On the basis of the knowledge about this group accumulated up to now, arvicolids have a history of more than 5 Ma, and a Holarctic distribution during Late Cenozoic. Among micromammals, fossil arvicolids usually draw more attention especially when chronology and biostratigraphy of continental deposits of late Cenozoic are taken into account. This is not only owing to the facts that they have abundant fossil records and a relatively rapid evolutionary rate like other rodent taxa, but also the fact that their evolutionary trend over time within Late Cenozoic can be clearly reflected in several gradual changes on their dental morphology, such as: 1) increasing hyposodonty; 2) appearance of crown cement; 3) increasing undulation of the sinuous line; 4) disappearance of enamel islet in the first lower molar; 5) reduction of roots; and 6) change of enamel band differentiation from *Mimomys*-type (negative type) to *Microtus*-type (positive type) etc.. Furthermore, some of these changes, like 3) and 6), can be even quantified to demonstrate the evolutionary gradualism through time. REPENNING ET AL. (1990) stated that when combined with external age control data, it was possible to distinguish age differences as brief as 100,000 years during the past 5

million years if arvicolid history was well known in the region of concern. It is due to this merit that particular attention has been paid to fossil arvicolids, which leads to a tremendous amount of accumulation of literatures and knowledge about this group. At the same time, since the first fossil arvicolid from the Issoire region of France was referred to as *Arvicola amphibius cizae* by CROIZET and JOBERT in 1828 (KRETZOI, 1990), excessive amounts of taxonomic names have been proposed all over the world up to now, and the amount is still growing, so that it is nearly impossible for every single researcher or researchers from every single region to discuss the phylogeny of regional arvicolid species and interregional correlations of arvicolid faunas from a panoramic global view or, more specifically, from a panoramic Holarctic view without interregional cooperations. For that reason, in this dissertation, the discussion of arvicolid species within China will be mainly focused on. When necessary and possible, just simple reviews on related species outside China are going to be made.

III. Mammal Chronology in Europe, North America and China

One of the most important things after we discovered fossils is to determine the age of them. LINDSAY (1990) summarized three basic strategies used by vertebrate palaeontologists to establish the age of a fossil assemblage: 1) stratigraphic superposition, 2) stage of evolution, and 3) mammal dispersal events. Among these three strategies, the stratigraphic superposition is only applicable where widely distributed, continuous, and stable strata occur, like most of the marine strata. But for the only restrictedly distributed, uncontinuous and unstable terrestrial sediments, on the other hand, it is too difficult to apply the stratigraphic superposition strategy, if two distant terrestrial sections have totally different sedimentary facies and sequences even they are of similar age. So it is more common for vertebrate palaeontologists who mainly deal with terrestrial deposits to use the other two strategies to determine the age of the fossil assemblages they discovered. Even though, sometimes, it is thought that age determination based only on "stage of evolution" was hazardous, when mammal faunas had been well studied, with several widely distributed lineages well established, the age assignment of a particular faunal assemblage is usually straightforward in a relative sense. In fact, several biochronological frameworks have been established in Europe, North America and China, respectively, based on these strategies.

A. Mammal Neogene zones of Europe (MN) and European Land Mammal Ages (ELMA)

P. MEIN compiled the fossil mammal data of 190 sites or faunas from 14 countries throughout Europe and North Africa, ordered these mammal faunas sequentially as a series of biochrons, and presented his result in a chart at an international colloquium on continental biostratigraphy at Montpellier and Madrid in 1974. MEIN organized these mammal sites into 16 zones termed MN (=Mammal Neogene) zones, plus an earlier Paleogene zone (MN O), and a younger Quaternary zone (MN Q1). Each of MEIN's zones, with both large and small mammals listed, was characterized by (1) characterizing species of well established evolutionary lineages (e.g., used for interpretation of stage of evolution), (2) important genera appearing in each zone, and (3) important genera disappearing in each zone. These zones were expanded and formally presented the next year at the RCMNS (Regional Committee on Mediterranean Neogene Stratigraphy) meeting held in Bratislava (MEIN, 1975). The updated chart listed 221 mammal sites and included Yugoslavia in addition to the countries utilized in the previous chart. Many more characterizing species, generic first appearances, and generic associations were added. The MN zones were revised again at the next meeting of RCMNS at Athens (MEIN, 1979). And a further and the most recent comprehensive revision of MN zones is presented by MEIN (1990). In this most recent update of Mammal Neogene zones, each zone was represented by the localities of Western Europe, Central Europe, Eastern Europe, Southeastern Europe, Western Asia and North Africa, and characterized by common taxa (genera), first appearance genera, and last occurrence genera. A typical locality was assigned to each Mammal Neogene zone, and the faunal list from this locality was given.

This biochronological framework (European MN zones) will continue to develop and be revised as new discoveries are made; the data base will become more stable with time. However, a problem with use of European MN zones, as with any relative chronologic framework, is that it cannot be calibrated unless tied to some other independent chronologic framework.

The recognition of the requirement for a uniform and inclusive chronologic framework for European mammal faunas brought off another significant step in the advancement of European mammal biochronology, the Munchen symposium held in April 1975. Fahlbusch (1976) reported the result of the meeting. Forty five reference localities were selected, and grouped into 13 mammal ages. Reference localities for the Neogene had already been placed within MN zones, so the Neogene European land mammal ages had a sequential

organization. For example, mammal age Ruscinian is equivalent to MN14+MN15, and Villanyian equivalent to MN16+MN17. Mammal age Biharian is represented by *Allophaiomys* faunas. Where appropriate, faunal events would serve as boundaries between land mammal ages, and for convenience references to previous marine stage correlations were given. Characterizing assemblages for the land mammal ages would consist of the faunal lists of designated reference localities. The resulting biochronologic framework, base on mammal evolution in Europe, provided the possibility of refinement, revision and precise boundary definition as needed. But the same in nature as MN zones, it is also a relative chronologic framework.

B. North American Land Mammal Ages (NALMA)

The North American Land Mammal Ages were first formally defined by Wood et al. (1941) , a seven-person committee made up of vertebrate paleontologists, several years after the publication of the first North American stratigraphic code to keep North American continental chronologic framework consistent with practice and philosophy. The Wood Committee named 17 land mammal ages, plus naming an older Lance Cretaceous interval and a younger Pleistocene interval. Each North American land mammal age was characterized by (1) a type fauna, commonly the accumulated fossil remains from some restricted lithostratigraphic unit (e.g., Blancan is based on the local fauna at Mt. Blanco and adjoining draws near the "old rock house," north of Crawfish Draw, Crosby County, Texas), (2) principal correlative faunas, (3) index fossils (considered restricted to that land mammal age), (4) genera appearing in that land mammal age, (5) genera last recorded from that land mammal age, and (6) genera characteristic of that land mammal age. Thus, each land mammal age was defined on paleontologic data from an identified lithostratigraphic unit and a geographically restricted area. However, lithostratigraphic and geographic characterizations were not included. Tedford (1970) pointed out that North American land mammal "ages" are neither equivalent to geochronologic ages (Viz. divisions of epochs) nor to their equivalent chronostratigraphic stages. So North American land mammal ages are biochronological units, representing spans of time during which the characterizing fauna lived. The recent volume "Cenozoic Mammals of North America" edited by WOODBURNE (1987) and "Late Cretaceous and Cenozoic Mammals of North America" edited by WOODBURNE (2004) are the comprehensive published review of North American land mammal ages, which broadened and clarified the characterization for each land mammal age to ponder accurate definitions for each age.

Probably the most significant problem in application of any mammal chronology is the definition and recognition of the boundary between two units. Two faunal assemblages in separate chronologic intervals that are close to the same boundary are more easily united than separated. Thus, definition of boundaries between chronologic intervals must be well defined and rigorously characterized. In recent stratigraphic codes the lower boundary of chronologic units is always addressed, and is usually based on the appearance of a new taxon or taxa. Overlying (and younger) chronologic boundaries are usually not addressed, but are designated when the next (younger) chronologic unit is defined. This practice has been widely applied by vertebrate paleontologists in North America in the North American land mammal ages system.

In fact, the development of North American Land Mammal Ages were enhanced because terrestrial deposits that yielded diagnostic fossils were occasionally superposed. That is to say the fossils can be placed in an ordered stratigraphic sequence. And what's more, there are plentiful external age controls for the terrestrial deposits yielding diagnostic fossils. For example, BELL ET AL. (2004) listed 19 well dated volcanic units of the past 5 Ma useful in correlating North American Mammal faunas. So it is possible to determine the boundaries for the land mammal ages in the way introduced above. Because the NALMAs were calibrated by superposition, stage of evolution, and various external age controls, this system in itself is probably the best on in the sense of LINDSAY (2003).

C. Chinese Neogene Mammal Ages and Mammal Faunal Units (NMU)

In China systematic research on Neogene stratigraphy started in late 1970s. Since then, Chinese paleontologists have carried through a chronological sequencing system of Chinese Neogene mammalian faunas, which is independent from the biochronological frameworks mentioned above, but, apparently, strongly influenced by the European MN and ELMA systems. CHIU ET AL. (1979) grouped the Chinese Neogene faunas into six biochrons with three of them in Miocene and three of them in Pliocene, which can be thought as the inception of Chinese Neogene Mammal Ages system. After that, it was updated with newly discovered faunal data several times by LI ET AL. (1984), QIU AND QIU (1995), and TONG ET AL. (1995), but the concept stayed the same in all these contributions, among which Chinese Neogene was divided into several mammal ages in them. Each of these mammal ages was represented by one typical fauna and other related faunas. Moreover, all the mammal ages were also embedded into the geological time scale to represent a geological time interval. As pointed out by QIU (1990), these mammal ages were, essentially, only a series of disjunct samples in a line. The system in itself is merely a

sequencing system of faunas but a biochronological system that could meet basic demands. For that reason, instead of mammal ages, QIU (1990) used another informal name "Neogene mammal faunal units" proposed by STEININGER ET AL. (1990) for these ages. He proposed six units at that time. The former four were for Miocene, and the latter two were for Pliocene and Early Pleistocene. Furthermore, to keep away from the conflict concerning the MN, ELMA and NALMA with the International Stratigraphic Guide (SALVADOR, 1994), QIU ET AL. (1999) defined the Neogene mammal faunal unit (NMU) as: a time interval with fuzzy boundaries, thus is mainly fauna and/or locality based unit. Each of these NMUs is established by referring a representative fauna and several referable faunas. They totally established 11 NMUs for the Chinese Miocene. The most recent update of Chinese NMU system was made by DENG (2006). A lot of new faunal and geomagnetic data was appended to calibrate this system and make it more precise. Besides, the former mammal age, Yushean, was divided into Gaozhuangian and Mazegouan.

D. What on earth is biochronology?

As mentioned above, biochronological concepts have been employed for decades by vertebrate paleontologists to order faunal assemblages of mammals collected from terrestrial deposits. As a result, several independent frameworks have been proposed and become widely accepted and applied by the vertebrate paleontologists all over the world. These biochronological systems include NALMA (North America Land Mammal Ages), ELMA (European Land mammal Ages), MN (Mammal Neogene zones of Europe, MEIN, 1975), NMU (Chinese Neogene Mammal Faunal Units) etc., which have proved to be most effective and practical frameworks for the correlation of terrestrial deposits inter-regionally, and furthermore, if undergoing sufficient study and meeting necessary requirements ("golden strike"-like external age controls and acceptable stratotypes), they can also become the foundation for subdividing Late Cenozoic geochronologically at the age level and chronostratigraphically at the stage level accordingly. In view of the importance and significance of biochronology, LINDSAY (2003) made a comprehensive historical review on chronostratigraphy and biochronology to clarify their conceptual essences and make them rigorous enough to be accepted as a reliable method for geochronology in stratigraphic guides. Some important concepts of biochronology recommended by LINDSAY (2003) are listed as follows:

> **Biochronology:** the organization of geologic time according to the irreversible process of evolution in the organic continuum (cited from Berrggren and van

Couvering, 1978: 39).

Land mammals ages: a relatively short interval of geologic time that can be recognized and distinguished from earlier and later such units (in a given region or province) by a characterizing assemblage of mammals.

Stage of evolution: the chronological ordering of faunal assemblages based on morphological differences observed in members of one phyletic lineage recorded in different assemblages within the same deposit or basin or biogeographic region; advanced evolutionary stages are ranked higher in the order.

Chronostratigraphic marker: any physical event recorded in the stratigraphic record whose biological, chemical, or physical properties yield chronological significance by direct association with any other chronostratigraphic marker.

Datum events: any chronostratigraphic marker.

Furthermore, LINDSAY (2003) emphasized that the application of datum events, such as first appearance datum (FAD) and last appearance datum (LAD) etc., should be confined to biological events that are tied to directly to a chronostratigraphic marker, i.e. the datum events should be tied to certain strata and should not be only mental event without stratal support.

From the definitions recommended by LINDSAY (2003) and the various widely accepted and applied independent biochronological systems mentioned above, we can find that 1), for the chronological ordering, the phylogeny of the same members from different assemblages takes a fundamental role, so systematic or phylogenetic studies can be thought as the base of biochronology; and 2), biochronology itself is in fact just a relative concept and we can only tell the relative sequences of different assemblages but not the absolute ages of them, so the temporal intervals of the biochronological units such as NALMA, ELMA etc. and the corresponding strata, if available, have to be mapped to the absolute timescale (e.g., GPTS) to become usable for geochronology and chronostratigraphy. In fact, there have been several attempts to establish chronostratigraphic stages based on their biochronologic equivalents, e.g., Vallesian "Stage" (CRUSAFONT-PAIRO, 1950, 1951), Turolian "Stage" (CRUSAFONT-PAIRO, 1965; MARKS, 1971) in Europe, and Clarkforkian Stage, Wasatchian Stage, Clarendonian Stage (SAVAGE, 1955, 1977; ROSE, 1981) in North America etc.. Besides the significance on geochronology and chronostratigraphy, a well-dated biochronological framework is also critical to solve phylogenetic, biogeographic and systematic problems. Like the biochronological frameworks mentioned above, they are all independent of each other,

because of the different biogeographic provinces and distinctive faunas they are based on. However, they can usually be correlated to each other at the same time if the faunal assemblages they are based on include shared members. In such cases, to demonstrate the phylogeny and the migration route of the shared members the well-dated biochronological framework will be critically beneficial.

IV. A Review of Arvicolid Biochronology

Derived from the definition of biochronology proposed by LINDSAY (2003), arvicolid biochronology can be briefly understood as the accomplishment of biochronology based on arvicolids. The reason why fossil arvicolids are dominantly suitable for the establishment of biochronological framework has been introduced in the chapter of introduction. In fact, there have been quite a few instances of studies mainly based on fossil arvicolids devoted to the establishment of biochronological framework of Late Cenozoic, especially Neogene, all over the world. Some of them can be regarded as in agreement with the strict sense of biochronological rules proposed by LINDSAY (2003), but some of them are not.

REPENNING (1987) refined the North American mammalian biochronology framework of Late Cenozoic by ten microtine events on the basis of more than 80 microtine localities. More than half of these localities have external age controls, so each of these ten microtine events was assigned to a comparatively precise absolute age. Then REPENNING (1987) used each of these microtine events to define the boundaries of Hemphillian, Blancan, Irvingtonian, Rancholabrean NLMAs and their subages. Some typical microtine species, both immigrants and native species, were also listed out for each of these NLMAs or it subages. Apparently, the arvicolid species of North America show great provincialism, compared with arvicolids of Eurasia continent. This framework can be theoretically thought to be a biochronological framework in the sense of LINDSAY (2003).

FEJFAR AND HEINRICH (1989) made a comprehensive review on the muroid rodent biochronology of the Neogene and Quaternary in Europe. Even though this framework is not totally based on arvicolid rodents, but the Pliocene~Pleistocene parts of this framework are all determined by arvicolid rodents. In this framework, Pliocene is divided into two superzones: *Trilophomys-Ruscinomys* superzone and *Borsodia-Villanyia* superzone. Each of these superzone is defined by the concurrent range of the genera in the name of the superzone. The lower and upper boundaries of these superzones are also defined. For example, the lower boundary of the *Borsodia-Villanyia* superzone is defined

as the FAD of *Borsodia*, and the upper boundary of it is defined as the FAD of *Microtus* (*Allophaioms*). Both superzones are further subdivided into four and three zones, respectively. For example, the *Trilophomys-Ruscinomys* superzone includes *Promimomys insuliferus* zone, *Promimomys moldavicus* zone, *Mimomys* (*Mimomys*) *davakosi* zone, and *Mimomys* (*Mimomys*) *occitanus* zone. Each of these zones is defined as the total range of the species included in the zone name. The *Borsodia-Villanyia* superzone comprises *Mimomys* (*Mimomys*) *hajnackensis* zone, *Mimomys* (*Mimomys*) *polonicus* zone, and *Mimomys* (*Mimomys*) *pliocaenicus* zone. Like Pliocene, Pleistocene is also divided into two superzones and several zones. The two superzones of Pleistocene are *Microtus-Mimomys* superzone, and *Arvicola-Microtus* superzone. The *Microtus-Mimomys* superzone is subdivided into *Mimomys* (*M.*) *savini-M.* (*Cseria*) *pusillus* zone and *Mimomys* (*M.*) *savini* zone. The *Arvicola-Microtus* superzone is subdivided into *Arvicola cantiana* zone and *Arvicola terrestris* zone. Each of these superzones is also correlated to each of the ELMAs. For example, the *Trilophomys-Ruscinomys* superzone is correlated to the Ruscinian age; the *Borsodia-Villanyia* superzone is correlated to the Villanyian age; the *Microtus-Mimomys* superzone is correlated to the Biharian age, and so on. Each of the zones of Pliocene is also correlated to a MN zone or MN subzone. For example, *Promimomys insuliferus* zone -> MN14a; *Promimomys moldavicus* zone -> MN14b; *Mimomys davakosi* zone -> MN15a; *Mimomys occitanus* zone -> MN15b; *Mimomys hajnackensis* zone -> MN16a; *Mimomys polonicus* -> MN16b; *Mimomys pliocaenicus* -> MN17, and so on. FEJFAR ET AL. (1997) updated this framework by incorporating a lot of new sites from both Europe and Asia. Several superzones and corresponding ELMAs are redefined by some new-found arvicolid forms, but the nature of this framework has not changed. Not like the NALMAs refined by REPENNING (1987) based on the ten microtine events with comparatively precise external age controls, by nature, the FEJFAR AND HEINRICH (1989) framework is, in fact, a framework totally depending on the stage of evolution, but without a direct connection to geological time scale. It is, in all respects, a sequencing framework of discrete or overlapped time interval. For example, it is very likely that there is gap or overlap between the *Promimomys insuliferus* zone and the *Promimomys moldavicus* zone of the *Trilophomys-Ruscinomys* superzone according to the definitions of both zones.

AGUSTÍ ET AL. (2001) calibrated Mammal Neogene (MN) zones of Western Europe on the basis of the significant magnetobiostratigraphic framework developed in the last decade in a number of Spanish basins: Ebro, Calatayud-Daroca, Vallè-Penedès, Teruel, Fortuna, Cabriel and Guadix-Baza. The lower boundaries of the MN zones were established based on the first appearance (FAD) of selected small and large mammal taxa.

By small mammal taxa, arvicolid species took decisive effect on the Pliocene and Pleistocene part of the calibration made by AGUSTÍ ET AL. (2001). In this "State of the art" calibration called by AGUSTÍ ET AL., the lower boundary of MN14 is defined by the FAD of *Promimomys*. And the first appearances of three *Mimomys* species, *Mimomys occitanus*, *M. vandemeuleni*, *M. davakosi*, are used to define the lower boundary of MN15. The lower boundary of MN16 is defined by the first appearances of *Kislangia ischus*, *Mimomys polonicus*, *Kislangia cappettai*, *Mimomys hajnackensis*. That of MN17 is defined by the first appearances of *Kislangia gusi*, *Mimomys tornensis*, *M. pliocaenicus*, *M. reidi*. AGUSTÍ ET AL. (2001) also calibrated each of these boundaries on the basis of the magnetobiostratigraphic framework. The best estimate of the MN14 lower boundary is found in the Cabriel section, where the Fuente del Viso mammal site is correlated in chron C3n.3r, at 4.9Ma. The MN14/MN15 boundary is well constrained and correlated to 4.2 Ma, at the C3n/C2Ar transition according to the data from the Alfambra area in the Teruel Basin. The boundary between MN15 and MN16 is established at 3.2 Ma, between the chrons C2An.2r and C2An.2n, according to the results in the sections of Galera (GARCÉS ET AL., 1997) and Zújar (OMS ET AL., 1999). The lower boundary of the MN17 is dated to about 2.5 Ma, close to the C2An/C2r boundary. If we call the original Mammal Neogene (MN) framework a preliminary biochronological framework, this calibrated "State of the art" MN framework should be regarded as one in the strict sense of LINDSAY (2003).

The latest and the most comprehensive review on arvicolid biochronology should be the one contributed by REPENNING ET AL. (1990) at the "INTERNATIONAL SYMPOSIUM EVOLUTION, PHYLOGENY AND BIOSTRATIGRAPHY OF ARVICOLIDS (Rodentia, Mammalia)" held in Rohanov (Czechoslovakia), May 1987. In this contribution, REPENNING ET AL. (1990) incorporated the arvicolid biochronology data from Eurasia and North America into an arvicolid biochronology framework of the Northern Hemisphere. The arvicolid data from China, contributed by ZHENG AND LI (1990) for the symposium, is also included in this framework. Even though the conspicuous provincialism of arvicolid faunas from different continents and even within the same continent and the differences of arvicolid taxonomy in different regions created considerable difficulties for this incorporation, with the assumption that dispersal rates were instantaneous within presently attainable time discrimination, the temporal calibration of the arvicolid biochronology throughout the Northern Hemisphere, both Europe and North America, was combined. As a result, this framework was integrated into one big table with each region having a column of its own arvicolid biochronology ages and their typical arvicolid species. Mentioned by REPENNING ET AL. (1990), with this age refinement, a suitable

arvicolid fauna anywhere in the Northern Hemisphere, except where the biochronology is not yet well known, can be dated, on the average, to within 200,000 years during the last 5 million years.

In brief, fossil arvicolids can play a very important role when talking about the mammal biochronology of Late Cenozoic.

V. Introduction of Arvicolid Fossil Localities

A. Bilike

The locality Bilike (42°08′11.5″N, 114°29′35.0″E) is situated about 1.5 km south of the Bilike Village, Dagaitan District, Huade County, Inner Mongolia Autonomous Region, China. It was first discovered by ZHANXIANG QIU (IVPP) and others in 1978. In 1986 ZHUDING QIU (IVPP) tried collecting samples from this locality, and reported a preliminary list of 30 taxa later (QIU, 1988). In 1991 Sino-German collaborate team made an excavation with the support of the Academia Sinica and the Max-Planck-Gesellschaft for Sino-German scientific cooperation in vertebrate paleontology. Thousands of specimens belonging to 20 taxa of micromammals were added to the fauna (QIU AND STORCH, 2000). After the excavation, the locality was destroyed because of railway construction. QIU AND STORCH (2000) proposed a new form of arvicolid, *Aratomys bilikeensis*, and correlated the Bilike fauna to MN14 (equivalent of early Ruscinian, ELMA; early Early Pliocene) partially based on the evolutionary stage of this arvicolid form. This form was first informally referred to the genus *Mimomys* as *Mimomys* (*Aratomys*) *bilikeensis* by REPENNING (2003). In the present study, the same material is restudied and REPENNING's opinion on its referral is adopted.

B. Gaotege

The locality Gaotege (43°29′55.3″N, 115°26′38.3″E) is situated about 73 km southwest of Xilinhaote City, Inner Mongolia Autonomous Region, which is an inselberg with a gray aspect if observed far away. This locality was first discovered by the French priests as well as paleontologists PÈRE TEILHARD DE CHARDIN and EMILE LICENT in 1924, when they were on a geological investigation in Hebei and Inner Mongolia area of China. TEILHARD DE CHARDIN (1926) described briefly 20 forms of fossils they discovered from this locality. After that, no study had been carried on with this locality until Dr. XIAOMING WANG (Natural History Museum of Los Angeles County) and his colleagues of IVPP tracked it

down again in 2000. Since then, several screen-washings have been carried out and the fauna list of the locality grew from 20 species to 46 species. LI ET AL. (2003) preliminarily reported the successive works, and LI (2006) systematically described the rodents, discussed the age of the fauna, and demonstrated the relation of it with other Neogene faunas of North China in his doctoral thesis. The present author appreciates greatly the generosity of Dr. LI who grants the author this opportunity to restudy all the arvicolid materials from this locality.

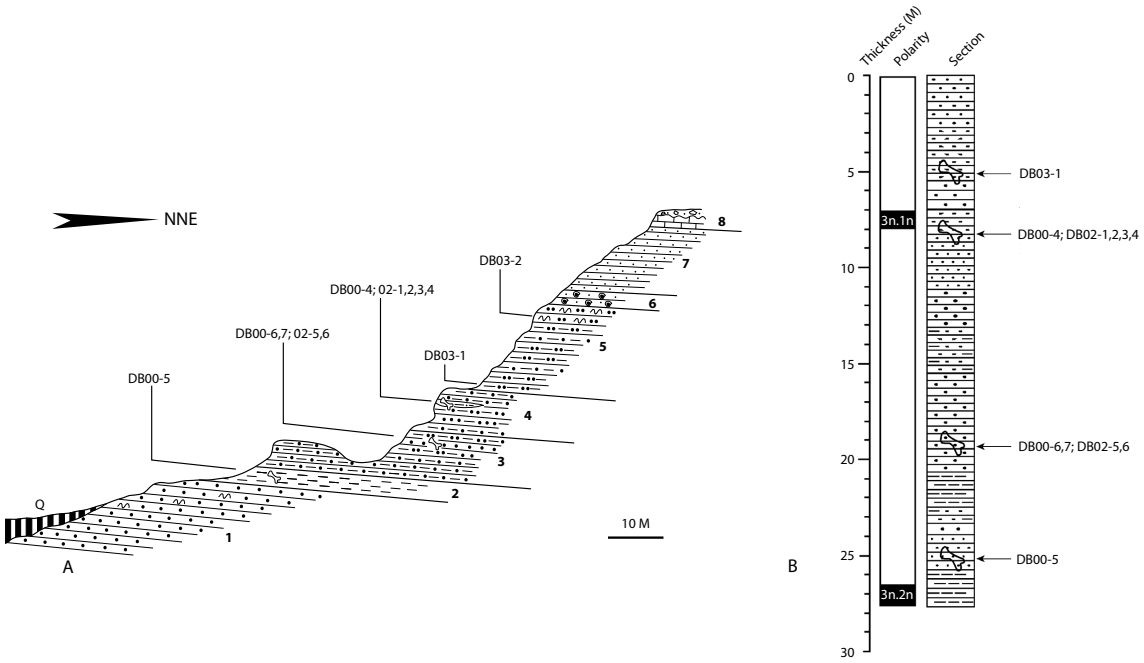

Figure 2. Gaotege section (A: after LI, 2006) and its magnetostratigraphic study result (B: modified from Fig. 7 of XU ET AL., 2007)

Gaotege section with an exposed thickness less than 70 m was lithologically divided into eight layers from the top down (Figure 4). The arvicolid materials were collected from layer 3, 4 and 5. In the faunal list of LI ET AL. (2003), only one arvicolid species, *Mimomys* cf. *M. bilikeensis* (=*Artatomys* cf. *A. bilikeensis*) was given. In his doctoral dissertation, LI (2006) described three forms of arvicolids: a new form *Mimomys teilhardi* sp. nov. from the same layers (DB02-5~6 and DB02-1~4) as *Mimomys* cf. *M. bilikeensis* (LI ET AL., 2003) and one new layer (DB03-1), *Mimomys* cf. *M. orientalis* and ?*Borsodia* sp. from another new layer (DB03-2). In the present re-study on the same arvicolid materials as in LI (2006), three more forms are identified: *Villanyia* sp. nov. from DB02-5~6, DB02-1~4 and DB03-1, and *Villanyia* sp. 1, *Villanyia* sp. 2 from DB03-2. The doubtful form, ?*Borsodia* sp., is referred to *Villanyia* sp. 2.

XU ET AL. (2007) brought out the result of the magnetostratigraphic study on this section. They sampled nearly half of the section (27.65 m) including the upper part of layer

2, layer 3, layer 4, and the lower part of layer 5. They recognized two magnetozones, N1 at 7.05~7.85 m, and N2 at 26.60~27.65 m on the sampled section from the top down, respectively. Furthermore, they correlated N2 to C3n.1n (Cochiti subchron), and N1 correspond to upper part of C3n.2n (Nunivak subchron) on the basis of the faunal comparisons between the Gatege fauna and other typical faunas of northern China from Gaozhuang Formation of the Yushe Group (FLYNN, 1997), Zone IV of the Lingtai composite section (ZHENG AND ZHANG, 2001), and Bilike. As a result, the age of the main fossil-bearing strata, viz. DB02-5~6 of layer 3 was thought to be 4.38 Ma; DB02-1~4 of layer 4 about 4.34 Ma; DB03-1 of layer 5 about 4.15 Ma, respectively. The age of the arvicolid-bearing layer, DB03-2 was thought to be <4.072 Ma, because no magnetosgratigraphic sampling was done on that part of the section.

C. Renzidong

The fossil locality of Renzidong Cave is situated near the south bank of the Yangtze River in Fanchang County of Anhui Province, China. The sediments of Renzidong Cave can be divided lithologically into 8 layers. Among them, the first 7 layers with a total thickness of about 15 m comprise the upper part of the sediments, which is composed mainly of brown to reddish brown mud or sandy mud with limestone breccia. This part yielded abundant mammalian remains including the vole remains described here. The eighth layer with a thickness more than 15m comprises the lower part, which is composed mainly of gray sandy mud, sand and rounded gravel. This part contains few mammalian remains. JIN ET AL. (2000) listed more than 67 forms of mammals from this site, and assigned the age of the site to the time interval between 2.0 and 2.4 Ma by the faunal data. This interval falls into the Early Pleistocene in the chronological sense generally accepted in China, but Late Pliocene in this dissertation. Among the mammalian forms listed out, 35.8% of them are Palaearctic elements, and 34.4% are Oriental elements. The remaining 29.9% are widespread forms in Eurasia. The present zoogeographic boundary between the Palaearctic and Oriental Regions is far to the north of Renzidong Cave. Thus, JIN ET AL. (2000) concluded that a cooling event at the beginning of the Pleistocene caused southward migration of the Palaearctic elements. JIN ET AL. (2000) listed three arvicolid forms: *Mimomys* cf. *M. peii*, *Borsodia* sp., and *Mimomys* cf. *M. gansunicus* (=*Cromeromys* cf. *C. gansunicus*). Among these three forms, ZHANG ET AL. (in press) named one of them, *Borsodia* sp., as *Villanyia fanchangensis*. As for the other forms, in this study, the former *Mimomys* cf. *M. peii* is identified as a new form, *Omniprocessimys parallelus* gen. et sp.

nov., and the former *Mimomys* cf. *M. gansunicus* as *M. gansunicus*. Based on the study here, the age assigned by JIN ET AL. (2000) to Renzidong fauns is thought to be acceptable.

D. Lingtai

Lingtai is the name of a county in Gansu Province. During 1971~1972, WANPO HUANG ET AL. from IVPP investigated the area near Leijiahe Village of Lingtai County and found some mammalian fossils in Xiaoshigou. The faunal list was reported at the 3rd meeting of Chinese Association for Quaternary Research in 1979. LI ET AL. (1984) called this fauna Leijiahe Fauna and thought its age should be Early Pliocene. During 1991~1993, WANPO HUANG (IVPP) and HIDEO NAKAYA (Japan) reinvestigated Xiaoshigou, Wenwanggou and Renjiagou near Leijiahe Village. By then, five main localities found near Leijiahe Village were 72074(1), 72074(3), 72074(4) in Xiaoshigou, and 93001, 93002 in Wengwanggou. Among these localities, 93001, 93002 and 72074(4) yielded more abundant fossil materials and ZHENG (1994) made a preliminary report on them. In 1997, SHAOHUA ZHENG, ZHAOQUN ZHANG (IVPP) ET AL. resampled 72074(4) and 93001 (including 93002 with a single fossil-bearing layer) to make a more precise biostratigraphic study. Their works were published in a serier of papers (ZHENG AND ZHANG, 2000, 2001; ZHANG AND ZHENG, 2000, 2001). ZHENG AND ZHANG (2000) reported the comprehensive biostratigraphic study result of 93001 section. The whole section was divided into five biozones, and three arvicolid forms, *Mimomys gansunicus* (=*Cromeromys gansunicus*), *Borsodia* n. sp., and *Allophaiomys terrae-rubrae* were listed. The paleomagnetic correlation of the section was basically based on the magnetostratigraphic study result of WEI ET AL. (1993), and they made some modification according to CK95 GPTS and the Geochronology Time Scale of BERGGREN ET AL. (1995), and new chronological interpretation was given owing to the fact that there was a big hiatus in the section. According to their biozone division, all the *Mimomys gansunicus* layers and most of the *Borsodia* n. sp. layers fell into Zone 4 to which the time interval 3.6~2.6 Ma was assigned; all the *Allophaiomys terrae-rubrae* layers and one *Borsodia* n. sp. layer fell into Zone 5 to which the time interval 2.5~1.8 Ma was assigned. ZHANG AND ZHENG (2001) reported the biostratigraphic study result of 72074(4) section at Xiaoshugou. Two arvicolid species, *Mimomys bilikeensis* (=*Aratomys bilikeensis*) and *Mimomys gansunicus* (=*Cromeromys gansunicus*) were listed. The *Mimomys bilikeensis* layers fell into the Zone III, and the only *Mimomys gansunicus* layer fell into Zone IV of this section. ZHENG AND ZHANG (2001) reported the composite biostratigraphic study result of the three sections, 93001, 93002, and 72074(4). In the taxon list of this composite section, the number of arvicolid species increased from four

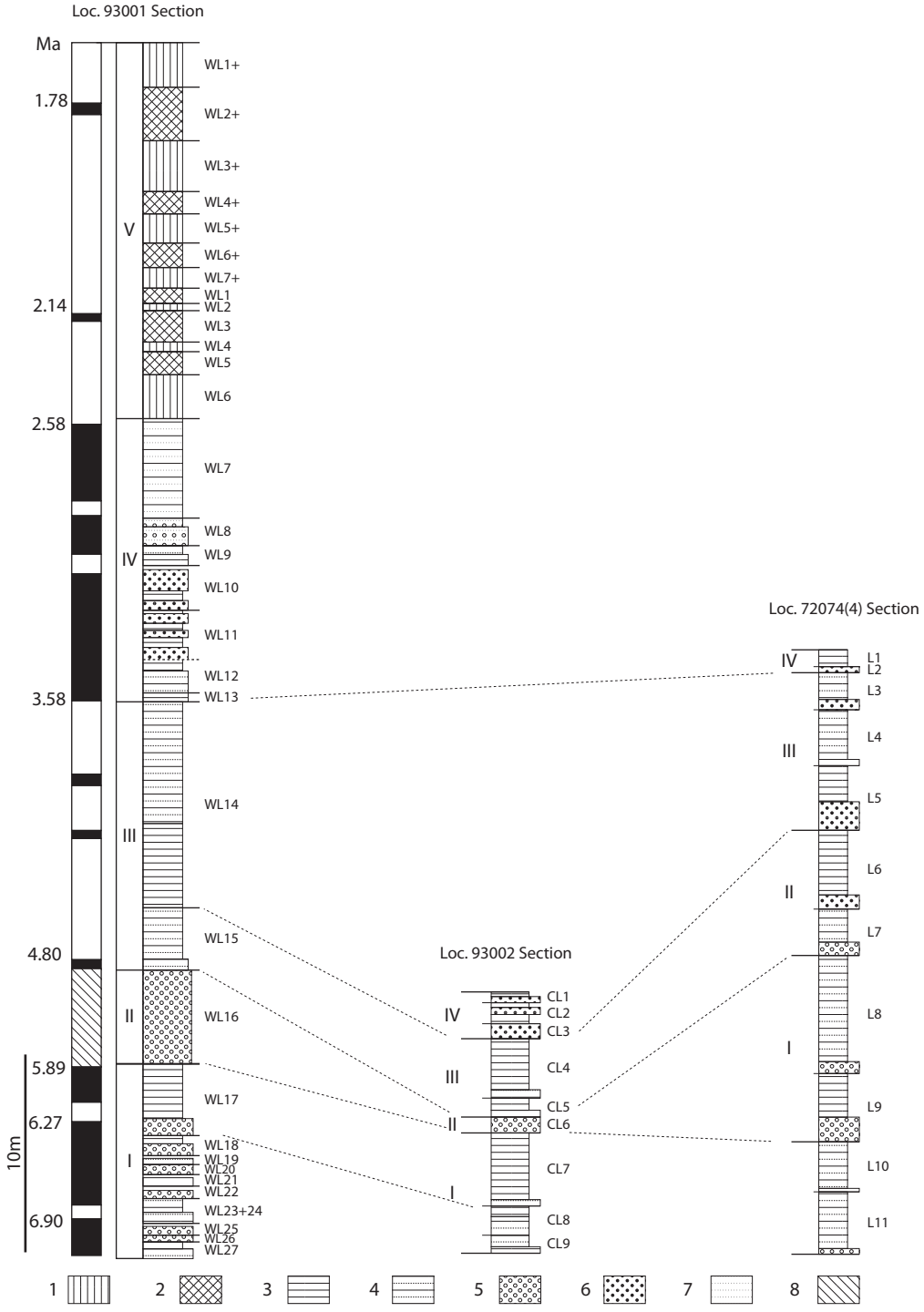

Figure 3. Lithostratigraphic correlation of three sections in the Leijiahe area, Lingtai, Gansu (after ZHENG AND ZHANG, 2001)

1. loess; 2. paleosol; 3. mud stone; 4. silt stone;

5. conglomerate with carbonate nodules; 6. conglomerate; 7. sand stone; 8. no data.

* Only 93001 Section and 72074(4) Section are involved in the present study

(*Mimomys gansunicus* from both 93001 and 72074(4), *Mimomys bilikeensis* from 72074(4), and *Allophaiomys terrae-rubrae*, *Borsodia* n. sp. from 93001; no arvicolid species

were discovered from 93002 section) to seven, with *Allophaiomys pliocaenicus*, *Proedromys* sp., and *Hyperacrius yenshanensis* added as a result of the re-identification and resample of overlying supplemental layers WL7+~1+ on 93001 section. The composite section was divided into six biozones, and the Zone V of 93001 (time interval 2.5~1.8 Ma) was partly correlated to the Zone VI of the composite section; the Zone IV of 93001 (time interval 3.6~2.6 Ma) and the Zone IV of 72074(4) was completely and partly correlated to Zone V of the composite section, respectively; the Zone III of 72074(4) was correlated to the Zone IV of the composite section, and the Zone III of 93001 was correlated to Zone III +IV of the composite section. In this dissertation, the author re-identified all the arvicolid materials from both 93001 and 72074(4) as follows: *Mimomys* cf. *M. bilikeensis* and *M. gansunicus* from 72074(4) section, *Mimomys gansunicus*, *Villanyia* cf. *V. fanchangensis*, *Allophaiomys deucalion*, *Proedromys bedfordi*, *Borsodia* sp. and Arvicolinae gen. et sp. indet. from 93001 section. Moreover, the paleomagnetic correlation and the age of 93001 section is reexamined based on the study here.

E. Xiaochangliang

The Xiaochangliang site is situated near the east-north-eastern end of the Nihewan Basin in Hebei Province. Around the site, Pliocene and Pleistocene sediments are well exposed. CAI ET AL. (2004) divided the sediments in the area, from the bottom up, into four units: 1) "Hipparion red clay" of early Pliocene age, 2) red, gray and grayish black fluvio-lacustrine silty clay of late Pliocene age, 3) brownish yellow to grayish yellow fluvio-lacustrine clay and gravel of Pleistocene age, and 4) overlying loess. The unit 3 is sometimes subdivided into the Nihewan Formation of Early Pleistocene age and the Xiaodukou Formation of Middle Pleistocene age (YANG ET AL., 1996 ; WEI, 1999, etc.).

At the Xiaochangliang section, the units 1 and 2 of CAI ET AL. (2004) are lacking, and only the units 3 and 4 are deposited. The unit 3 overlies directly the Jurassic basement rocks with an unconformity and is covered by the unit 4. ZHU ET AL. (2001) showed a detailed stratigraphic sequence of the section with a thickness of 73m, which was composed mainly of silt and/or clay (Figure 3). They also described a thicker sequence of the Donggou section 1km west-south-west of the Xiaochangliang site, which is correlative with the Xiaochangliang section because of the identical sedimentary sequences of the two sections. They carried out detailed paleomagnetic measurements, and found out two normal and two reversed magnetozones in the Xiaochangliang section (N1, N2 and R1, R2), and three normal and two reversed magnetozones in the Donggou section (N1, N2, N3 and R1, R2). They correlated the magnetozones with the standard geomagnetic

timescale, as shown in Figure 3. N3 correlative with the Olduvai Subchron is recognized only in the Donggou section, while N2 correlative with the Jaramillo Subchron is found in both sections. The author sampled the artifact layer, right below the sedimentological marker layer, a black silty clay layer about 2 cm according to ZHU ET AL. (2001), in the summer of 2005 (SH in Figure 3). Instead of determine the age of the artifact layer directly, ZHU ET AL. (2001) estimated the age of the equivalent marker layer on Donggou section to be 1.36Ma by the average accumulation rate of the sediments between the two subchrons identified, and this age was taken as the age of the artifact layer of Xiaochangliang site.

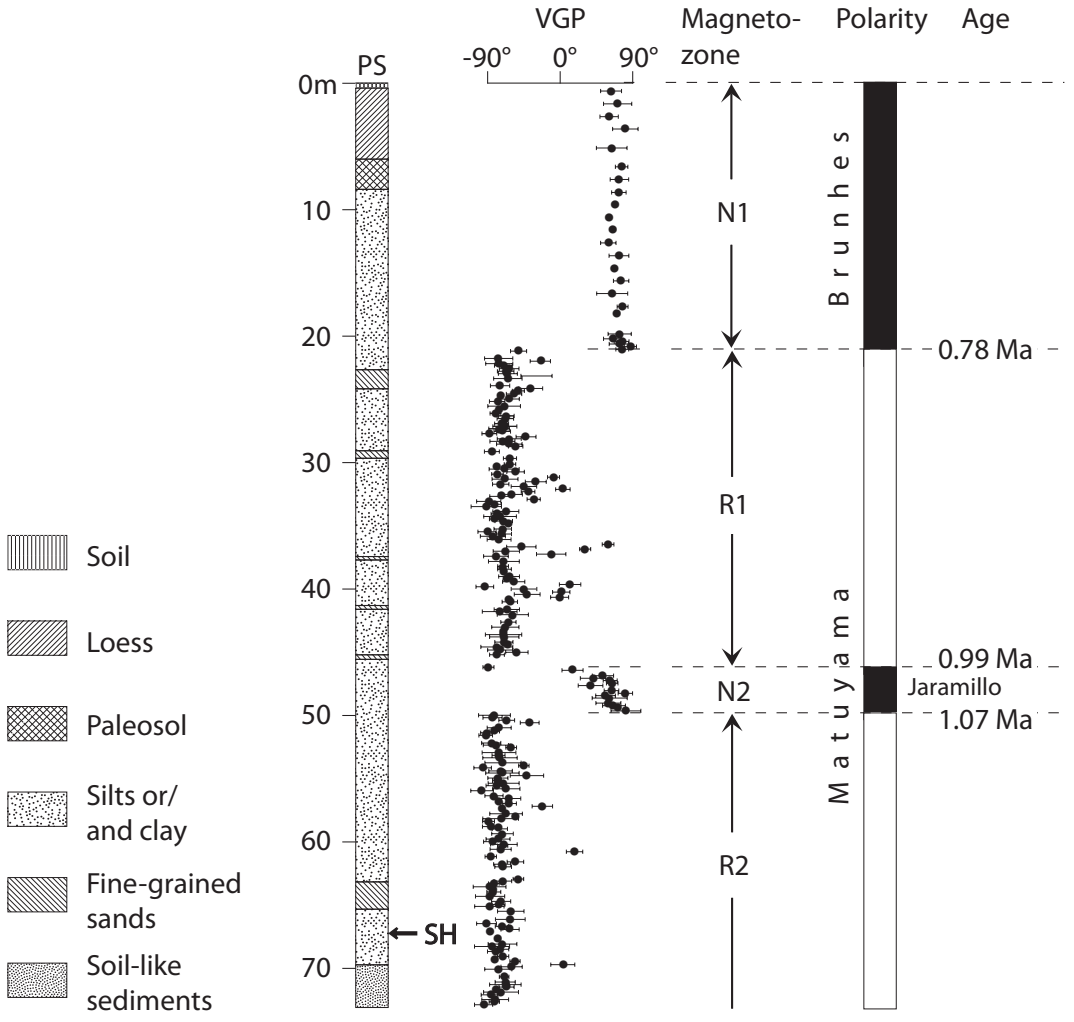

Figure 4. Columnar section and paleomagnetic data of the Xiaochangliang site (modified from ZHU ET AL., 2001).

* The section shows the lithofaces of the sediments from the plateau surface (PS) to the sampling horizon (SH) which is equivalent to the artifact layer of the site. On the basis of the paleomagnetic data (VGP: virtual geomagnetic pole), ZHU ET AL. (2001) correlated and dated the sediments as shown in the right side of this figure.

In the past studies on this Paleolithic site, only two forms of arvicolids, *Allophaiomys* cf. *A. pliocaenicus* and *Borsodia chinensis* (=*Mimomys chinensis*) were reported once by TANG ET AL. (1995). But there was only one broken right M_1 for the former, and one right M_2 for the latter one. In the present study, 73 molars referred to *Borsodia chinensis* and 61 molars referred to *Allophaiomys deucalion* obtained by our sampling and screen-washing are going to be described and discussed.

F. Other related localities and species

Besides all the localities described above, the author is also offered the opportunities to observe the specimens from other localities. For example, the author observed nearly all the specimens involved in ZHENG AND LI (1986), such as *Borsodia chinensis* form Xiaoshagou, Nihewan (PLATE 30, Figs. 5~6), Linxi, Liaoning (PLATE 30, Figs. 7~9), Heshui, Gansu (PLATE 30, Figs. 10~11); *Mimomys orientalis* from Youhe, Weinan, Shaanxi (PLATE 30, Fig. 1), Yushe, Shanxi (PLATE 30, Fig. 2); *Omniprocessimys banchiaonicus* from Heshui, Gansu (PLATE 30, Fig. 15); *Mimomys youhenicus* from Youhe, Weinan, Shaanxi (PLATE 30, Figs.3~4); *Mimomys gansunicus* from Heshui, Gansu (PLATE 30, Fig. 12); *Mimomys* cf. *intermedius* from Lishi, Shanxi (PLATE 30, Figs. 13~14); *Omniprocessimys peii* from Dachai, Shanxi (PLATE 31). The author also observed the specimens of the arvicolid species reported by FLYNN ET AL. (1997), such as (1) Upper Gaozhuang Formation: *Mimomys* sp.; (2) Mazegou Formation: *Mimomys* (*Cromeromys*) *irtyshensis*; (3) Haiyan Formation: *Borsodia chinensis*, *Mimomys gansunicus*, ?*Villanyia* sp. (the opinion of the present author).

VI. Systematic Descriptions

A. Descriptive terminology and measuring methods

As introduced in the introduction part, the study on arvicolids has a history of nearly two centuries. During the time, many arvicolid researchers had proposed their own terminologies, such as HINTON (1926), VAN DER MEULEN (1973), RABEDER (1981), and so on. At present, the study of fossil arvicolids is still mainly subject to the morphologies of molars. However, among fossil arvicolids, the differences whether between primitive forms and advanced forms or between different forms of the same age are so conspicuous that a set of universal terminology is absolutely necessary for the study. The terminology for the occlusal surface description of VAN DER MEULEN (1973) has been accepted by many

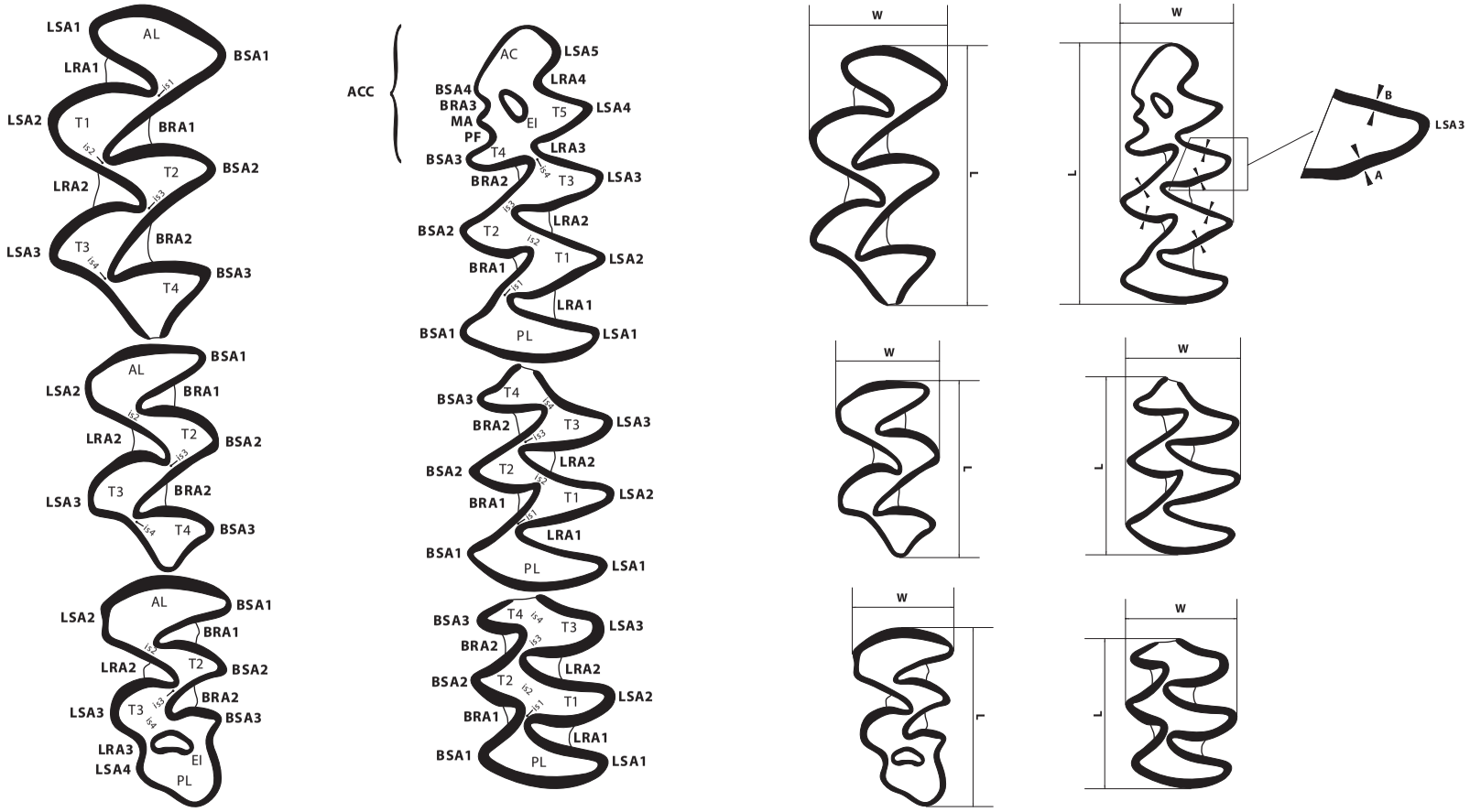

Figure 5. Terminology and measuring methods for the occlusal surface of arvicolid molars (occlusal views after CARLS AND RABEDER, 1988)

MA: *Mimomys*-angle; **PF:** prism fold; **AC:** anterior cap; **AL:** anterior loop; **PL:** posterior loop; **ACC:** anteroconid complex; **LSA:** lingual salient angle; **LRA:** lingual reentrant angle; **is:** isthmus; **T:** triangle; **EI:** enamel islet; **L:** length of occlusal surface; **W:** width of occlusal surface; **A:** thickness of the anterior enamel wall of triangle; **B:** thickness of the posterior enamel wall of triangle.

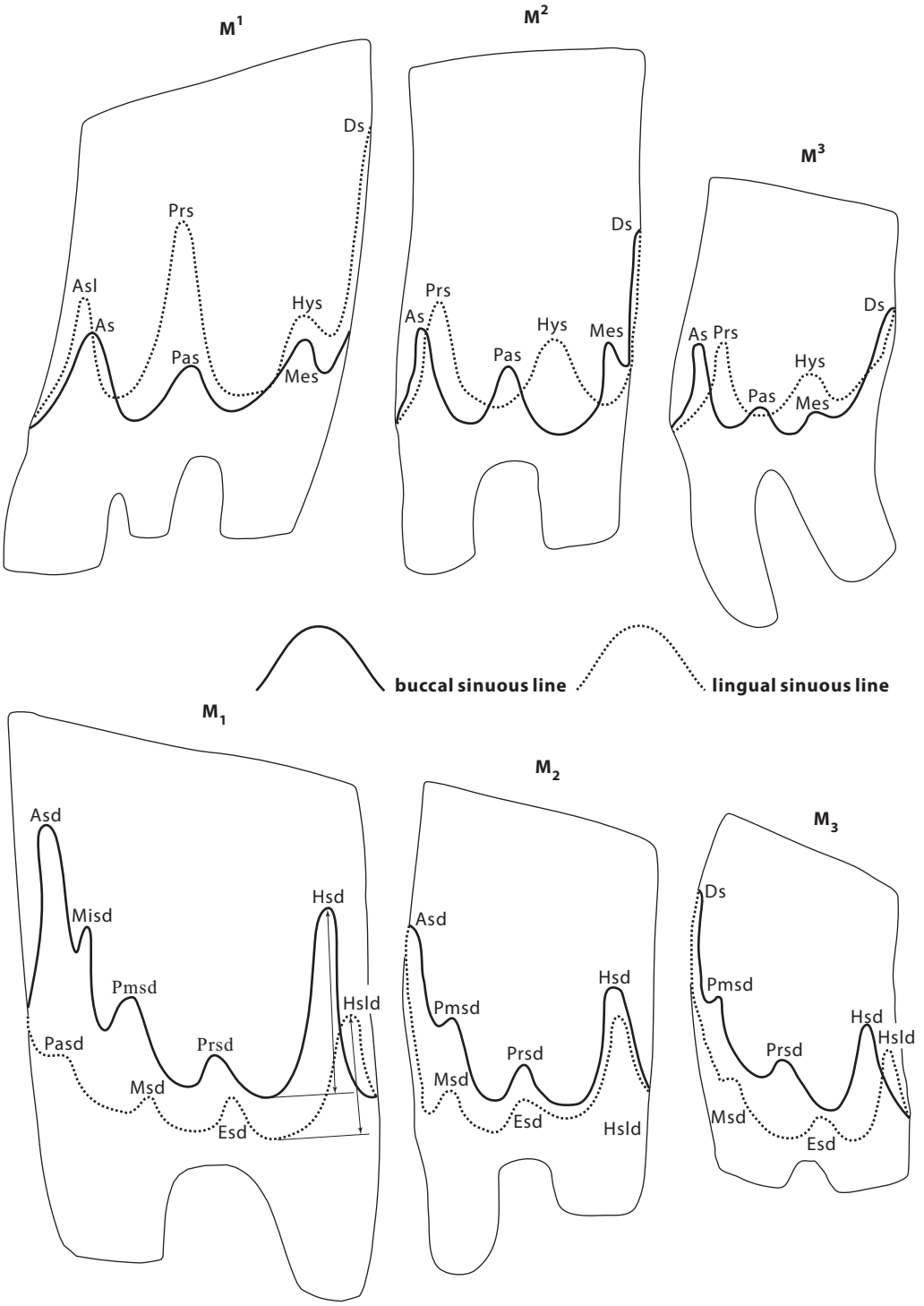

Figure 6. Terminology and measuring method for sinuous line of arvicolid molars (after CARLS AND RABEDER, 1988)

Upper molars - As: anterosinus; **Asl:** anterosinulus; **Ds:** distosinus; **Hys:** hyposinus; **Mes:** metasinus; **Pas:** parasinus; **Prs:** protosinus.

Lower molars - Asd: anterosinuid; **Esd:** entosinuid; **Hsd:** hyposinuid; **Hsld:** hyposinulid; **Misd:** mimosinuid (sinuid of Mimomys-angle); **Msd:** metasinuid; **Pasd:** parasinuid; **Pmsd:** prismosinuid (sinuid of prismenkate); **Prsd:** protosinuid.

researchers. VAN DER MEULEN first introduced the term anteroconid complex (ACC) in his terminology, which improved the convenience of the application. In this terminology, triangle on $M^{2\sim3}$ counts form two because of the consideration of cusp homology. Accordingly, lingual salient angle also counts form two for the same reason. In the present study, the terminology of VAN DER MEULEN (1973) are adopted, and some other terms, such as *Mimomys*-angle (MA), prism fold (PF), and so on, are added. Besides, the counting method of isthmus of KAWAMURA (1988) is also introduced. The whole terminology for the description of occlusal surface characters and measuring methods for occlusal surface is shown in Figure 5. As for the terminology for the sinuous line on lateral sides of molars, the terminology of CARLS AND RABEDER (1988) is adopted as shown in Figure 6.

B. Calculating method for quantified characters

SDQ (Schemelzband Differentiation Quotient), which was first introduced by HEINRICH (1978), is a quantitative index of the enamel band differentiation type. The calculating method adopted here is following HEINRICH (1982) as follows:

$$SDQ_{LSA3}=A_{LSA3}\div B_{LSA3}\times 100$$

$$SDQ=(SDQ_{LSA2}+SDQ_{BSA2}+SDQ_{LSA3})\div 3\times 100$$

Based on this index, the enamel band differentiation type of the species whose SDQ is more than 100 is thought to be negative type or *Mimomys*-type; on the contrary, if less than 100, it is called positive type or *Microtus*-type. The measuring method for A and B is shown in Figure 5.

HH-index CARLS AND RABEDER (1988) proposed this index as a indirect indicator for the crown height. Here HH means hyposinuid-hyposinulid. The measuring method for both sinuids is shown in Figure 6. And the calculating method is as follows:

$$HH\text{-}index=SQRT(Hsd^2+Hsld^2)$$

C. Systematic descriptions

Order RODENTIA ROCHEBRUNE, 1883

Family CRICETIDAE GRAY, 1821

Subfamily ARVICOLINAE GRAY, 1821

Dental diagnosis (following REPENNING, 1988): Cricetid rodents with hypsodont, triangularly prismatic cusps on their cheek teeth; M_1 with posterior loop and three basic

alternating triangles; anteriorconid complex with single rounded to globular cap; M^3 with alternating triangles.

Included tribes: Arvicolini, Clethrionomyini, Lagurini, Microtini, Pitymyini, Lemmini, and Synaptomyini.

Remarks: The classification of fossil arvicolids (in the sense of REPENNING ET AL., 1990) has been undergoing controversy and not completely settled yet. Different researchers hold different opinions on it. GROMOV AND POLYAKOV (1977) introduced the brief history of taxonomy and classification of voles. According to them, Miller (1896) identified two suprageneric groups of voles, viz. Lemmi and Microti, with three genera in the former and four in the latter, and thought of them as a subfamily of the rat family Muridae. Mehely (1914) held similar opinion with Miller (1896), but he separated the rooted-toothed voles as an independent subfamily. The classification of Hinton (1910, 1926), like Miller's, contained few changes but significant additions, especially at the generic and subgeneric levels. Simpson (1945) considered voles as a subfamily of the small hamster family Cricetidae, and raised both suprageneric groups of Miller and Hinton to the rank of tribe: Lemmini and Microtini. He further separated Ellobiini as an independent tribe. Kretzoi (1955) considered voles as an independent family Arvicolidae of Myomorpha. In his classification, he included seven subfamilies: Baranomyinae, Microtoscoptinae, Ellobiinae, Prometheomyinae, Lemminae, Myospalacinae, Arvicolinae. What's more, he also included five tribes in the subfamily Arvicolinae: Arvicolini, Ondatrini, Microtini, Lagurini and Dicrostonychini. While Hooper and Hart (1962) viewed voles as a subfamily Microtinae of the rat family Muridae. He included eight tribes in this subfamily: Lemmini, Clethrionomyini, Prometheomyini, Dicrostonychini, Neofibrini, Ondatrini, Microtini and Ellobiini. GROMOV AND POLYAKOV (1977) basically inherited the classification of Hooper and Hart (1962), but they added some new tribes. The tribes they included in the subfamily were: Microtoscoptini, Ondatrini, Clethrionomyini, Lagurini, Dicrostonyxini, Lemmini, and Microtini. After that, REPENNING (1987) reviewed the classification of arvicolids (=microtine rodents) in his comprehensive contribution about the biochronology of microtine rodents of the United States. He stated that arvicolids were a polyphylentic group of rodents and consisted of five separate cricetid subfamilies representing five separate evolutionary lineages. There five subfamilies were: Lemminae, Prometheomyinae, Arvicolinae, Ondatrinae, and Dicrostonychinae. When they reviewed the arvicolid biochronology of the Northern Hemisphere, REPENNING ET AL. (1990) used the same classification and listed the tribes and genera included in each subfamily. For example, they listed five tribes for the subfamily Arvicolinae: Arvicolini, Clethrionomyini,

Microtini, Pitymyini, and Lagurini. FEJFAR AND REPENNING (1998) eliminated the subfamily Lemminae and placed two more tribes Lemmini and Synaptomyini in the subfamily Arvicolinae. In addition to the classifications above, MCKENNA AND BELL (1997) thought voles as a subfamily of the rat family Muridae, and they included seven tribes in this subfamily: Arvicolini, Clethrionomyini, Dicrostonychini, Ellobiini, Lagurini, Lemmini, and Prometheomyini. In the classification of living mammals of WILSON AND REEDER (1993), voles were also thought of as a subfamily arvicolinae of the rat family Muridae. In the present study, the idea of REPENNING (1987), REPENNING ET AL. (1990) and FEJFAR AND REPENNING (1998) will be followed, and voles are thought of as four subfamilies of the hamster family Cricetidae. The subfamily arvicolinae is also in the sense of them.

Tribe ARVICOLINI KRETZOI, 1954

Dental diagnosis (following REPENNING AND GRADY, 1988 and REPENNING, 1992): Genera of tribe Arvicolini have a first lower molar with posterior loop, preceded successively by three substantially closed and alternating triangles and terminated by and anteroconid complex with confluent, lingual and buccal primary wings and an uncomplicated, more or less globular cap. M^3 with no more than two completely formed alternating triangles. Most genera have rooted cheek teeth, and increasingly stronger undulation of sinuous line characterizes increasing hyposodonty.

Included genera (partially): *Allophaiomys*, *Arvicola*, *Borsodia*, *Mimomys*, *Promimomys*, *Omniprocessimys* gen. nov. and *Villanyia*.

Genus *Mimomys* FORSYTH-MAJOR, 1902

Type species— *Mimomys pliocaenicus* FORSYTH-MAJOR, 1902

Diagnosis— Molars rooted. No or little cementum in ancestral forms, but abundant in advanced forms. Enamel islet and *Mimomys*-angle on M_1 strongly developed in ancestral forms, but becoming weaker or totally disappear in advanced forms. Upper molars all with three roots in ancestral forms, and loss of roots occurring with the progress of evolution. Only M^1 even in advance forms still having three roots, but with the anterior two fused together. M^3 with two enamel islet in ancestral forms, but in advanced forms, the anterior one reduced. Sinuous line flat in ancestral forms, but sinuses (sinuids) getting high-positioned with the progress of evolution.

Remarks The genus was proposed by FORSY-MAJOR (1902) based on a fossil arvicolid form, *Mimomys pliocaenicus*, from northern Italy that he had placed in the genus *Arvicola* 20 years earlier. He also included in *Mimomys* two species from Britain that Newton

(1882) had placed in *Arvicola*, but he forgot selecting a type species. Of these three species, Méhely (1914) selected *Mimomys pliocaenicus* as the type sepcies, as it was this form that Forsyth-Major had personally described. Since then, numerous species and subgenera have been referred to this genus. In the present study, subgenus are not going to be assigned to the species described here. The included subgenera are partially listed according to some authors. But the included species are too many to be covered completely.

Included subgenera (partially, following REPENNING AND GRADY, 1988; KOWALSKI, 2001; GROMOV AND POLYAKOV, 1977; REPENNING, 2003): *Aratomys*, *Cromeromys*, *Cseria*, *Mimomys*, *Cosomys*, *Ogmodontomys*, *Ophiomys*, *Pusillomys*, *Kislangia*, and *Microtomys*.

Mimomys bilikeensis (QIU AND STORCH, 2000)

PLATE 1~3

Synonymy—

Aratomys bilikeensis QIU AND STORCH, 2000; QIU AND STORCH (2000). Senckenbergiana lethaea 80 (1), p195, Pl. 8 figs 26~31.

Original diagnosis— See QIU AND STORCH, 2000.

Emended diagnosis— Enamel band undifferenciated (SDQ approximately 102). No crown cementum. Anteroconid complex of M_1 short and mushroom-shaped, *Mimomys* angle weak, enamel islet developed, and vanishing after about 50% loss of crown height through wear as *Mimomys* angle, is2 comparatively wider than the other isthmuses. Formation of enamel islet on M_1 by folds that penetrate the anteroconid complex from the mesial (in most cases) or lingual tooth margin (occasionally). M^3 with two enamel islets, the anterior one vanishing earlier than the posterior one. Location of anterior and posterior root of M_3 dorsally and labially, respectively, of the incisor. Very primitive enamel microstructure.

Biochronological range— Early Gaozhuangian of DENG, 2006.

Studied locality and materials—

Bilike

2 maxillary fragments with M^1 (V11909.1~2); 37 mandible fragments: 28 with M_1 (11909.16~43), 7 with M_2 (11909.44~50), 1 without tooth (11909.51), 1 with M_3 (11909.52); 311 M^1 (11909.53~363); 346 M^2 (11909.364~709); 347 M^3 (11909.719~1065); 244 M_1 (11909.1067~1310); 316 M_2 (11909.1337~1652); 342 M_3 (11909.1678~2019).

Measurements— See Table 1.

Description—

There is no cementum in reentrant angles of the molars. Root development is so early that the formation of it can be observed even on nearly unworn molars. The sinuous lines generally undulate smoothly in all molars and the positions of the sinuses (-ids) are very low. Enamel band tends to become thicker with wear.

M^1: The occlusal patterns of M1 comprises four alternating triangles behind the anterior loop. On juvenile specimens, the posterior walls of LRA1, 2 are seemingly parallel to the anterior walls of BRA1, 2 respectively, which leads to the zigzag shape of the whole dentine field being equally semi-confluent at each dentine isthmus; and the posterior end of the tooth is pointed posteriorly, where the enamel band becomes distinctly much thinner and seemingly discontinuous. With the process of wear, the the parallel walls of reentrant angles turns to normal occlusal pattern and the dentine field becomes separate at is1, 3, but keeps semi-confluent at is2, 4; the posterior end turns to round-shaped, and the enamel band there restore to normal thickness as that of other parts. The buccal sinuous line undulates smoothly with all sinuses at nearly the same level parallel to the masticatory surface, while the lingual sinuous line rises higher at the protosinus (Prs) with the other part nearly flat. Not less than 257 of 313 available specimens ("not less than" comes up because not all specimens are observable for root formation, sic passim) are observed to have three roots with the middle root on mesial side above T1. Not less than 22 of 313 available specimens have four roots with the fourth root on mesial side above T3.

M^2: There are three alternating triangles behind the anterior loop. Among all the salient angels, BSA1 looks slimmer than the others. On juvenile specimens, the anterior wall of AL is sometimes concave on its buccal side; the posterior wall of BRA1 and the anterior wall of BRA2 are seemingly parallel to anterior and posterior walls of LRA2, respectively, which also leads to the zigzag shape of the whole dentine field being equally semi-confluent at each dentine isthmus like on M^1. On mature and aged specimens, the dentine field is separated at is2, 3, but keeps semi-confluent at is4. The apex of BRA2 tends to be more posteriorly pointed than that of BRA1. Not less than 291 of 345 available specimens have three roots; not less than 4 of 345 available specimens have two roots; and not less than 1 of 345 specimens has four roots. Other characters, such as the posterior end of the teeth, the enamel band thickness at the posterior end, and the sinuous lines etc., are similar with that on M^1.

M^3: The occlusal pattern of M3 is basically composed of an anterior loop, a semicircular-shaped and comparatively short posterior loop and one feeble triangle between them. There are always two reentrant angles on buccal side and one on lingual side. Salient angle can count to three on both buccal and lingual side if including the angles on both sides of

the posterior loop. On some specimens, there is a narrow and shallow reentrant fold right next to BSA3 on the buccal side of PL. LSA2 is usually robust and blunt. BSA1 is usually slimmer. The apex of BRA2 is nearly opposite to that of LRA2. On some juvenile specimens, the anterior wall is concave and the BSA1 is flat-headed. An enamel island always appears on the posterior loop and lasts until nearly the whole crown is worn out. When this island will form varies considerably from juvenile to aged stage depending on the close of an extra reentrant fold that develops on the lingual side of the posterior loop. It sometimes closes early even on juvenile specimens, and sometimes it last long but never gets so close to the lingual sinuous line as LRA2 in lingual view. Usually, an enamel island also appears around the anterior loop, but only on mature or aged specimens. On juvenile specimens, the apex of BRA1 extends deep inwards close to the anterior wall of LRA2, which makes dentine field of AL is separate form that of T2. This situation will change on mature or aged specimens with wear of the teeth, where the former apex part of BRA1 is isolated and forms the anterior enamel island, and the new apex withdraws outwards a little. At the same time, BRA1 becomes shallower and AL becomes confluent with T2 with the enamel island in the middle though. Even though, the anterior enamel island forms later than the posterior one, it usually doesn't last long and disappears earlier. The sinuous line on both buccal and lingual side is nearly flat with only Prs a little higher positioned. Among all 347 available specimens, not less than 83 teeth have two roots; not less than 206 teeth have three roots.

Mandible: The mental foramen is small, and situated somewhat anteroinferiorly to M_1. The lower masseteric crest is stout, and originates from the position about 0.5 mm posterior to the mental foramen. The crest is slightly convex ventrally, and extends to the lower margin of the angular process. The upper masseteric crest, the characteristic "arvicoline groove" (Repenning, 1968), runs parallel to the anterior edge of the ascending ramus, and connects to the lower masseteric crest by an acute angle. The anterior edge of the ascending ramus originates from the position beside the posterior loop of M_1. The internal temporal fossa between the ramus and the alveoli of the molar is broad and shallow, especially beside M_3. The lower incisor with a triangular section runs by the lingual side of both roots of M1, anterior root of M_2, and the buccal side of both roots of M_3, and is overlain by the posterior root of M_2.

M_1: There are three alternating triangles between the anterior cap (equivalent to ACC here) and the posterior loop. An round- or oval-shaped enamel islet always appears on the anterior cap. If oval-shaped, it extends anteropsoteriorly. It doesn't last a lifetime, and will be worn out on mature or aged individuals. The outline of the anterior cap varies greatly

on juvenile to young specimens before the enamel islet vanishes suffering from wear. Especially on juvenile specimens whose roots begin to form or just formed, a number of extra irregular secondary folds can be observed on the anterior and/or lingual side of the anterior loop. *Mimomys*-angle usually develops, but sometimes doesn't last long. Using the duration of the enamel islet as a reference, it can be observed that 94 out of 142 specimens with enamel islet still present, but only 43 out of 131 specimens with enamel islet already worn out have *Mimomys*-angle developed. On all other specimens, *Mimomys*-angle can not be observed. The development of LRA4 on lingual side of the anterior loop is conspicuous on younger specimens, but it is much shallower than the other reentrant angles behind the anterior loop especially on the aged specimens on which it becomes a very smooth concave curve. BRA3 is only observable on juvenile to young specimens as a smooth and slightly concave curve. On aged specimens, all extra secondary folds disappears, and the outline of the anterior loop becomes smooth, and on the lingual side it becomes straight (except those with *Mimomys*-angle developed in front of BSA3 where it curves a little) and runs obliquely like the posterior walls of the buccal reentrant angles. The apex of LRA3 is obliquely opposite to that of BRA2. The dentine isthmus is2 is distinctly wider than is1, 3. The enamel band can be considered as undifferentiated because the SDQ is calculated at 102.36. The buccal sinuous line undulates more than the lingual one and a comparatively higher position of Hsd and Asd can be observed. There are always two roots, but on very few specimens, a third hair root can be observed in the middle of the two normal roots.

M_2: There are four alternating triangles in front of the posterior loop. Buccal triangles are distinctly smaller than lingual ones. T1~T2 and T3~T4 are semi-confluent with each other respectively, which means that the apices of BRA1, 2 are anterior to that of LRA1, 3 respectively and the dentine isthmuses is2, 4 are distinctly wider that is1, 3. On young specimens, the front end of the tooth is pointed anteriorly and the enamel band there becomes much thinner and seemingly discontinuous. But on older specimens, the outline of the front end of the tooth becomes smoothly, and anteriorly convex and the thickness of the enamel band there also return to normal as the other part. The buccal sinuous line, with three sinuids nearly at the same level, undulates more than the lingual one. Two roots.

M_3: There are four triangles in front of the posterior loop, with T1 and T2 alternating with each other, T3 and T4 opposite to or alternating with each other. Buccal triangles are distinctly smaller that lingual ones. On young specimens, the apex of T3 tilts anteriorly sometimes, and the enamel band becomes distinctly thinner at the front end of the tooth.

Triangles T1, T2 are semi-confluent, and T3, T4 are confluent or semi-confluent. The sinuous lines on both sides are nearly flat. Two roots.

Remarks and comparisons—

QIU AND STORCH (2000) proposed a new form of arvicolids under the name of *Aratomys bilikeensis*. But REPENNING (2003) thought of *Aratomys* as a subgenus of *Mimomys*, and referred this species to *Mimomys*. The author agrees with the opinion of REPENNING (2003). This is the most primitive *Mimomys* species in North China. Many researchers believe that *Mimomys* is derived from *Promimomys*, and *Promimomys* derived from *Microtodon*. FAHLBUSCH AND MOSER (2004) reported the abundant materials of *Microtodon atavus* from Ertemte and Harr Obo, Inner Mongolia. But, until now, *Promimomys* has not been found in Northern China, except *Promimomys aisaticus* from Xindong, Huainan, Anhui reported by JIN AND ZHANG (2005). There's only one left mandible with $M_{1\sim2}$ for *Promimomys aisaticus*, besides, there, indeed, are some morphological conflicts between it and the most primitive *Mimomys*, *M. bilikeensis*, in North China. So, even though, there are abundant materials for *Microtodon atavus* and the most primitive *Mimomys* species, *M. bilikeensis*, in North China, more evidence is still required to prove the transition from *Promimomys* to *Mimomys* in North China.

Mimomys bilikeensis differs from *Mimomys teilhardi*, *M. orientalis*, and *M. youhenicus* mainly in that it has a weaker *Mimomys*-angle, BRA3 on M_1, and weaker undulation of sinuous line; it differs from the *Villanyia* and *Borsodia* species described here in having a enamel islet developed on ACC of M_1; it differs from the *Allophaiomys* and *Proedromys* species in having rooted molars and no cementum deposited in the reentrant angles of molars.

Mimomys cf. *M. bilikeensis* (QIU AND STORCH, 2000)

PLATE 24, Figs. 9~15

Synonymy—

Aratomys bilikeensis; ZHANG AND ZHENG (2001). Vertebrata PalAsiatica 39 (1), Fig. 3.

Aratomys bilikeensis; ZHENG AND ZHANG (2001). Vertebrata PalAsiatica 39 (3), p. 57, Fig. 1.

Studied locality and materials—

Lingtai (personal number):

72074(4)— L5 L5-3: 1 broken left M_1 (03), 1 right M_2 (02), 1 left M_3 (01); L5-2: 1 left M^2 (03), 1 right M^2 (02), 1 right M_2 (04), 1 left M_3 (01).

Measurements— See Table 1.

Description—

There is no cementum in reentrant angles of all the molars.

M^2: There are three alternating triangles behind the anterior loop. T3 and T4 are much more confluent with each other at is4 than T2 and T3. Among all the salient angels, BSA1 looks slimmer than the others. The apexes of both BRA1 and BRA2 tend to be posteriorly pointed. The sinuous line undulates smoothly, similar with *Mimomys bilikeensis* The only two available specimens both have three roots, but the anterior two roots are fused together near the base, and then are separated from each other.

M_1: The only one broken left M_1, with its anterior cap and enamel layer of buccal side damaged, has few informative characters observable. There are three alternating triangles between the anterior cap (equivalent to ACC here) and the posterior loop. The apex of LRA3 is obliquely opposite to that of BRA2. The dentine isthmus is2 is wider than is1, 3. The lingual sinuous line undulates smoothly, same as in *Mimomys bilikeensis*. This only one specimen has two roots.

M_2: There are four alternating triangles in front of the posterior loop. Buccal triangles are distinctly smaller than lingual ones. T1~T2 and T3~T4 are semi-confluent with each other, respectively, which means that the apices of BRA1, 2 are anterior to that of LRA1, 3, respectively and the dentine isthmuses is2, 4 are distinctly wider than is1, 3. The outline of the front end of the tooth is not anteriorly pointed. The buccal sinuous line, with three sinuids nearly at the same level, undulates more than the lingual one. Two roots.

M_3: There are four triangles in front of the posterior loop, with T1 and T2 alternating with each other, T3 and T4 opposite to each other. Buccal triangles are distinctly smaller that lingual ones. Triangles T1, T2 are semi-confluent, and T3, T4 are completely confluent. The sinuous lines on both sides are nearly flat. Two roots.

Remarks and comparisons

There is no key molar to give us enough confidence to make a further specific identification. So our referral is mainly base on the following morphological characters: 1) the apexes of BRA2 and LRA3 on the only broken M_1 are opposite to each other; 2) the sinuous line on the lingual side of this molar is as flat as *Mimomys bilikeensis*; 3) it seems that there's no more other folds developed on its ACC; and 4) the sinuous lines on all the other molars referred to this species are also as flat as that in *Mimomys bilikeensis*.

Mimomys teilhardi Li, 2006

PLATE 4

Synonymy—

Mimomys teilhardi Li, 2006; Li (2006). Doctoral Dissertation of CAS, p52. (in part)

Original diagnosis— See LI, 2006.

Emended diagnosis— Root number pattern of all molars in order of M^1, M^2, M^3, lower molars is 3, 3, 2, 2. No cementum deposited in reentrant angles of molars. Enamel islet and *Mimomys*-angle on M_1 strongly developed. M^3 with two enamel islets. The undulation of sinuous line stronger than *Mimomys bilikeensis*.

Biochronological range— Early Gaozhuangian of DENG, 2006.

Studied locality and materials—

Gaotege (number from original author):

83 M_1— DB02-1 (32) VXXX19.1, 150~152, 154~156, 161, 165~167, 169, 171~174, 176~178, 180, 188, 189, 191~194, 197, 199~201, 203, 205, 207. **DB02-2 (19)** VXXX19.386~390, 392, 393, 395~397, 399~401, 403~406, 408, 409. **DB02-3 (16)** VXXX19. 532, 534, 537, 539~541, 543, 545, 547~554. **DB02-4 (4)** VXXX19. 632, 633, 636, 637. **DB02-5 (1)** VXXX19.656. **DB02-6 (3)** VXXX19.657, 661, 662. **DB03-1 (7)** VXXX19.688~690, 692, 694~696.

Measurements— See Table 1.

Description—

There is no cementum in reentrant angles of the molars. Root formation is early. The sinuous lines undulate little more stronger than that of *Mimomys bilikeensis*.

M_1: There are three alternating triangles between ACC and the posterior loop. An round- or oval-shaped enamel islet always appears on the anterior cap. It does not last a lifetime, and will be worn out on mature or aged individuals. On juvenile specimens whose roots begin to form or just formed, less extra irregular secondary folds can be observed on the anterior and/or lingual side of the anterior loop than in *Mimomys bilikeensis*. The anterior loop usually extends anterolingually. *Mimomys* angle always develops, and lasts lifetime. The development of LRA4 on lingual side of the anterior loop is conspicuous on younger specimens, but it is much shallower than the other reentrant angles behind the anterior loop especially on the aged specimens on which it becomes a very smooth concave curve. BRA3 is strong on juvenile to young specimens. The apex of LRA3 is usually obliquely opposite to that of BRA2. The dentine isthmus is2 is distinctly wider than is1, 3. The enamel band can be considered as weak *Mimomys* type or positive type because the SDQ is 111. The sinuous line undulates stronger than that of *Mimomys bilikeensis.* And the buccal sinuous line undulates more than the lingual one and a comparatively higher position of Hsd and Asd can be observed. There are always two roots, but on very few specimens, a third hair root can be observed in the middle of the two normal roots.

Remarks and comparison—

LI (2006) assigned all the arvicolid materials from DB02-5~6, DB02-1~4, and DB03-1 of Gaotege section to this new species. Based on the author's observation, it is believed that there should be two forms mixed together in these materials. These two forms have distinctively different characters on M_1, but, for the other molars, no noticeable differences can be detected. Here the specific name *Mimomys teilhardi* proposed by LI (2006) is still used to represent the form with a strong enamel islet, a un-necked anterior cap, and a distinctly smaller HH-index (0.39 mm, See Table 1) on M_1. It is in direct contrast to the other form with no enamel islet, with a necked anterior cap, and a distinctly greater HH-index (0.76 mm, Appendix Table 1) on M_1, which here is assigned to the genus *Villanyia* as an unnamed new species, *Villanyia* sp. nov.. As a comprise, presently clear distinction between these two forms is only going to be made on M_1, and temporarily the author takes all the materials of the other molars as *Mimomys teilhardi - Villanyia* sp. nov. complex, which means that they presently can be assigned to any of them and will be described later.

Mimomys teilhardi mainly differs from *Mimomys bilikeensis* by a stronger *Mimomys*-agnle; from *Mimomys orientalis*, and *Mimomys youhenicus* in having a smaller HH-index; from *Villanyia* and *Borsodia* species in having a enamel islet developed on ACC of M_1; from *Allophaiomys deucalion*, *Proedromys bedfordi* in having rooted molars and lacking cementum deposited in the reentrant angles; from *Mimomys gansunicus*, *M. banchiaonicus*, and *M. peii* in lacking cementum deposited in the reentrant angles.

Mimomys cf. *M. orientalis* YOUNG, 1935

PLATE 7

Synonymy—

Mimomys cf. *M. orientalis*; LI (2006). Doctoral Dissertation of CAS, p57. (in part)

Studied locality and materials—

Gaotege (personal number):

DB03-2 LI (2006): 7 left M^1 (06~12), 5 right M^1 (01~05), 1 left M^2 (13), 2 left M^3 (17~18), 1 right M^3 (16), 2 left M_1 (19, 23), 2 broken right M_1 (20, 22), 3 right M_2 (30~31, 39); LI 2007.05: 6 left M_1 (02~07), 3 right M_1 (08, 10, 12).

Measurements— See Table 1.

Description—

There is little cementum deposited at the bottom of the reentrant angles. But sometimes cementum can not observed, especially on M_1 and M^3. The sinuous lines are typical *Mimomys* type, and the undulation is much stronger than that of *Mimomys bilikeensis*, *M. teilhardi*.

M^1: The occlusal patterns of M^1 comprises four alternating triangles behind the anterior loop. The dentine field is separate at is separate at every isthmus, which menas all the isthmuses are equally closed. Cementum can be observed on all the available specimens. And all the available specimens have three independent roots.

M^2: There are three alternating triangles behind the anterior loop. BSA1 looks slimmer than the other salient angles. The dentine field is separated at is2, 3, 4. Cementum can be observed on the only referred specimen, and it has two roots.

M^3: The occlusal pattern of M^3 is basically composed of an anterior loop, a comparatively long posterior loop and one triangle T2 between them. There are always two reentrant angles on buccal side and one on lingual side. Salient angle can count to three on both buccal and lingual side if including the angles on both sides of the posterior loop. LSA2 is usually robust and blunt. BSA1 is usually slimmer. The apex of BRA2 is nearly opposite to that of LRA2. On juvenile specimen (PLATE 7, Fig. 14), the anterior wall is concave and the BSA1 is flat-headed. An enamel island always appears on the posterior loop and lasts until the whole crown is nearly worn out. Sometimes (PLATE 7, Figs. 15~16) the extra reentrant fold on the lingual side of the posterior loop, which seems like LRA3, lasts so long that the formation of this island is also very late. Even though the enamel island around the anterior loop can not be observed on the occlusal views of all three referred specimens (PLATE 7, Figs 14~16), but we can find that it will be formed with the wear of the crown from the buccal view, when the former apex part of BRA1 is isolated and forms the anterior enamel island, and the new apex withdraws outwards a little. At the same time, BRA1 will become shallower and AL becomes confluent with T2 with the enamel island in the middle though. No cementum can be observed on all the three specimens. Of the three specimens, one has three roots, and the other two have two roots.

M_1: There are three alternating triangles between ACC and the posterior loop. An enamel islet always appears on the anterior cap. It doesn't last long, and will be worn out after about 1/4 wear of the crown height. The anterior cap is usually lingually pointed on young and mature individuals. On juvenile specimens whose roots have not been formed, a number of extra irregular secondary folds can be observed on the anterior and/or lingual side of the anterior loop. *Mimomys*-angle can be seen on 9 out of 12 observable specimens, and the other three specimens don't have *Mimomys*-angle developed. The development of LRA4 on lingual side of the anterior loop is conspicuous. BRA3 is more developed that *Mimomys teilhardi*. The apex of LRA3 is in front of that of BRA2 on most specimens, except on Li200705-02 where it is opposite to that of BRA2. The dentine isthmus is2 is slightly wider than is1, 3. The enamel band differentiation is typically *Mimomys* type,

because the SDQ is calculated at 122. Two roots.

M_2: There are four alternating triangles in front of the posterior loop. T1~T2 and T3~T4 are semi-confluent with each other, respectively, which means that the apices of BRA1, 2 are anterior to that of LRA1, 3, respectively and the dentine isthmuses is2, 4 are distinctly wider that is1, 3. Little cementum can be observed in the bottom of the salient angles of all the referred specimens. Two roots.

Remarks and comparison—

LI (2006) referred part of the arvicolid materials from DB03-2 of the Gaotege section to this form. The author agrees with him because both the morphology, especially the HH-index of M_1 (please see Table 1 for details) are indicative of its similar stage of evolution with *Mimomys orientalis*. It is left as cf. because there are few specimens for *Mimomys orientalis* and the only complete M_1 for this species is a young individual. It is apparent that this form shows several more advanced character than the *Mimomys* species from the lower layers on the same section. These characters include greater HH-index, the commencement of cementum deposit in the reentrant angles of molars, and so on. It differs from *Mimomys youhenicus* by a smaller HH-index; from *Mimomys gansunicus* in having a comparatively strong *Mimomys*-angle and less cementum deposited in the reentrant angles of molars; from *Allophaiomys deucalion* and *Proedromys bedfordi* in having rooted molars and less cementum deposited in the reentrant angles of molars; from all *Villania* and *Borsodia* species in having a strong enamel islet developed on ACC of M_1.

Mimomys gansunicus ZHENG, 1976

PLATE 8~13

Synonymy (only concerning the studied localities)—

Cromeromys cf. *C. gansunicus*; JIN ET AL. (2000). Acta Anthropologica Sinica, 19 (3), p190.

Cromeromys gansunicus; ZHENG AND ZHANG (2000). Vertebrata PalAsiatica, 38 (1), Fig. 2.

Cromeromys gansunicus; ZHANG AND ZHENG (2001). Vertebrata PalAsiatica, 39 (1), p57, Fig. 1.

Cromeromys gansunicus; ZHENG AND ZHANG (2001). Vertebrata PalAsiatica, 39 (3), Fig. 3.

Original diagnosis— Medium size. M_1 has a broad prim fold that can reach the base of the crown and a narrow islet fold that disappears at a higher position of the crown; no islet on M_1; the positions of the sinuids high. $M^{1\sim2}$ with 2 roots. Abundant cementum in molars. (Translated from ZHENG and LI, 1986)

Emended diagnosis— Root number pattern of all molars in order of M^1, M^2, M^3, lower molars is 2 or 3, 2, 2, 2. Abundant cementum deposited in reentrant angles of molars.

Enamel islet developed on ACC of M_1, but duration short. *Mimomys*-angle on M_1 developed or vanishing. If developed, it is far away from BSA3 like a independent salient angle. M^3 with only anterior enamel islet. The Hsd and Hsld are too high for the HH-index to be measured.

Biochronological range— Nihewanian (MN17)

Studied localities and materials—

Renzidong

1 left broken maxilla with $M^{1\sim3}$ (V13990.25); 1 right broken maxilla with $M^{1\sim3}$ (V13990.26); 1 left broken maxilla with $M^{2\sim3}$ (V13990.27); 1 left broken maxilla with $M^{1\sim2}$ (V13990.28); 176 left and right M^1 (V13990.451~626); 152 left and right M^2 (V13990.627~778); 83 left and right M^3 (V13990.779~861); 4 broken left mandibles with $M_{1\sim3}$ (V13990.1~4); 4 broken left mandibles with $M_{1\sim2}$ (V13990. 5~7, 23); 1 broken left mandible with I and M_1 (V13990.8); 3 broken left mandibles with M_1 (V13990.9, 10, 16); 1 broken left mandible with I and $M_{1\sim2}$ (V13990.11); 1 broken left mandible with M_2 (V13990.12); 1 broken left mandible with I and M_2 (V13990.13); 1 broken right mandible with I and $M_{1\sim2}$ (V13990.14); 4 broken right madibles with $M_{1\sim2}$ (V13990.15, 17, 18, 24); 4 broken right mandibles with M_1 (V13990.19~22); 181 left and right M_1 (V13990.29~209); 153 left and right M_2 (V13990.210~362); 88 left and right M_3 (V13990.363~422).

Lingtai (personal number):

93001— WL15 WL15-2: 1 right M_3 (03). **WL11** WL11-7: 3 right M^3 (03~05), 1 left M_1 (01), 1 left M_2 (02); WL11-6: 1 right M^1 (04), 1 right M^2 (03), 1 left M_1 (05), 1 left M_2 (01), 1 left M_3 (02); WL11-5: 1 left M^2 (04), 2 right M^2 (02, 03), 1 right M^3 (06), 2 broken left M_1 (09, 10), 1 left M_3 (08), 1 right M_3 (07); WL11-4: 1 right M^3 (01), 1 left M_2 (02); WL11-3: 1 left M^1 (01), 1 left M^2 (02), 1 right M^2 (03), 1 right M^3 (04), 1 left M_1 (11), 2 left M_2 (08, 09), 2 left M_3 (06~07), 1 right M_3 (05); WL11-2: 1 left M^2 (02), 1 broken M^3 (01); WL11-1: 1 broken left mandible with $M_{1\sim2}$ (01). **WL10** WL10-11: 2 left M^1 (01, 02), 1 right M^2 (03), 1 left M_1 (08), 1 right M_1 (07); WL10-10: 1 left M^1 (01), 1 right M^2 (02), 1 broken left M^3 (04), 1 left M^3 (05), 1 right M^3 (03); 1 broken right M_1 (07), 1 broken left M_2 (06); WL10-8: 2 left M^1 (01, 02), 3 right M^1 (03~05), 1 left M^2 (06), 2 left M^3 (09~10), 1 broken right M^3 (08), 1 right M_1 (12), 1 left M_2 (11), 1 right M_3 (07); WL10-7: 1 right M^3 (03), 1 broken left mandible with $M_{1\sim3}$ (01), 1 left M_2 (02); WL10-6: 1 left M^1 (01); WL10-5: 1 left M_1 (01); WL10-4: 1 broken left M_1 (01), 1 broken right M_2 (02), 1 right M_3 (03); WL10-2: 1 left M^1 (05), 1 right M^3 (02), 1 left M_2 (01); WL10-1: 1 broken left M^3 (01); WL10: 1 left M^1 (08), 2 right M^1 (05~06), 2 left M^2 (01~02), 2 right M^2 (03~04), 1 broken left M_1 (09), 1 right M_1 (11), 1 left M_3 (13), 1 right M_3 (14). **WL8** WL8: 1 left M^3 (04), 2 right M^3 (02~03), 1 right

M_2 (05); WL8_1: 6 left M^1 (09~11, 13~15); 6 left M^2 (01~06), 1 right M^2 (07), 3 left M^3 (31~33), 1 broken right M^3 (30), 1 broken right mandible with $M_{1\sim2}$ (39), 1 left M_1 (37), 1 right M_1 (38), 2 broken right M_1 (34, 36), 3 left M_2 (19~21), 1 right M_2 (18), 3 left M_3 (23~25), 3 right M_3 (27~29).

72074(4)— L1-1 1 left mandible with $M_{1\sim2}$ (01).

Measurements— See Table 1.

Description—

There is plentiful cementum in all reentrant angles of the molars. The crown is obviously higher than the *Mimomys* species described above. Both walls of all the triangles are seemingly posteriorly curved on lower molars, and anteriorly curved on upper molars. The sinuous line belongs to typical *Mimomys* type and the undulation of sinuous lines is much stronger than the species described above. Usually, on lower molars, the sinuids Hsd, Hsd, and Asd are so high that they will penetrate the all crown before (all except M_3) or right after (M_3) the roots' formation, which makes the enamel bands of them interrupted at the apexes of BSA1, LSA1 and front end from the occlusal view, respectively, and on upper molars, the sinuses As, Asl and Ds act in the same way. The Enamel band tends to become thicker with wear.

M^1: The occlusal patterns of M^1 comprises four alternating triangles behind the anterior loop. The dentine field is completely separated at all the isthmuses, and all the isthmuses are completely closed. Besides the usual high positioned sinuses As, Asl and Ds, Prs is also very high and makes the enamel band interrupted at the apex of LSA2 from occlusal view. All the specimens have three roots, but the anterior two are fused together around the base of them and become separated from each other later.

M^2: There are three alternating triangles behind the anterior loop. Among all the salient angels, BSA1 looks slimmer and LSA2 more blunt than the others. The dentine field is separated at all the isthmuses. All the specimens have two roots.

M^3: The occlusal pattern of M^3 is basically composed of an anterior loop, a posterior loop and two triangles (T2 and T3) between them. There are always two reentrant angles (BRA1, 2) on buccal side and one, sometimes two (PLATE 10, Figs. 1, 6, 8, 9; PLATE 13, Figs. 2, 8, 10, 14) reentrant angles on the lingual side. Usually, salient angle can count to three on both buccal and lingual side, but sometimes a feeble pointed LSA4 can be observed (PLATE 10, Figs. 3, 7). On young individuals, BSA3 is very pointed, but it usually becomes blunt on aged individuals. LSA2 is usually robust and blunt. BSA1 is usually flat-headed on young individuals, and becomes slimmer and pointed on aged individuals. LSA2 is comparatively robust and blunt. The apex of BRA2 is distinctly posterior to that of

LRA2. An enamel island always appears on the posterior loop but doesn't lasts very long. It will be worn out around the time when the roots is formed. The formation of this island varies greatly. It can be formed by the simplification of the extra fold on lingual side of PL (PLATE 10, Figs. 11, 15, 16; PLATE 13, Figs. 13, 16) or by that of BRA2 (PLATE 10, Fig. 4). There is no enamel island developed around the anterior loop. So the is2 is nearly closed. All the specimens have two roots.

M_1: There are three alternating triangles between ACC and the posterior loop. An round-shaped enamel islet always appears on the anterior cap. It doesn't last long, and will be worn out before the roots are formed. The anterior cap is usually lingually pointed on young individuals. A extra salient angle, or the so-called *Mimomys*-angle can be observed on most specimens from Renzidong, but differing from the *Mimomys*-angle of *Mimomys teilhardi* and *Villanyia* sp. nov. that will be described below, this so-called *Mimomys*-angle is located far away from BSA3 (PLATE 8, Figs. 6~9, 11, 13~15), which makes it more like an independent salient angle than a *Mimomys*-angle. On other specimens from Renzidong, the so-called *Mimomys*-angle can not be observed. This so-called *Mimomys*-angle cannot be observed on all the specimens from 93001 and 72074(4), Lingtai. LRA4 is very strong, but it is much shallower than the other reentrant angles behind the anterior loop. BRA3 (or the so-called PF for the specimens from Renzidong that have the so-called *Mimomys*-angle) is also very strong. The apex of LRA3 extends anteriorly to the front of that of BRA2. The dentine isthmuses is1~4 are equally closed. The differentiation of the enamel band can be considered as *Mimomys*-type or negative type, because the SDQ is calculated at 141 for the specimens from Renzidong, and 144 for the specimens from Lingtai. All the specimens have two roots.

M_2: There are four alternating triangles in front of the posterior loop. T1~T2 are separated from each other and T3~T4 are semi-confluent with each other, which means that the dentine isthmuses is1~3 are nearly closed, but is 4 is not closed. Two roots.

M_3: There are four triangles in front of the posterior loop, with T1~T2 and T3~T4 are alternating with or opposite to each other, respectively. Buccal triangles are distinctly smaller that lingual ones. Two roots.

Remarks and comparison—

The species, *Mimomys gansunicus*, has been put into the Russian subgenus *Cromeromys* proposed by ZAZHIGIN (1980) from time to time, e.g. the synonyms listed above. But according to the author's personal communication with Alexey S. Tesakov (Professor of Geological Institute, RAS), the diagnosis of this subgenus should be: "Cement in molar reentrants present. Simplification of paraconid part of M_1 occurs by simple increasing

fusion of its elements in course of ontogeny. Hollow column of enamel in anterior loop absent. No simplified elements in M^3. Enamel outline of M^3 similar with that of *Dolomys milleri* NEHRING." He also mentioned that the most important in the *Cromeromys* concept is the combination of M_1 without enamel islet and the M^3 with the posterior lingual reentrant (LRA3) never closed with the formation of enamel islet. However, the enamel islet on ACC of M_1 and the posterior enamel islet on M^3 of *Mimomys gansunicus* do exist (e.g. PLATE 8, Figs 1, 6, 14~16; PLATE 10, Figs 1, 3, 5, 7~8, 12~16; PLATE 13, Figs 4, 6, 15~16). So it is not suitable to put this species into the Russian subgenus, which maybe represents a different evolutionary lineage. And the author still insists on putting this species into the genus *Mimomys* without subgeneric assignation.

The author observed the type specimen, one broken right M_1 with broken anterior cap (V4765), and found that there are no remarkable differences on the occlusal surface and the pattern of sinuous line between the type specimen and the materials studied here. But there are some slight differences in some of the specimens from Renzidong, such as an enamel islet, and a "so-called" *Mimomys*-angle on ACC of M_1. These two characters can not be observed on the type specimen, and all the M_1s from 93001 and 72074(4) of Lingtai. But the author still insists on assigning the materials from Renzidong to this species, because not all the specimens have these characters. Maybe *Mimomys gansunicus* from Renzidong is a little more primitive than that from Lingtai, and than the type.

Mimomys gansunicus mainly differs from the *Borsoida* and *Villanyia* sepcies, *Mimomys bilikeensis*, and *M. teilhardi* in having cementum deposited in the reentrant angles of molars; from *Mimomys orientalis* in much stronger undulation of sinuous line; from *Allophaiomys deucalion*, *Omniprocessimys parallelus* gen. et sp. nov. and *Proedromys bedfordi* in rooted molars; from *Omniprocessimys peii* in having normal *Mimomys* type of sinuous line pattern.

Genus *Allophaiomys* KORMOS, 1932

Type species— *Allophaiomys pliocaenicus* KORMOS, 1932

Diagnosis— Molars rootless. Abundant cementum deposited in the reentrant angles of all molars. ACC of M_1 trefoiled, with T4, T5 and AC confluent with each other. AC lingually skewed. M^3 lacking a fully developed T4.

Remarks— According to REPENNING (1992), the oldest records of *Allophaiomys* in western Europe appeared to be at the base of the Olduvai event and may be slightly older in the Black Sea area, where the oldest *Allophaiomys* appeared to be pre-Olduvai. And by faunal approximation, the type locality, Betfia-2, Hungary, was presumed to be about as

old as the end of the Olduvai event, or at the Pliocene-Pleistocene boundary. He also stated that the oldest record of *Allophaiomys* in North America was possibly during the oldest part of the Olduvai event or just before it. Furthermore, he also mentioned that the oldest dated records of *Allophaiomys* were from Zone IV deposits of China, but his conclusion was based on ZHENG AND LI (1990). Apparently, the paleomagnetic correlation of the zones proposed by ZHENG AND LI (1990) was, in fact, not based on magnetostratigraphic study, but faunal correlation, so they were, in fact, not dated. Besides, ERBAJEVA (1998) also mentioned that the extinct genus *Allophaiomys* was an important component of Early Pleistocene small mammalian faunas of Eurasia and North America. As for the origin of this genus, few researchers have talked through it up to now. Here based on our study, it is believed that the genus *Allophaiomys* probably stemmed out from one of the *Mimomys* species, *Mimomys gansunicus*, during Early Pleistocene, which is going to be discussed in detail in the following texts.

Allophaiomys deucalion KRETZOI, 1969

PLATE 25~26

Synonymy (only concerning the studied localities)—

Allophaiomys terrae-rubrae; ZHENG AND ZHANG (2000). Vertebrata PalAsiatica, 38 (1), Fig. 2.

Allophaiomys terrae-rubrae, *Allopahiomys pliocaenicus*; ZHENG AND ZHANG (2001). Vertebrata PalAsiatica, 39 (3), Fig. 3.

Diagnosis— Rootless. Abundant cementum deposited in reentrant angles of molars. No enamel islet and *Mimomys*-angle developed on M_1. M^3 with LRA3 strongly develop.

Biochronological range— MQ1

Studied localities and materials—

Xiaochangliang

Culture Layer 3 left M^1 (V15325.1~3), 4 right M^1 (V15325.4~7), 3 left M^2 (V15325.8~10), 6 right M^2 (V15325.11~16), 6 left M^3 (V15325.17~22), 5 right M^3 (V15325.23~27), 4 left M_1 (V15325.28~31), 8 right M_1 (V15325.32~39), 8 left M_2 (V15325.40~47), 7 right M_2 (V15325.48~54), 4 left M_3 (V15325.55~58), 3 right M_3 (V15325.59~61).

Lingtai (personal number)

93001— WL6 1 broken left M_1 (03), 1 left M_3 (01), 1 right M_3 (02). **WL5** 1 right M^1 (05), 1 broken M^2 (02), 1 left M^3 (03), 1 broken left mandible with $M_{1\sim2}$ (08), 1 broken left M_2 (06). **WL4** 1 broken left M_1 (05), 1 right M_1 (06), 1 broken right M_3 (02). **WL3** 1 right

M_1 (08), 1 broken left M_2 (01), 1 left M_2 (05), 1 right M_3 (04). **WL7+** 1 broken right M^3 (01). **WL5+** 2 broken left M^3 (11~12), 1 left M^3 (13), 1 left M_1 (14), 1 broken right M_1 (15), 1 right M_1 (16), 1 broken left M_3 (05), 1 broken right M_3 (02). **WL2+** 1 left M^3 (02), 1 broken left M_1 (03).

Measurements— See Table 1.

Description—

The molars are rootless. There is abundant cement in the reentrant angles of the molars but little or lacking in those of fresh teeth. On upper molars, both the anterior and posterior walls of the reentrant angles are convex anteriorly, but the posterior walls are more convex, which makes the apex of the reentrant angels tend to extend posteriorly; on the contrary, on the lower molars, the situation is reversed, which means that both the anterior and posterior walls of the reentrant angles are convex posteriorly, and the posterior walls are more convex, which makes the apexes of the reentrant angles tend to extend anteriorly. On the occlusal surface, the enamel band is usually interrupted at the apexes of LSA1, BSA1 and, as common in arvicolid species, at posterior edge on upper molars, while on the contrary anterior edge on lower molars.

M^1: There are four interlaced triangles behind the anterior loop. The buccal reentrant angles extend deeper lingually than the lingual ones do. On the occlusal surface, the enamel band is also interrupted at the apex of LSA2, which makes the apex of it more obtuse than that of others, whereas on one less worn specimen, it is continuous at the apexes of LSA1 and BSA1. The dentine isthmuses are closed comparatively tightly.

M^2: There are three interlaced triangles behind the anterior loop. Isthmuses are closed tightly. BSA1 is slimmer and more acute while LSA1 is more obtuse than the other salient angles.

M^3: This tooth shows more variation than the others. Basically, there are three triangles behind the anterior loop. Among these three interlaced triangles, T3 is the robustest, and T4 is the feeblest. LSA3 is usually obtuse, while BSA2 and BSA3 are acute. is2 and is3 are usually closed, but the closeness of is4 shows some variation. On 4 out of 11 specimens, it is completely closed, and the apex of LRA3 is a little more posteriorly situated than that of BRA2; on 5 of them LRA3 is quite weak and is4 is nearly open. On 3 specimens, the rudiment of t5 can be observed. On one specimen, another tiny salient angle posterior to t4 can be observed.

M_1: Between the anteroconid complex and the posterior loop, there are three interlaced triangles. The triangles on the labial side are more or less robuster than those on the lingual side. is1~4 are closed tightly. The apex of LRA3 is usually situated in front of that of

BRA2, except on one specimen, they are opposite to each other and make the is4 closed. But there is still some distance for between the apex of LRA3 and the enamel wall of BRA3 for the closeness of is5 on the anteroconid complex, so t4, t5 and the anterior cap on it are confluent with each other. LRA4 and BRA3 are usually shallow and the apexes of them are not acute as those of the other reentrant angles, but smoothly obtuse. On one specimen of a very fresh tooth still with the extra folds in the front of the anterior cap, an enamel island can be observed but it is very shallow, and will be disappear soon because of wear.

M_2: In front of the posterior loop, there are 4 interlaced triangles, the lingual ones of which are more or less stronger than those of labial ones. is1~3 are closed. The apex of the BRA2 doesn't reach the anterior wall of BSA3, is4 is open.

M_3: In front of the posterior loop, there are 4 nearly oppositely displaced triangles, the lingual ones of which are distinctly robuster than those of the labial ones. T1 is anterolabially confluent with T3. And T3, t4 are completely confluent. T4 is rather weak and on one specimen it is nearly completely reduced.

Remarks and comparison—

Allophaiomys KORMOS, 1933 probably represents the ancestral genus of living *Microtus*. As the oldest species of this genus, *A. deucalion* (KRETZOI, 1969) was quantitatively defined by VAN DER MEULEN (1974) based on the type population from Villány-5 to distinguish it from *A. pliocaenicus* KORMOS, 1932 due to the gradually changed morphologies. VAN DER MEULEN (1974) proposed three parameters, A/L, B/W and C/W to distinct these two species. According to his definition, the quantitative characteristics of *A. deucalion* are: A/L<42; B/W≥33.0; C/W≥20.0. The author measured the specimen assigned to this species here, the results are as follows: A/L=42.85 (N=4); B/W=37.7 (N=8); C/W=22.8 (N=8). Even though the A/L exceeds the range of definition a little, it is maybe because of the deficiency of specimens. So the author insists the assignation due to following arguments: 1), B/W and C/W, especially the former (a distinctive character of *A. deucalion*) matches the definition very well; 2), according to the description by *van der Meulen* (1974), the weak development of LRA3 on M3 of *A. deucalion* here (5 out of 11 specimens) also reinforced the assignation.

***Omniprocessimys* gen. nov.**

Type species— *Omniprocessimys parallelus* gen. et sp. nov.

Diagnosis— Molars rooted in early forms, but lost in later forms. Cementum plentifully deposited in the reentrant angles of molars. All the sinuses (sinuids) ascend high. *Mimomys*-angle strong. Anterior cap of M_1 necked and usually round-shaped. The enamel

islet on ACC of M_1 only appears in early forms. Only a posterior enamel islet developed on M^3.

Differential Diagnosis— All the sinuses (sinuids) ascend high, which distinguishes this genus from all the other arvicolid genus and other species of *Mimomys*.

Etymology— The latin root "Omni" means each; "processi" means advance; "Omniprocessi" means that all the sinuses (sinuids) ascend very high simultaneously.

Included species— *O. banchiaonicus* (ZHENG ET AL., 1975), *O. peii* (ZHENG, 1986), *O. parallelus* gen. et sp. nov.

Remarks— This is probably a special domestic group that only existed in North China.

***Omniprocessimys parallelus* sp. nov.**

PLATE 14~16

Synonymy—

Mimomys cf. *M. peii*; JIN ET AL. (2000). Acta Anthropologica Sinica, 19 (3), 190.

Holotype— 1 broken left mandible with $M_{1\sim3}$ (VXXXXX)

Type Locality— Renzidong

Etymology— "parallelus" is a adjective latin word that means parallel. It means all the sinuses on M_1 of this species are parallel to each other.

Diagnosis— Rootless. Abundant cementum deposited in reentrant angles of molars. No enamel islet developed on ACC of M_1. *Mimomys*-angle on M_1 strong. M^3 with only posterior enamel islet.

Hypodigm— Renzidong: 1 broken maxilla with M1~2 (VXXXXX.4), 64 left and right M^1 (VXXXXX.164~227), 60 left and right M^2 (VXXXXX.228~287), 34 left and right M^3 (VXXXXX.288~321), 1 broken left mandible with $M_{1\sim3}$ (VXXXXX.2), 1 broken right mandible with $M_{2\sim3}$ (VXXXXX.1), 1 broken right mandible with $M_{1\sim2}$ (VXXXXX.3), 74 left and right M_1 (VXXXXX.5~78), 42 left and right M_2 (VXXXXX.79~120), 43 left and right M_3 (VXXXXX.121~163).

Biochronological range— Nihewanian (MN17)

Measurements— See Table 1.

Description—

The crown is high. There is abundant cementum in reentrant angles of the molars. All the molars don't have roots. Differing from the typical *Mimomys*-type of sinuous line, all the sinuses on lower molars and sinuids on upper molars go up very so high along the ridges of all the salient angles and the anterior ends of lower molars or the posterior ends of upper molars that they penetrate the whole crown height and make the enamel band

interrupted at the apex of each salent angle on both lower and upper molars. Both walls of all the triangles are seemingly posteriorly curved on lower molars, and anteriorly curved on upper molars. Enamel band tends to become thicker with wear.

M^1: The occlusal patterns of M^1 comprises four alternating triangles behind the anterior loop. The dentine field is completely separated at all the isthmuses, which menas all the dentine isthmuses are nearly closed.

M^2: There are three alternating triangles behind the anterior loop. Among all the salient angels, BSA1 looks slimmer than the others. The dentine field is equally separated at all the dentine isthmuses.

M^3: The occlusal pattern of M^3 is basically composed of an anterior loop, a posterior loop and two (e.g. PLATE 16, Figs 1~2, 7 and so on) or three (e.g. PLATE 16, Figs 5~6, 15) triangles between them. There are usually three (e.g. PLATE 16, Fig. 2) and sometimes three (e.g. PLATE 16, Figs. 5, 15) reentrant angles on buccal side and usually two on lingual side. Salient angle can usually count to three on buccal and lingual side, but sometimes four (e.g. PLATE 16, Figs. 5, 7, 15) on lingual side. LSA2 is usually robust and blunt. BSA1 is usually slimmer. The apex of BRA2 extends far posteriorly from that of LRA2 and opposite to that of LRA3 if it appears (PLATE 16, Figs. 10, 16). Sometimes if LRA3 appears, the apex of it extends to the back of that of BRA2 (PLATE 16, Fig. 15). An enamel island always appears on the posterior loop, which is usually formed by the simplification of LRA3 if it appears . But it doesn't last long. The posterior enamel island never appears around the anterior loop. The dentine isthmuses is2~3 are usually closed.

M_1: There are three alternating triangles between ACC and the posterior loop. No enamel islet appears on the anterior cap. The anterior cap is usually round-shaped. The apexes of BRA3 and LRA4 are usually opposite or obliquely opposite to each other forming a closed or open neck, which separates AC from the other part of ACC. Occasionally, LRA4 is located in front of LRA4 , which leads to a 7-shaped AC (PLATE 14, Fig. 14). *Mimomys*-angle is strongly developed, located close to BSA3, and lasts a lifetime. The apex of LRA3 is in front of that of BRA2. The dentine isthmuses is1~4 are all equally closed. The differentiation of the enamel band can be considered as typical *Mimomys*-type or negative type, because the SDQ is calculated at 124.

M_2: There are four alternating triangles in front of the posterior loop. T1~T2 and T3~T4 are semi-confluent with each other, respectively, which means that the apexes of BRA1, 2 are anterior to that of LRA1, 3, respectively and the dentine isthmuses is2, 4 are distinctly wider that is1, 3. On aged individuals, the enamel band of the anterior wall of T4 completely diminished.

M_3: There are four triangles in front of the posterior loop, with T1 and T2 alternating with each other, T3 and T4 alternating with (young individuals) or opposite to (aged individuals) each other. Buccal triangles are distinctly smaller that lingual ones. Triangles T1, T2 are semi-confluent, and T3, T4 are semi-confluent or confluent. T4 is distinctly feeble compared with the other triangles. On aged individuals, the enamel band of the anterior walls of T3 and T4 completely diminished.

Remarks and comparison—

Among the three species assigned to this new genus, this new form is the most advanced form, which can be indicated by: rootless molars; loss of the enamel islet on ACC of M_1, and much stronger undulation of sinuous lines. The other species, *Omniprocessimys peii* and *O. banchiaonicus* both have rooted molars (PLATE 30, Fig 15; PLATE 31). According to the description of ZHENG AND LI (1986), on a young individual of *Omniprocessimys peii*, a broken right M_1 with only the anterior half preserved (V8113), a enamel islet can be observed on ACC. But this enamel islet can not be observed even on the juvenile specimens of the new form.

Genus *Villanyia* KRETZOI, 1956

Type species— *Villanyia exilis* KRETZOI, 1956

Diagnosis— Rooted vole with cementless molars; M^1 with three roots; M^2 with three roots in primitive species, but with two roots in advanced species; M^3 with one or two enamel islands, of which the anterior on tends to be reduced in advanced species; posterior loop of M^3 short and broad; M_1 with enamel island; *Mimomys* angle usually present; enamel band differentiation quotient (SDQ) close to or more than 100; posterior root of M_2 sits on the incisor in primitive species, but slides to its buccal side in advanced species.

Included species— *Villanyia petenyii* (MEHELY, 1914) including "*Mimomys praehungaricus* SCHEVTSCHENKO, 1965" and "*Mimomys tanatica* SCHEVTSCHENKO, 1965"; *Villanyia eleonorae* ERBAJEVA, 1976; *Villanyia novoasovica* (TOPACHEVSKY AND SCORIK, 1977); *Villanyia stklovi* ZAZHIGIN, 1980; *Villanyia betekensis* ZAZHIGIN, 1980; *Villanyia hengduanshanensis* (ZONG, 1987); *Villanyia fanchangensis* ZHANG ET AL. (in press).

Remarks— The distinction between *Villanyia* KRETZOI, 1956 and *Borsodia* JÁNOSSY AND VAN DER MEULEN, 1975 has been obscure, because several related species have been put back and forth between the two genera by several authors (GROMOV AND POLYAKOV, 1977; ZAZHIGIN, 1980; TESAKOV, 1993; KOWALSKI, 2001). When JÁNOSSY and VAN DER MEULEN (1975) proposed *Borsodia* as a subgenus of *Mimomys*, they gave out the diagnosis of the

subgenus as follows: A group of *Mimomys* species with molars which lack crown-cementum and in which the enamel at the occlusal surface is thicker at the anterior side of the triangles in the lower molars and thicker at the posterior sides in the upper molars. From this definition we can see that the genus *Borsodia* has its own distinctive morphological features and this definition should be followed when we refer species to this genus. And *Villanyia* should represent a different genus, of which some species probably gave rise to *Borsodia* (TESAKOV, 1993). So, the authors of the present paper think it's necessary to divide the two genera clearly based on the differential diagnosis given above, because they have distinct morphological features and represent different evolutionary stages. The included species of *Villanyia* is based on our emended diagnosis and the descriptions or revisions given by GROMOV AND POLYAKOV (1977), ZAZHIGIN 1980), KOWALSKI (2001), JÁNOSSY AND VAN DER MUELEN (1975), TESAKOV (1993). Other related species, such as "*Villanyia klochnevi*" ERBAJEVA, 1998 etc., are re-referred to *Bosodia* (see the discussion later).

Villanyia sp. nov.

PLATE 17

Synonymy—

Mimomys teilhardi LI, 2006; LI (2006). Doctoral Dissertation of CAS, p. 52. (in part)

Diagnosis— Root number pattern of all molars in order of M^1, M^2, M^3, lower molars is 3, 3, 2, 2. No dental cementum deposited in reentrant angles of molars. M^3 with two enamel islands developed. No enamel islet developed on ACC of M_1. *Mimomys*-angle strong.

Biochronological range— Early Gaozhuangian of DENG, 2006.

Studied locality and materials—

Gaotege

29 M_1— DB02-1 (15) VXXX19.153, 163, 164, 168, 170, 175, 185~187, 190, 195, 198, 202, 204. **DB02-2 (4)** VXXX19. 318, 391, 398, 402. **DB02-3 (6)** VXXX19.531, 533, 536, 542, 544, 546. **DB02-4 (2)** VXXX19.634, 635. **DB02-6 (1)** VXXX19.663. **DB03-1 (2)** VXXX19.691, 693.

Measurements— See Table 1.

Description—

There is no cementum in reentrant angles of the molars. Both walls of all the triangles go straight and don't curve. Root formation is early. The undulation of the sinuous lines is little stronger than that of *Mimomys teilhardi*, and of course, *Mimomys bilikeensis*.

M_1: There are three alternating triangles between ACC and the posterior loop. There is no

enamel islet developed around the anterior cap. The anterior cap is generally round- or subround-shaped. The apexes of BRA3 and LRA4 are usually obliquely opposite to each other developing a neck that is usually open for the anterior cap. *Mimomys*-angle is usually developed and located close to BSA3. Occasionally, *Mimomys*-angle can not be observed on some specimens (e.g. PLATE 17, Fig. 6). The apex of LRA3 is obliquely opposite to that of BRA2. The dentine isthmus is2 is distinctly wider than is1, 3. The enamel band can be considered as *Mimomys*-type or negative type, because the SDQ is calculated at 112. Two roots.

Remarks and comparison—

This is the most primitive *Villanyia* species in North China. As stated before, it comes from the same layers of Gaotege section as *Mimomys teilhardi*, and except on M_1, there are no noticeable differences that can distinguish the two species from each other on the other molars. On M_1, it apparently differs from *Mimomys teilharid* in clearly greater HH-index and in having no enamel islet developed on ACC. Here the species name is left blank for future consideration.

Villanyia fanchangensis ZHANG ET AL. (in press)

PLATE 18~20

Synonymy—

Borsodia sp.; JIN ET AL. (2000). Acta Anthropologica Sinica, 19 (3), p. 190.

Diagnosis— Medium-sized species with three roots in M^1 and two roots in M^2 and M^3; M^1 and M^2 without "lagurine" structure; M^3 with two enamel islands, two or three salient angles and one or two re-entrant angles on the lingual side, two or three salient angles and re-entrant angles on its buccal side, anterior loop broadly confluent with T2, isthmus between T2 and T3 narrow or closed; anterior cap of M_1 simple in shape, isthmus between the anterior cap and T5 showing a clear constriction, anteroconid complex of M_1 having neither enamel island, islet fold, *Mimomys* angle nor prism fold, T4 and T5 of M_1 broadly confluent with each other; in M_2 and M_3, T1 and T3 broadly confluent with T2 and T4 respectively; both roots of M_2 slides to the buccal side of the incisor; both roots of M_3 sits on the incisor.

Type locality— Renzidong

Biochronological range— Nihewanian (MN17)

Studied locality and available materials

Renzidong

1 left mandible with I and $M_{1\sim3}$ (V13991); 1 premaxilla-maxilla with left incisor and M^1, and with right incisor, M^1 and M^2 (V13991.8); 213 isolated M^1 (V13991.825~V13991.1037); 189 isolated M^2 (V13991.1038~V13991.1226); 133 isolated M^3 (V13991.1227~V13991.1359); 3 right mandibles with I and $M_{1\sim3}$ (V13991.1~V13991.3); 2 right mandibles with $M_{1\sim3}$ (V13991.4, 13991.5); 1 left mandible with $M_{1\sim2}$ (V13991.7); 1 right mandible with M_1 (V13991.6); 461 isolated M_1 (V13991.9~V13991.469); 261 isolated M_2 (V13991.470~V13991.730); 94 isolated M_3 (V13991.731~V13991.824).

Measurements— See Table 1.

Description—

Small-sized. There is no cementum in reentrant angles of the molars. The sinuous line belongs to the typical *Mimomys*-type. Usually, on lower molars, the sinuids Hsd, Hsd, and Asd are so high that they will penetrate the all crown before (all except M_3) or right after (M_3) the roots' formation, which makes the enamel bands of them interrupted at the apexes of BSA1, LSA1 and front end from the occlusal view, respectively, and on upper molars, the sinuses As, Asl and Ds act in the same way. Both walls of all the triangles go straight and don't curve. The Enamel band tends to become thicker with wear.

Premaxilla-maxilla and upper incisor: This part is preserved only in one specimen (V13991.8). The incisive foramen is slender, 4.2mm in length and about 0.5mm in width. It terminates anteriorly at the position about 1.9mm behind the posterior margin of the alveolus of the upper incisor. The posterior end of the foramen is situated slightly anterior to the anterior margin of the alveolus of M^1 (about 0.5mm). The upper incisor is broadly triangular in cross section, and has no groove on its enamel surface.

M^1 and M^2: The occlusal patterns of M^1 and M^2 comprise four and three alternating triangles behind each anterior loop respectively. LRA2 is normal in shape, and shows the same feature as the other re-entrant folds. The "lagurine" structure is not observed there. In young individuals, the anterior wall of T3 is nearly parallel to the posterior wall of T2, so that T3 and T2 make a parallelogram totally (PLATE 19, Figs. 8, 13). In older individuals, however, such a feature is not observed. The lingual re-entrant angles are nearly as deep as the buccal ones. In M^1, the sinuous line also ascends high on the lingual side along the ridge of LSA2.

M^3: The pattern of M^3 shows more conspicuous variation than those of M^1 and M^2. It comprises two alternating triangles (T2 and T3) between the anterior and posterior loops.

The anterior loop has an enamel island except in young and aged individuals. In young individuals, BRA1 deeply penetrates lingually into the central part of the crown (PLATE

20, Figs. 1, 2, 5). The lingual part of BRA1 becomes the island by the advance of wear, where its buccal part remains as a shallow fold (PLATE 20, Figs. 8, 9). Moreover in aged individuals, the island disappears, so that the anterior loop is broadly confluent with T2 (PLATE 20, Figs. 4, 10, 14, 16). BRA1 is also shallow in these individuals. The anterior wall of the anterior loop is slightly concave. LSA2 is more robust than and not as acute as BSA1. BRA2 is much shallower than LRA2, but developed. The isthmus between T2 and T3 is narrow or closed. T3 and the posterior loop are confluent with each other, and form a large dentine field that accommodates the posterior enamel island. This island is formed by the isolation of the lingual part of BRA3, as observed in a very young individual (PLATE 20, Fig. 2). The island disappears by wear in very old individuals (PLATE 20, Figs. 14, 16), where the island in the anterior loop was already extinguished. Thus no island is seen in these individuals. LSA3 is well developed, but LRA3 is shallow and indistinct. BSA3 is well developed in 66% of the examined specimens, but it is indistinct or absent in the remaining specimens. BRA3 is sometimes observed, but shallow.

Mandible and lower incisor: The mental foramen is small, and situated somewhat anterior to the front margin of M_1. The lower masseteric crest is stout, and originates from the position about 0.5 mm posterodorsally to the mental foramen. The crest is slightly convex ventrally, and extends to the lower margin of the angular process. The upper masseteric crest runs parallel to the anterior edge of the ascending ramus, and connects to the lower messteric crest by an acute angle. The anterior edge of the ascending ramus originates from the position beside the posterior loop of M_1. The internal temporal fossa between the ramus and the alveoli of the molars is broad a shallow, and elongates anteroposteriorly. The lower incisor with a triangular section passes on the lingual sides of the roots of M_1 and M_2, while it is overlain by the roots of M_3.

M_1: The occlusal pattern of M_1 comprises five triangles between the anterior cap and posterior loop. The anterior cap is simple, shows a round or elliptical shape, and is relatively short anteroposteriorly. It has no enamel island. The buccal wall of the anterior cap is smooth in almost all the specimens, but weak BSA4 is observed in few specimens (about 1.3% of the examined specimens; PLATE 18, Fig. 5). LRA4 and BRA3 are generally well developed, but shallower than the other lingual and buccal re-entrant angles respectively. In few specimens, however, LRA4 and BSA3 are weak or absent (PLATE 18, Fig. 10). The isthmus between the anterior cap and T5 is broad, but shows a clear constriction in the anteroconid complex. T5 and T4 is opposite in position and completely confluent with each other to form a single dentine field which elongates obliquely to the transverse axis of the crown. The anterior wall of T4 has no *Mimomys*-angle in almost all

the specimens, but a feeble salient angle, possibly a degenerate *Mimomys*-angle, is observed in few specimens (about 1.3%; PLATE 18, Fig. 20). The isthmus between T4 and T3 is narrow or closed. T3, T2 and T1 are alternate in position. The isthmus between T3 and T2 is narrow, while that between T2 and T1 are broad, and these triangles are generally confluent with each other. The isthmus between T1 and the posterior loop is generally closed. The axes of LRA3, LRA2 and LRA1 are nearly parallel to the transverse axis of the crown, while those of BRA2 and BRA1 are generally oblique to the axis. The posterior margin of the posterior loop is slightly convex posteriorly.

M_2 and M_3: The occlusal patterns of these molars comprise three dentine fields. T4 and T3 are opposite in position, and completely confluent with each other to form the lozenge-shaped anterior field. T2 and T1 are also opposite, and confluent to form the middle field with a more transversely elongated lozenge-shape. The isthmuses between the anterior and middle fields and that between the middle field and posterior loop are closed. The lingual re-entrant angles are deeper than the buccal ones. The axes of the lingual and buccal re-entrant angles are nearly parallel to the transverse axis of the crown.

Remarks and comparison—

On the basis of the descriptions and figures given by KOWALSKI (1960), GROMOV AND POLYAKOV (1977) and ZAZHIGIN (1980), *Villanyia exilis* differs from new species by the enamel differentiation and morphology of M^3, M_1 and M_2. The anterior enamel island of M^3 is mostly absent and possibly disappears earlier in *Villanyia exilis*. The *Mimomys*-angle is usually present and the isthmus between the anterior cap and T5 is less constricted in *Villanyia exilis*. T1 and T2 are alternating and separated from each other in M_2 of *Villanyia exilis*.

The description and figure of *Villanyia petenyii* given by ZAZHIGIN (1980) show clear differences from the present specimens. In *Villanyia petenyii*, M^3 has only one islet (posterior enamel islet), and M_1 has the *Mimomys*-angle. Furthermore, the posterior root of M_2 stands on the incisor in *Villanyia petenyii*.

Villanyia eleonorae differs from the new species by having in some M^2 three roots, and only posterior enamel islet in M^3. The *Mimomys*-angle of M_1 is usually present, and the isthmus between the anterior cap and T5 is less constricted in *Villanyia eleonorae* than in *Villanyia fanchangensis*.

The isthmus between T1 and T2 is closed in M_2 of *Villanyia eleonorae*. *Villanyia steklovi* differs from *Villanyia fanchangensis* by having in M^2 three roots and by its posterior root of M_2 which stands on the incisor. *Villanyia beketensis* differs from by having only the posterior enamel island in M^3 (ZAZHIGIN, 1980).

Villanyia novoasovica and *V. hengduanshanensis* differ from the present specimens in having the *Mimomys*-angle in M_1 (ZONG, 1987; TESAKOV, 1993).

ERBAJEVA (1998) mentioned a transitional form *Borsodia klochnevi* (=*Villanyia klochnevi*, this species has been referred to *Borsodia* by ZHANG ET AL., in press) between *Villanyia eleonorae* and *Borsodia chinensis laguriformes*. But based on our study here, the transition from *Villanyia* to *Borsodia* can not be concluded. On the contrary, they probably represent two concurrent lineages during Pliocene ~ Early Pleistocene of North China.

Villanyia cf. *V. fanchangensis* ZHANG ET AL. (in press)

PLATE 21~22

Synonymy—

Borsodia n. sp. ; ZHENG AND ZHANG (2000). Vertebrata PalAsiatica, 38 (1), Fig. 2. (in part)

Borsodia n. sp. and *Hyperacrius yenshanensis*; ZHENG AND ZHANG (2001). Vertebrata PalAsiatica, 39 (3), Fig. 3. (in part)

Studied locality and materials—

Lingtai (personal number):

93001— WL11 WL11-7: 1 left M^2 (10), 1 broken M^3 (01), 1 broken right M_1 (05), 1 left M_2 (09), 1 right M_2 (08), 1 left M_3 (02), 2 right M_3 (04, 06); WL11-6: 1 left M^1 (01); WL11-5: 1 left M^1 (02), 1 broken right M^2 (03), 1 broken left M^3 (04), 1 broken left M_1 (08), 2 right M_2 (06~07), 1 left M_3 (05); WL11-4: 1 right M^1 (03), 2 right M^2 (01~02), 1 left M_3 (04); WL11-3: 1 left M^2 (02), 1 right M^2 (03), 1 left M_1 (07), 1 left M_2 (08), 1 left M_3 (09), 1 right M_3 (11); WL11-2: 1 left M_3 (01). **WL10** WL10-11: 1 left M^1 (06), 1 right M^2 (05), 1 right M^3 (04), 1 left M_3 (02), 1 right M_3 (01); WL10-10: 1 broken left M^3 (02), 1 broken right M_3 (01); WL10-8: 1 left M^1 (01), 1 right M^1 (02), 1 left M^3 (05), 1 right M^3 (03), 1 left M_1 (10), 1 left M_2 (11), 1 right M_2 (08), 1 left M_3 (06); WL10-7: 1 broken left M_1 (01); WL10-6: 1 broken right M^1 (02), 1 right M^2 (01); WL10-5: 1 left M^2 (01); WL10-4: 1 left M_1 (01); WL10-2: 1 broken left M_1 (03), 1 right M_1 (04), 1 left M_2 (01), 1 right M_3 (02); WL10: 2 left M^1 (03~04), 1 right M^1 (05), 1 right M^2 (06), 1 broken right M^3 (01), 1 right M^3 (02), 1 left M^3 (08). **WL8** 1 left M^1 (07), 1 right M^2 (06), 2 left M^3 (01~02), 1 right M^3 (04), 1 broken right M_1 (08), 1 broken right M_2 (11), 1 right M_2 (12). **WL7** WL7-1: 1 left M_3 (01).

Measurements— See Table 1.

Description—

Small-sized. There is no cementum in reentrant angles of the molars. The sinuous line belongs to the typical *Mimomys*-type. Usually, on lower molars, the sinuids Hsd, Hsd, and

Asd are so high that they will penetrate the whole crown before (all except M_3) or right after (M_3) the roots' formation, which makes the enamel bands of them interrupted at the apexes of BSA1, LSA1 and front end from the occlusal view, respectively, and on upper molars, the sinuses As, Asl and Ds act in the same way. Both walls of all the triangles are seemingly posteriorly curved on lower molars, and anteriorly curved on upper molars.

M^1: The occlusal patterns of M^1 comprises four alternating triangles behind the anterior loop. On juvenile specimens, the anterior wall of LRA2 is seemingly parallel to the posterior wall of BRA2; and the posterior end of the tooth is pointed posteriorly. On mature and aged individuals, the the parallel walls of reentrant angles sometimes turns to normal occlusal pattern and the dentine field becomes almost separated at all the isthmuses (PLATE 22, Figs. 11~12), but sometimes they keep parallel to each other and the dentine field is separated only at is1, and semi-confluent at is2~4 (PLATE 22, Fig. 9). All the specimens have three roots, but the anterior two roots are fused together around the base of the roots, and will divide later.

M^2: There are three alternating triangles behind the anterior loop. Among all the salient angels, BSA1 looks slimmer than the others. On some specimens, the anterior wall of AL is sometimes concave on its buccal side; the anterior wall of BRA2 is seemingly parallel to the posterior wall of LRA2, which causes the dentine field to be semi-confluent at is3 (PLATE 22, Figs. 15~16). On the other, the dentine field is equally but not completely separated at is2~4. All the specimens have two roots.

M^3: The occlusal pattern of M^3 is basically composed of an anterior loop, a posterior loop and two or three salient angles between them. There are always two reentrant angles on buccal side and one, occasionally two (PLATE 21, Fig. 16), on lingual side. Salient angle can count to three on both buccal and lingual side. LSA2 is usually robust and blunt. BSA1 is usually slimmer. The apex of BRA2 is nearly opposite to that of LRA2. On some juvenile specimens, the anterior wall is concave. An enamel island can be observed around the posterior loop on four specimens (PLATE 21, Figs. 9, 11, 12, 15). On the other specimens, the enamel islet can not be observed, it possibly has been worn out. view. The anterior enamel island around the anterior loop can only be observed on two specimens (PLATE 21, Figs. 11~12). On these two specimens, the anterior enamel islet is formed by the simplification of BRA1, which extends deep inwards close to the anterior wall of LRA2 when the individuals are young, and makes dentine field of AL is separate from that of T2. This situation will change when the individuals are getting old, when the former apex part of BRA1 is isolated and forms the anterior enamel island, and the new apex withdraws outwards a little. At the same time, BRA1 becomes shallower and AL becomes confluent

with T2 with the enamel island in the middle though. Even though, the anterior enamel island forms later than the posterior one, it usually doesn't last long and disappears earlier. All the specimens have two roots.

M_1: There are three alternating triangles between ACC and the posterior loop. No enamel islet appears on the anterior cap. The anterior cap is generally round-shaped with a normally open neck formed by LRA4 and BRA3 obliquely opposite to each other. *Mimomys*-angle is not developed. T4 and T5 are also obliquely opposite and wide open to each other. The apex of LRA3 is obliquely opposite to that of BRA2. The comparatively more open dentine isthmus is2 than is1, 3 can be observed on Plate 21, Figs. 2~3, 7. The differentiation of the enamel band can be considered as *Mimomys*-type or negative type, because the SDQ is calculated at 122. Two roots.

M_2: There are four alternating triangles in front of the posterior loop. T1~T2 and T3~T4 are slightly semi-confluent or completely confluent with each other, respectively, which means that the apexes of BRA1, 2 are slightly anterior or opposite to that of LRA1, 3, respectively and the dentine isthmuses is2, 4 are open, while is1, 3 are closed. Two roots.

M_3: There are four triangles in front of the posterior loop, with T1~T2 and T3~T4 opposite to and confluent with each other. Buccal triangles are smaller than lingual ones. On young specimens, the apex of T3 tilts anteriorly sometimes, and the enamel band becomes distinctly thinner at the front end of the tooth. Two roots.

Remarks and comparison—

Here our referral is mainly on account of: no cementum on most of the specimens (Plate 21, Fig 2 has cementum but it represents a aged individual); the apexes of LRA3 and BRA2 on M_1 are opposite to each other; T4 and T5 of M_1 are complete confluent; no *Mimomys*-angle can be observed on any of the M_1s; the existence of two enamel islets on M^3 can be indicated at least on two specimens (PLATE 21, Figs 11~12), and even though on those specimens that have no enamel islets, similar morphotypes in *Villanyia fanchangensis* can still be found (PLATE 21, Fig 10 — PLATE 20, Fig 16; PLATE 21, Fig 16 — PLATE 20, Fig 12; and so on).

Villanyia sp. 1

PLATE 23, Figs. 1~7

Synonymy—

Mimomys cf. *M. orientalis*; Li (2006). Doctoral Dissertation of CAS, p57. (in part)

Studied locality and materials

Gaotege (personal number):

DB03-2 LI (2006): 3 left M^2 (14~15, 43), 2 left M^3 (44, 47); LI 2007.05: 1 left M_1 (01), 1 broken right M_1 (13).

Measurements— See Table 1.

Description—

There is no cementum in reentrant angles of the molars. The sinuous line belongs to the typical *Mimomys*-type. And the undulation is stronger than that of *Mimomys teilhardi*, *Villanyia* sp. nov., and of course, *Mimomys bilikeensis*, but weaker than that of *Mimomys* cf. *M. orientalis* and other advanced species. Usually, on lower molars, the sinuids Hsd, Hsd, and Asd ascend high, and on upper molars, the sinuses As, Asl and Ds act in the same way.

M^2: There are three alternating triangles behind the anterior loop. Among all the salient angels, BSA1 looks slimmer than the others. The dentine field is equally separated at all isthmuses. Both walls of all the triangles are seeming anteriorly curved. Among all the three referred specimens, one (PLATE 23, Fig. 4) has three roots, but the anterior tow are fused together around the base of them. And the other two have 2 roots.

M^3: Only two specimens are referred to this species. Based on the observation on them, the occlusal pattern is basically composed of an anterior loop, a short posterior loop and two triangles between them. There are two reentrant angles on buccal side and one on lingual side. Salient angle can count to three on both buccal and lingual side for the specimen of PLATE 23, Fig. 6. But, for the specimen of PLATE 23, Fig. 7, it can only count to two on buccal side, because BSA3 is not developed. LSA2 is robust and blunt. BSA1 is slimmer. The apex of BRA2 is nearly opposite to that of LRA2. The anterior wall is concave. No enamel island can be observed around either the posterior loop or the anterior loop of the two referred specimen. It is probably because they have been worn out. Because there is no enmal islet around the anterior loop, and BRA1 is very shallow, AL is confluent with T2 on both specimens. The PL of specimen of PLATE 23, Fig. 6 is distinctly shorter than that of PLATE 23, Fig. 7. Both specimens have two roots.

M_1: Only two specimens are referred to this species. Based on the observation on them, there are three alternating triangles between ACC and the posterior loop. No enamel islet appears on the anterior cap. On the specimen of PLATE 23, Fig. 2, the anterior cap is broken; and *Mimomys*-angle is developed; a nearly closed neck of the AC is formed by LRA4 and BRA3 opposite to each other. On the specimen of PLATE 23, Fig. 1, the AC is semicircular-shaped and with several secondary extra folds on the anterior and buccal of it; *Mimomys*-angle is not developed; the apex of BRA3 is opposite to that of LRA3 instead of LRA4. The apex of LRA3 is located slightly in front of that of BRA2. Both walls of all the

triangles go straight and don't curve. The differentiation of the enamel band can be considered as *Mimomys*-type or negative type, because the SDQ is calculated at 114. Two roots.

Remarks and comparison—

This is a species slightly more primitive than *Villanyia* sp. nov., because this form has a greater HH-index, but without other noticeable differences from *Villanyia* sp. nov.. The indistinct materials from *Mimomys* cf. *M. orientalis* listed is owing to the fact that both forms comes from the same layer, DB03-2, of Gaotege section, and that there is only little cementum deposited in the molars of *Mimomys* cf. *M. orientalis*. It is possible that in young individuals the deposit of cementum has not started when no cementum can be observed. In this occasion, it will be difficult to distinguish these two forms. So, also as a compromise, these specimens are temporarily taken as indistinct for the future consideration.

Villanyia sp. 2

PLATE 24, Figs. 1~8

Synonymy—

Mimomys cf. *M. orientalis*; LI (2006). Doctoral Dissertation of CAS, p57. (in part)

Borsodia? sp.; LI (2006). Doctoral Dissertation of CAS, p62.

Studied locality and materials—

Gaotege (personal number):

DB03-2 LI (2006): 2 right M^1 (45, 48), 1 left M^2 (46), 1 right M^2 (49), 1 right M^3 (50), 1 broken left M_1 (28), 1 left M_1 (25), 1 right M_1 (21); LI 2007.05: 1 left M_1 (11).

Measurements— See Table 1.

Description—

There is no cementum in reentrant angles of the molars. The sinuous line belongs to the typical *Mimomys*-type. And the undulation is stronger than that of *Mimomys* cf. *M. orientalis*, *Villanyia* sp. 1, *Mimomys teilhardi*, *Villanyia* sp. nov., and of course, *Mimomys bilikeensis*. Usually, on lower molars, the sinuids Hsd, Hsd, and Asd ascend high, and on upper molars, the sinuses As, Asl and Ds act in the same way.

M^1: The occlusal patterns of M^1 comprises four alternating triangles behind the anterior loop. On the two referred specimens, the posterior wall of LRA2 is seemingly parallel to the anterior wall of BRA2, which leads to the semi-closeness of is3. The posterior end of the tooth is conspicuously pointed posteriorly. Both referred specimens have three roots.

M^2: There are three alternating triangles behind the anterior loop. Among all the salient

angels, BSA1 looks slimmer than the others. On the two specimens, the anterior wall of AL is concave on its buccal half. The posterior end of the tooth is conspicuously pointed posteriorly. The dentine field is separated at all dentine isthmuses. One of the referred specimen has two roots, the other's root number is not observable.

M^3: Only one specimen is referred to this species. The occlusal pattern is composed of an anterior loop, a bar-like and comparatively longer posterior loop and two triangles between them. There are two reentrant angles on buccal side and one on lingual side. Salient angle can count to two on buccal side and three on lingual side. LSA2 is robust and blunt. BSA1 is slimmer. The apex of BRA2 is opposite to that of LRA2. The anterior wall is concave. No enamel island appears on either the posterior loop or the anterior loop. The dentine field belongs to the typical tow-field type, which means AL is confluent with T2 and T3 is confluent with PL. Two roots.

M_1: There are three alternating triangles between ACC and the posterior loop. No enamel islet appears on the anterior cap. *Mimomys*-angle is not developed, either. The anterior cap looks comparatively longer, bar-like. LRA4, especially BRA3, looks flatter, so the anterior cap is confluent with the other part of ACC. The apex of LRA3 is obliquely opposite to that of BRA2. The dentine isthmuses is1~32 seems equally closed. The differentiation of the enamel band can be considered subtly as *Mimomys*-type or negative type, because the SDQ is calculated at 108. Two roots.

Remarks and comparison—

This is probably a form where *Borsodia* stems out. But the characters of this form does not agree with the diagnosis of the genus *Borsodia* because of its nearly uniform enamel band differentiation type., so these materials are temporarily assigned as sp. in the genus *Villanyia* for the future consideration. This form noticeably differs from *Villanyia* species by an un-necked and comparatively longer anterior cap of M_1. Furthermore, it differs from *Villanyia* sp. nov. and *Villanyia* sp. 1 by lacking of *Mimomys*-angle.

Genus *Borsodia* JÁNOSSY AND VAN DER MEULEN, 1975

Type species— *Borsoida hungaricus* (KORMOS, 1938)

Diagnosis— (following JÁNOSSY AND VAN DER MEULEN, 1975) No cementum deposited in the reentrant angles of all molars. The differentiation of the enamel band belongs to *Microtus*-type or positive type.

Borsodia chinensis (KORMOS, 1934)

PLATE 27

Synonymy (partially)—

Mimomys chinensis; KORMOS (1934), p. 6, text-fig. 1c.

Mimomys (*Villanyia*) *laguriformes*; ERBAJEVA (1973), p.136, text-figs. 1~3.

Diagnosis— Molars rooted. No cementum deposited in the reentrant angles of all molars. The differentiation of the enamel band belongs to *Microtus*-type or positive. M_1 without *Mimomys*-angle and enamel islet; AC proportionally longer. M^3 with two-field dentine field, no enamel islet developed, BSA3 reduced, slim and long PL.

Biochronological range— MQ1

Studied locality and materials—

Xiaochangliang

Culture Layer 6 left M^1 (V15323.1~6), 9 right M^1 (V15323.7~15), 3 left M^2 (V15323.16~18), 4 right M^2 (V15323.19~22), 4 left M^3 (V15323.23~26), 7 right M^3 (V15323.27~33), 3 left M_1 (V15323.34~36), 6 right M_1 (V15323.37~42), 5 left M_2 (V15323.43~47), 12 right M_2 (V15323.48~59), 6 left M_3 (V15323.60~65), 8 right M_3 (V15323.66~73).

Measurements— See Table 1.

Description—

The molars are rooted. There is no cement in the reentrant angles of the molars. The enamel is differentiated in Microtus-type or positive type. On the occlusal surface, the enamel is usually interrupted at the apexes of LSA1, BSA1 and, as common in arvicolid species, at posterior edge on upper molars, while on the contrary anterior edge on lower molars.

M^1: There are four interlaced triangles behind the anterior loop. The anterior margin is more or less posteriorly concave. The enamel is interrupted at the apexes of BSA1, LSA1, LSA2 and the posterior end of the tooth on the occlusal surface. The posterior end of the tooth is acute and pointed posteriorly like a spur. The dentine isthmuses are normally closed, but is2 and is4 tend to become more open along with the crown wear especially when approaching to the roots. LRA2 is bi-apexed, which means that besides the normal apex, there is also another apex opposite to that of BRA1. The enamel between these two apexes is normally straight, but a slightly lignually convex angle can be observed on 3 out of 7 specimens, which is called “Lagurus-agnle” in the Lagurus species. This tooth has 2 roots, but the former one is, in fact, a merged combination of a small root right beneath T1 and the normal anterior root. This root is bifurcated when it grows long enough, which can be observed on one nearly worn-up specimen.

M^2: There are three interlaced triangles behind the anterior loop. BSA1 is much feebler

and more acute compared with LSA2 which is robust. LRA2 is bi-apexed like that on M1, and the so-called "Lagurus-angle" can be observed on 1 out of 9 specimens. The dentine isthmuses are closed, and the posterior end is the same with that of M1.

M^3: There are 2 triangles behind the anterior loop. Because the anterior loop and T3 are confluent with T2 and the posterior loop respectively, and is3 is the only closed isthmus on this tooth, the dentine is normally divided into two fields. On 2 out of 11 specimens, is3 is not closed tightly. LSA2 is robuster and obtuse. LRA2 is distinctly broader than the other reentrant angles. On 5 out of 11 specimens, the rudiment of BSA3 is visible. The posterior loop is slim, long, bar-like, and extends posteriorly or slightly posterobucally.

M_1: Between the anteriorconid complex and the posterior loop, there are three interlaced triangles. The anterior loop is rounded, and more or less extends buccally. The posterior edge of the posterior loop is more or less concave anteriorly. The apex of LRA3 is opposite to that of BRA2 or slightly anteriorly situated. The anterior cap, T4 and T5 are confluent. is1~4 are nearly closed. On 2 specimens, is2 is a little more open than the other three. 2 roots.

M_2: In front of the posterior loop, there are 4 interlaced triangles. is1~3 is closed, and is4 is open. Sometimes, is2 is more open than is1 and is2, but more closed than is4. The anterior end of the tooth is spur-like and anteriorly pointed. 2 roots.

M_3: There are 4 interlaced triangles in front of the posterior loop. Except is4, all dentine isthmuses are closed, but, sometimes, is2 is a little more open. The anterior end of the tooth is spur-like and anteriorly pointed. 2 roots.

Remarks and comparison—

Borsodia (JÁNOSSY and VAN DER MEULEN, 1975) is characterized by the lack of cement in reentrant angles of molars and Microtus or positive type of enamel differentiation. The morphologies of Xiaochangliang form totally match those of the only Chinese species of this genus, *B. chinensis* (KORMOS, 1934).

***Borsodia* sp.**

PLATE 28

Synonymy—

Borsodia n. sp. ; ZHENG AND ZHANG (2000). Vertebrata PalAsiatica, 38 (1). (in part)

Borsodia n. sp. and *Hyperacrius yenshanensis*; ZHENG AND ZHANG (2001). Vertebrata PalAsiatica, 39 (3). (in part)

Studied locality and materials—

Lingtai (personal number):

93001— WL11 WL11-7: 1 right M^3 (11); WL11-5: 1 left M_1 (01); WL11-3: 1 right M^3 (01); WL11-1: 1 right M_3 (01). **WL10** WL10-11: 1 broken left M^3 (03); WL10-10: 1 left M^3 (03); WL10-8: 1 broken right M^3 (04); WL10: 2 left M^3 (07, 09), 2 right M_2 (10~11), 1 broken left M_3 (12). **WL8** 1 right M^3 (03), 1 broken right M_1 (10), 1 broken right M_3 (13). **WL3** 1 broken right M_1 (03), 1 broken left M_2 (01).

Measurements— See Table 1.

Description—

There is no cementum in reentrant angles of the molars. The sinuous line belongs to the typical *Mimomys*-type. Usually, on lower molars, the sinuids Hsd, Hsd, and Asd are so high that they will penetrate the whole crown before the roots' formation, which makes the enamel bands of them interrupted at the apexes of BSA1, LSA1 and front end from the occlusal view, respectively, and on upper molars, the sinuses As, Asl and Ds act in the same way. Both walls of all the triangles are seemingly posteriorly curved on lower molars.

M^3: The occlusal pattern of M^3 is basically composed of an anterior loop, a bar-like and comparatively long posterior loop and two triangles between them. There are always two reentrant angles on buccal side and one on lingual side. Salient angle can count to two on the buccal side, but three on the lingual side, that is, there is no BSA3 developed on the buccal side. LSA2 is usually robust and blunt. BSA1 is usually slimmer. The apex of BRA2 is nearly opposite to that of LRA2. On some young specimens, the anterior wall is concave. No enamel island appears on either the posterior loop or the anterior loop. The dentine field belongs to the typical two-field type, which means that AL is confluent with T2, and T3 is confluent with PL. On some specimens, "lagurine" structure can be observed at the bottom of LRA2 (PLATE 28, Figs. 11, 14, 16). All the specimens have two roots.

M_1: There are three alternating triangles between ACC and the posterior loop. No enamel islet appears on the anterior cap. The anterior cap looks proportionally longer and bar-like. LRA4, especially BRA3, is flatter, so AC is confluent with the other part of ACC. T4 and T5 are obliquely confluent with each other. A feeble *Mimomys*-angle can be observed and it is located close to BSA3. The apex of LRA3 is slightly in front of that of BRA2. The differentiation of the enamel band can be considered as *Microtus*-type or positive type, because the SDQ is calculated at 82. Two roots.

M_2: There are four alternating triangles in front of the posterior loop. T1~T2 and T3~T4 are semi-confluent with each other, respectively, which means that the apices of BRA1, 2 are anterior to that of LRA1, 3, respectively and the dentine isthmuses is2, 4 are distinctly wider that is1, 3. Usually, the front end of the tooth is pointed anteriorly. Both walls of all the triangles are posteriorly curved. Two roots.

M_3: There are four triangles in front of the posterior loop, with T1~T2 and T3~T4 semi-confluent with each other, respectively, which means that the apices of BRA1,2 are anterior to that of LRA1, 3, respectively. Buccal triangles are distinctly smaller that lingual ones. Usually, the front end of the tooth is anterior pointed. Both walls of all the triangles are posteriorly curved. Two roots.

Remarks and comparison—

Our referral is mainly based on the lack of cementum and the *Microtus*-type of enamel band differentiation type of all the specimens referred to this species. But what is still not clear is that there is a weak *Mimomys*-angle developed on the only M1 referred here. But the author insist on the *Borsodia* generic assignment because of its *Microtus*-type of enamel band differentiation. All the other specimens also show great similarity on the morphology of occlusal surface.

Tribe MICROTINI KRETZOI, 1954

Dental diagnosis (following REPENNING AND GRADY, 1988 and REPENNING, 1992): Genera of tribe Microtini with rootless cheek teeth; the apexes of LRA3 and BRA3 opposite to each other and is5 closed; M^3 primitively simple.

Included genera (partially): *Lasiopodomys*, *Microtus*, and *Proedromys*.

Genus *Proedromys* THOMAS, 1911

Type species— *Proedromys bedfordi* THOMAS, 1911

Diagnosis— Molars rootless. Abundant cementum deposited in the reentrant angles of molars. M_1 with a round-shaped AC; no extra angle developed on the buccal side of AC; BRA3 and LRA3 opposite to each other and T4 completely separated from the the other parts of ACC by the closeness of them. T4 not developed on M_3. M^3 with only two triangles between AL and PL, and a reduced and hook-like PL.

Remarks—

This extant genus with single species, *Proedromys bedfordi*, is known from Sichuan and southern Gansu Province in North China. Pleistocene remains have been found over a considerably larger part of China.

Proedromys bedfordi THOMAS, 1911

PLATE 29, Figs. 1~6

Synonymy(only concerning the studied localities)—

Allophaiomys terrae-rubrae; ZHENG AND ZHANG (2000). Vertebrata PalAsiatica, 38 (1), Fig. 2. (in part)

Proedromys sp.; ZHENG AND ZHANG (2001). Vertebrata PalAsiatica, 39 (3), Fig. 3.

Diagnosis— The same with the diagnosis of the genus.

Biochronological range— MQ1

Studied locality and materials—

Lingtai (personal number)

93001— WL2 2 broken left M_1 (02, 04). **WL1** 1 broken left M^3 (01). **WL7+** 1 broken left M_1 (04). **WL5+** 1 broken right mandible with M_1 (19), 1 broken left M_1 (18), 1 left M_3 (04), 1 right M_3 (03). **WL4+** 1 broken right M^3 (02).

Measurements— See Table 1.

Description—

There is plentiful cementum in reentrant angles of the molars. All the molars have no root. The sinuous line belongs to the typical *Mimomys*-type. Usually, on lower molars, the sinuids Hsd, Hsd, and Asd are so high that they will penetrate the whole crown, which makes the enamel bands of them interrupted at the apexes of BSA1, LSA1 and front end from the occlusal view, respectively, and on upper molars, the sinuses As, Asl and Ds act in the same way. Both walls of all the triangles are seemingly posteriorly curved on lower molars, and anteriorly curved on upper molars.

M^3: The occlusal pattern of M^3 is basically composed of an anterior loop, a very short semi-circular posterior loop and two triangles between them. There are always only two reentrant angles on the buccal side and one on the lingual side. Salient angle can count to three on both buccal and lingual side. The apex of BRA2 is located far in front of that of LRA2. No enamel island appears on either the posterior loop or the anterior loop. The dentine field is completely separated at is2 and is3. is4 is closed, so T3 is confluent with PL. BSA3 and the PL form a hook together.

M_1: There are three alternating triangles between ACC and the posterior loop. No enamel islet can be observed on all the specimens. The anterior cap looks proportionally longer and oval-shaped. BRA3 is opposite to LRA3 instead of LRA4, and completely closed, so T4 is completely separated from the other part of ACC. But LRA4 does not separate AC, so AC is completely confluent with T5. *Mimomys*-angle is not developed. The dentine isthmuses is1~4 are equally close. The differentiation of the enamel band can be considered as typical *Mimomys*-type or negative type, because the SDQ is calculated at 125.

M_3: There are three triangles in front of the posterior loop. T1 and T2 are obliquely

confluent with each other. T4 is not developed. Buccal triangles are distinctly smaller that lingual ones. is1 and is3 are completely closed, and is2 is open.

Mimomys teilhardi - Villanyia sp. nov. COMPLEX

PLATE 5~6

Synonymy—

Mimomys teilhardi LI, 2006; LI (2006). Doctoral Dissertation of CAS, p52. (in part)

Biochronological range— Early Gaozhuangian of DENG, 2006.

Studied locality and materials—

Gaotege (number from original author):

DB02-1 54 M^1: VXXX19.2~55; 58 M^2: VXXX19.56~113; 36 M^3: VXXX19.114~149; 61 M_2: VXXX19.208~268; 47 M_3: VXXX19.269~315; 1 broken mandible with M_1: VXXX19.316. **DB02-2** 2 broken mandible with $M_{1\sim2}$: VXXX19.317~318; 32 M^1: VXXX19.319~350; 24 M^2: VXXX19.351~374; 11 M^3: VXXX19.375~385; 27 M_2: VXXX19.412~438; 12 M_3: VXXX19.439~450. **DB02-3** 31 M^1: VXXX19.451~481; 28 M^2: VXXX19.482~509; 21 M^3: VXXX19.510~530; 22 M_2: VXXX19.555~576; 22 M_3: VXXX19.577~598. **DB02-4** 11 M^1: VXXX19.599~609; 16 M^2: VXXX19.610~625; 5 M^3: VXXX19.626~630; 8 M_2: VXXX19.639~646; 7 M_3: VXXX19.647~653. **DB02-5** 2 M^1: VXXX19.654~655. **DB02-6** 1 broken mandible with M_1: VXXX19.657; 3 M^1: VXXX19.658~660; 3 M_2: VXXX19.664~666; 1 M_3: VXXX19.667. **DB03-1** 4 M^1: VXXX19.668~671; 9 M^2: VXXX19.672~680; 7 M^3: VXXX19.681~687; 6 M_2: VXXX19.697~702; 6 M_3: VXXX19.703~708.

Measurements— See Table 1.

Description—

M^1: The occlusal patterns of M^1 comprises four alternating triangles behind the anterior loop. On juvenile specimens, the posterior walls of LRA1, 2 are nearly parallel to the anterior walls of BRA1, 2, respectively, which leads to the zigzag shape of the whole dentine field being equally semi-confluent at each dentine isthmus; and the posterior end of the tooth is pointed posteriorly, where the enamel band is distinctly thinner and seemingly discontinuous. With the process of wear, the parallel walls of reentrant angles turns to normal occlusal pattern and the dentine field becomes separate at all isthmuses, but is2, 4 are sometimes distinctly open than is1, 3; the posterior end turns less pointed. The buccal sinuous line undulates with all sinuses a little higher than the bases of the reentrant angles and at nearly the same level parallel the masticatory surface, while the lingual sinuous line rises higher at the protosinus (Prs) than that at the anterosinulus (Asl)

and hyposinus (Hys), but all sinuses rise above the base line of the reentrant angles. All observable specimens have three roots with the middle root on mesial side above T1.

M^2: There are three alternating triangles behind the anterior loop. On juvenile specimens, the anterior wall of AL is sometimes concave on its buccal side, which makes BSA1 looks slimmer than the other salient angles; the posterior wall of BRA1 and the anterior wall of BRA2 are seemingly parallel to anterior and posterior walls of LRA2 respectively, which also leads to the zigzag outline of the whole dentine field being equally semi-confluent at each dentine isthmus like on M^1. On mature and aged specimens, the dentine field is separated at is2, 3, 4, but is4 is less closed. 96 out of 100 observed specimens have three roots, the other four have two roots. The sinuous line generally undulates little stronger that that of *Mimomys bilikeensis*.

M^3: The occlusal pattern of M^3 is basically composed of an anterior loop, a little more complicated and comparatively longer posterior loop and one feeble triangle between them. There are always two reentrant angles on buccal side and one on lingual side. A more independent but feeble BSA3 usually appears on buccal side of PL. If including the dependent angle on lingual side of PL, salient angle can also count to three on lingual side. LSA2 is usually robust and blunt, and BSA1 is usually slimmer. The apex of BRA2 is sometimes nearly opposite to, but sometimes extends to the back of that of LRA2. On some juvenile specimens, the anterior wall of AL is concave and the BSA1 is flat-headed. An enamel island always appears on the posterior loop and lasts before the crown is worn out. Usually, an enamel island also appears around the anterior loop, but only on mature or aged specimens. On juvenile specimens, the apex of BRA1 extends deep inwards close to the anterior wall of LRA2, which makes dentine field of AL is separate form that of T2. This situation will change on mature or aged specimens with wear of the teeth, where the former apex part of BRA1 is isolated and forms the anterior enamel island, and the new apex withdraws outwards a little. At the same time, BRA1 becomes shallower and AL becomes confluent with T2 with the enamel island in the middle. Even though, the anterior enamel island forms later than the posterior one, it usually doesn't last long and disappears earlier than the posterior one. The sinuous line on both buccal and lingual side is nearly flat with only Prs a little higher positioned. 4 out of 61 observable specimens have 3 roots, and all the other specimens have 2 roots.

M_2: There are four alternating triangles in front of the posterior loop. T1~T2 and T3~T4 are semi-confluent with each other, respectively, which means that the apexes of BRA1, 2 are anterior to that of LRA1, 3, respectively and the dentine isthmuses is2, 4 are distinctly wider that is1, 3. On young specimens, the front end of the tooth is pointed anteriorly and

the enamel band there becomes much thinner and seemingly discontinuous. But on older specimens, the outline of the front end of the tooth becomes smoothly and anteriorly convex and the thickness of the enamel band there also return to normal as the other part. The buccal sinuous line, with three sinuids nearly at the same level, undulates more than the lingual one. Two roots.

M_3: There are four triangles in front of the posterior loop, with T1 and T2 alternating with each other, T3 and T4 opposite to each other. Buccal triangles are distinctly smaller than lingual ones. On young specimens, the apex of T3 sometimes tilts anteriorly, and the enamel band at the front end of the tooth is distinctly thinner. Triangles T1, T2 are semi-confluent, and T3, T4 are confluent. The sinuous lines on both sides are nearly flat. Two roots.

Mimomys cf. *M. orientalis - Villanyia* sp. 1 COMPLEX

PLATE 23, Figs. 8~12

Synonymy—

Mimomys cf. *M. orientalis*; LI (2006). Doctoral Dissertation of CAS, p57. (in part)

Studied locality and materials—

Gaotege (personal number):

DB03-2 LI (2006): 5 left M_2 (34~38), 4 right M_2 (29, 32~33, 40), 1 left M_3 (42), 1 right M_3 (41).

Measurements— See Table 1.

Description—

M_2: There are four alternating triangles in front of the posterior loop. T1~T2 and T3~T4 are semi-confluent with each other, respectively, which means that the apices of BRA1, 2 are anterior to that of LRA1, 3, respectively and the dentine isthmuses is2, 4 are distinctly wider that is1, 3. Little cementum can be observed in the bottom of the salient angles of all the referred specimens. There is no cementum deposited in the salient angles. Two roots.

M_3: There are four triangles in front of the posterior loop, with T1 and T2 alternating with each other, T3 and T4 opposite to (PLATE 23, Fig. 11) or alternating with (PLATE 23, Fig. 12) each other. Buccal triangles are distinctly smaller that lingual ones. Triangles T1, T2 are semi-confluent, and T3, T4 are confluent (PLATE 23, Fig. 11) or semi-confluent (PLATE 23, Fig. 12). No cementum can be observed. Two roots.

Allophaiomys deucalion - Proedromys bedfordi COMPLEX

PLATE 29, Figs. 7~13

Synonymy(only concerning the studied localities)—

Allophaiomys terrae-rubrae; ZHENG AND ZHANG (2000). Vertebrata PalAsiatica, 38 (1), Fig. 2. (in part)

Proedromys sp.; ZHENG AND ZHANG (2001). Vertebrata PalAsiatica, 39 (3), Fig. 3.

Biochronological range— MQ1

Studied locality and materials—

Lingtai (personal number)

93001— WL2 1 right M^1 (01). **WL1** 1 broken left M^1 (05), 1 left M^2 (02), 1 left M_2 (03), 1 right M_2 (04). **WL5+** 3 broken left M^1 (08~10), 1 left M^2 (17), 1 right M^2 (01), 1 left M_2 (07), 1 right M_2 (06). **WL4+** 1 right M^2 (01), 1 broken M_2 (03). **WL2+** 1 broken left M^2 (01).

Measurements— See Table 1.

Description—

M^1: There are four interlaced triangles behind the anterior loop. The buccal reentrant angles extend deeper lingually than the lingual ones do. On the occlusal surface, the enamel band is also interrupted at the apex of LSA2, which makes the apex of it more obtuse than that of others, whereas on one less worn specimen, it is continuous at the apexes of LSA1 and BSA1. The dentine isthmuses are closed comparatively tightly.

M^2: There are three interlaced triangles behind the anterior loop. Isthmuses are closed tightly. BSA1 is slimmer and more acute while LSA1 is more obtuse than the other salient angles.

M_2: In front of the posterior loop, there are 4 interlaced triangles, the lingual ones of which are more or less stronger than those of labial ones. is1~3 are closed. The apex of the BRA2 doesn't reach the anterior wall of BSA3, is4 is open.

Arvicolinae gen. et sp. indet.

PLATE 29, Fig. 14

Studied locality and material—

Lingtai (personal number):

93001— WL8 1 broken left M_1 (14).

Measurements— See Table 1.

Description—

M_1: Only one specimen is referred to this species. Little cementum can be observed on this specimen. There are three alternating triangles between ACC and the posterior loop. No enamel islet can be observed on the anterior cap. The anterior cap is broken, but seems

Table 1. Measurements of Arvicolids from the Pliocene ~ Early Pleistocene of North China (Continued)

Locality	Species	M_1				M_2		M_3	
		L	W	SDQ	HH	L	W	L	W
Lingtai	*Mimomys* cf. *M. bilikeensis*	-	-	-	-	1.46|1.54|1.62	1.04|1.07|1.10 (2)	1.31|1.33|1.36	0.81|0.87|0.92 (2)
	Mimomys gansunicus	2.59|2.74|2.92	1.16|1.24|1.33 (15)	119|144|156 (16)	-	1.56|1.70|1.80	0.91|1.08|1.20 (15)	1.28|1.44|1.66	0.77|0.85|0.91 (16)
	Villanyia cf. *V. fanchangensis*	2.26|2.54|2.91	0.93|1.07|1.20 (4)	102|122|137 (4)	-	1.41|1.50|1.62	0.84|0.93|1.02 (9)	1.08|1.26|1.53	0.59|0.73|0.88 (13)
	Allopahiomys deucalion	2.54|2.68|2.81	1.00|1.05|1.09 (5)	107|116|131 (3)	-	1.48|1.56|1.64	0.90|0.93|0.96 (2)	1.39|1.45|1.52	0.64|0.69|0.75 (3)
	↕	-	-	-	-	1.51|1.60|1.68	0.79|0.94|1.03 (4)	-	-
	Proedromys bedfordi	2.94	1.12 (1)	125 (1)	-	-	-	1.35|1.40|1.45	0.72|0.76|0.80 (2)
	Borsodia sp.	2.42	0.99 (1)	82 (1)	4.19 (1)	1.56|1.57|1.59	0.97|0.99|1.00 (2)	1.41	0.82 (1)
	Arvicolinae gen. et sp. indet.	2.52	1.04 (1)	-	-	-	-	-	-
Renzidong	*Mimomys gansunicus*	2.63|2.86|3.12	1.19|1.32|1.50 (30)	112|141|165 (50)	-	1.68|1.81|1.98	0.99|1.16|1.34 (30)	1.45|1.57|1.71	0.79|0.90|1.02 (30)
	Villanyia fanchangensis	2.11|2.33|2.58	0.94|1.02|1.10 (30)	96|116|146 (50)	3.78|4.56|5.09 (45)	1.35|1.52|1.72	0.79|0.97|1.14 (30)	1.04|1.27|1.46	0.58|0.74|0.88 (30)
	O. parallelus gen. et sp. nov.	2.89|3.21|3.47	1.32|1.50|1.64 (30)	110|124|143 (39)	-	1.82|1.96|2.14	1.02|1.29|1.52 (25)	1.57|1.73|2.02	0.90|1.10|1.31 (30)
Xiaochangliang	*Allopahiomys deucalion*	2.32|2.61|2.77	0.97|1.06|1.13 (4)	91|95|101 (5)	-	1.57|1.66|1.74	0.99|1.01|1.04 (2)	1.38	0.71 (1)
	Borsodia chinensis	2.53|2.62|2.70	1.02|1.03|1.04 (2)	60|63|66 (2)	-	1.55|1.56|1.57	0.87|0.88|0.88 (2)	1.33|1.44|1.55	0.69|0.69|0.69 (2)
Bilike	*Mimomys bilikeensis*	2.15|2.39|2.65	0.90|1.09|1.42 (30)	85|102|125 (100)	0.10|0.20|0.28 (50)	1.54|1.74|1.88	0.98|1.15|1.30 (30)	1.25|1.42|1.59	0.76|0.94|1.10 (30)
Gaotege	*Mimomys teilhardi*	2.40|2.61|2.78	1.09|1.25|1.38 (32)	102|111|122 (32)	0.25|0.39|0.56 (47)	-	-	-	-
	↕	-	-	-	-	1.56|1.75|1.92	1.00|1.15|1.30 (41)	1.18|1.44|1.62	0.80|0.93|1.12 (35)
	Villanyia sp. nov.	2.26|2.54|2.84	1.01|1.14|1.27 (25)	100|112|134 (21)	0.60|0.76|1.10 (19)	-	-	-	-
	Mimomys cf. *M. orientalis*	2.53|2.85|3.21	1.13|1.34|1.46 (11)	106|122|146 (10)	0.95|1.29|1.66 (11)	1.72|1.81|1.86	1.06|1.18|1.28 (3)	-	-
	↕	-	-	-	-	1.57|1.67|1.80	1.04|1.10|1.18 (5)	1.56	0.86 (1)
	Villanyia sp. 1	2.85	1.32 (1)	114 (1)	0.96|1.03|1.10 (2)	-	-	-	-
	Villanyia sp. 2	2.43|2.60|2.75	1.01|1.11|1.19 (3)	104|108|117 (4)	1.14|1.40|1.66 (2)	-	-	-	-
ZHENG and LI (1986)	*Mimomys orientalis*	2.82|2.95|3.04	1.36|1.38|1.43 (3)	127|132|136 (2)	1.05 (1)	-	-	-	-
	Mimomys banchiaonicus	3.90	1.92 (1)	137 (1)	-	-	-	-	-
	Mimomys peii	3.47|3.64|4.01	1.46|1.67|1.76 (7)	114|129|137 (8)	-	2.06|2.10|2.14	1.42|1.47|1.52 (2)	1.68|1.85|2.04	1.02|1.19|1.42 (3)
	Mimomys youhenicus	2.71	1.28 (1)	125 (1)	2.76|3.07|2.41)2)	-	-	-	-
	Borsodia chinensis	2.39|2.61|2.73	1.06|1.09|1.15 (4)	52|57|60 (3)	-	1.56|1.68|1.78	0.98|1.00|1.03 (3)	1.56	0.85 (1)
	Mimomys gansunicus	2.76|2.97|3.18	1.23|1.37|1.51 (2)	126|137|147 (2)	-	2.04	1.41 (1)	-	-

Annotations and abbreviations: ↕, indistinct specimens; Min.|Mean|Max. (number of specimens); *L*, length; *W*, width; *SDQ*, enamel band (Schmelzband) differentiation Quotient, see Heinrich, 1982; *HH*, HH-index, see Carls and Rabeder, 1988.

Table 1. Measurements of Arvicolids from the Pliocene ~ Early Pleistocene of North China

Locality	Species	M^1		M^2		M^3	
		L	W	L	W	L	W
Lingtai	*Mimomys* cf. *M. bilikeensis*	-	-	1.76|1/76|1.76	1.25|1.28|1.30 (2)	-	-
	Mimomys gansunicus	2.14|2.38|2.58	1.25|1.37|1.50 (16)	1.55|1.77|1.95	1.01|1.15|1.29 (20)	1.45|1.65|1.78	0.74|0.90|0.99 (16)
	Villanyia cf. *V. fanchangensis*	1.90|2.12|2.29	1.00|1.15|1.27 (10)	1.53|1.67|1.83	0.82|1.02|1.14 (11)	1.18|1.32|1.45	0.62|0.76|0.82 (6)
	Allopahiomys deucalion	2.15	1.19 (1)	-	-	1.58|1.68|1.82	0.75|0.86|0.95 (3)
	↕	2.46	1.30 (1)	1.73|1.79|1.82	1.04|1.06|1.09 (4)	-	-
	Proedromys bedfordi	-	-	-	-	-	-
	Borsodia sp.	-	-	-	-	1.37|1.47|1.55	0.73|0.77|0.84 (5)
	Arvicolinae gen. et sp. indet.	-	-	-	-	-	-
Renzidong	*Mimomys gansunicus*	2.15|2.53|2.79	1.33|1.49|1.64 (30)	1.73|1.89|2.04	1.05|1.18|1.33 (30)	1.65|1.78|2.12	0.87|0.97|1.10 (30)
	Villanyia fanchangensis	1.87|2.14|2.37	0.80|1.14|1.33 (30)	1.58|1.69|1.87	0.87|1.02|1.15 (30)	1.15|1.44|1.65	0.63|0.78|0.96 (30)
	O. parallelus gen. et sp. nov.	2.52|2.74|3.03	1.46|1.64|1.76 (30)	1.90|2.13|2.29	1.22|1.38|1.51 (30)	1.56|2.07|2.29	0.95|1.14|2.05 (30)
Xiaochangliang	*Allopahiomys deucalion*	2.02|2.23|2.45	1.06|1.16|1.27 (2)	1.63|1.67|1.72	1.02|1.02|1.03 (2)	1.55|1.65|1.76	0.81|0.89|0.98 (3)
	Borsodia chinensis	2.13|2.22|2.31	1.02|1.14|1.25 (2)	1.82|1.87|1.91	0.97|0.99|1.01 (2)	1.38|1.53|1.62	0.63|0.77|0.87 (11)
Bilike	*Mimomys bilikeensis*	1.96|2.18|2.35	1.08|1.25|1.41 (30)	1.67|1.81|1.94	0.91|1.20|1.40 (30)	1.34|1.55|1.78	0.91|1.04|1.22 (30)
Gaotege	*Mimomys teilhardi*	-	-	-	-	-	-
	↕	2.16|2.32|2.48	1.16|1.35|1.50 (39)	1.64|1.87|2.08	0.99|1.19|1.50 (47)	1.28|1.53|1.82	0.84|1.00|1.20 (65)
	Villanyia sp. nov.	-	-	-	-	-	-
	Mimomys cf. *M. orientalis*	2.30|2.45|2.58	1.18|1.43|1.64 (8)	2.00	1.36 (1)	1.82|1.96|2.12	1.00|1.12|1.22 (3)
	↕	-	-	-	-	-	-
	Villanyia sp. 1	-	-	1.54|1.90|2.13	0.96|1.28|1.50 (3)	1.40|1.58|1.76	1.06|1.11|1.16 (2)
	Villanyia sp. 2	1.96|2.10|2.24	1.11|1.22|1.33 (2)	1.96|2.00|2.04	1.15|1.22|1.29 (2)	1.64	1.08 (1)
ZHENG and LI (1986)	*Mimomys orientalis*	-	-	-	-	-	-
	Mimomys banchiaonicus	-	-	-	-	-	-
	Mimomys peii	2.94|3.07|3.20	1.74|1.94|2.00 (8)	2.30|2.43|2.70	1.40|1.60|1.80 (5)	2.18|2.31|2.40	1.18|1.26|1.32
	Mimomys youhenicus	-	-	-	-	-	-
	Borsodia chinensis	2.28	1.36 (1)	1.74|1.75|1.75	0.95|1.02|1.10 (2)	-	-
	Mimomys gansunicus	-	-	-	-	-	-

like round-shaped. BRA3 and LRA4 are flat, so AC is not separated from the other part of ACC. T4 and T5 are also obliquely confluent with each other. *Mimomys*-angle is developed and located close to BSA3. The apex of LRA3 is slightly in front of that of BRA2. The dentine isthmus is2 is more open than is1, 3. Because the specimen is badly preserved, the differentiation of the enamel band can not be measured. The sinuous line belongs to the typical *Mimomys*-type. Two roots. On occlusal view, the enamel band is interrupted at the apexes of LSA1, BSA1 and the front of AC.

Remarks— It is difficult to make a further identification because of the poor preservation of the only specimen.

VII. Phylogenetic Analysis

It looks inconsistent that all the descriptions and taxonomies is done in a traditional way of systematics, then turn to phylogenetics while talking about the relatedness among all the species described above. Indeed, phylogenetics has been more and more popular and widely accepted by quite a lot of researchers whose work concerns the evolution, relationship of organism. Even though PhyloCode has been proposed for several years as a successor of the traditional Linnaean taxonomy system, it still sounds impossible to ask people to give up a system that has been use for more than two hundred years, not to mention that the controversy is still going on. Despite the fact that the author attempted to use the phylogenetic procedure to solve the the evolution and relationship problem of the taxa studied here, it proved impossible to do so because there are too many parallel evolutions occurring in the group studied here. But the phylogenetic method is still formally used, because even if in the traditional way, the intuition is still going to employ anyway. As a result, a intuitively acceptable phylogenetic hypothesis will be proposed, and all the other analysis is going to be based on this hypothesis. No taxonomic conflicts about monophyly or paraphyly between the two schools are going to be discussed. The phylogeny of the group studied here will be barely concerned.

A. Selected characters and character coding

As mentioned in the introduction part, the evolutionary trend of arvicolids over time can be clearly reflected in several changes on their morphology. And most of these gradually changing morphological characters are also used to do the classification of this group of rodents. But, in fact, most of them are proved to be parallel in different lineages, and it is nearly impossible to get a acceptable phylogenetic tree based on the maximum

parsimony criterion, or the so-called Occam's razor. So, in this study, instead of objective maximus parsimony criterion, a subjective phylogenetic tree will be reconstructed based on the character evolution reconstruction and coding listed below:

Table 2. Selected characters and character Coding

Characters	Coding	Illustration etc.
1 dental cementum	**0** completely no cementum **1** little cementum (invisible or nearly invisible) in reentrant angles **2** abundant cementum in reentrant angles	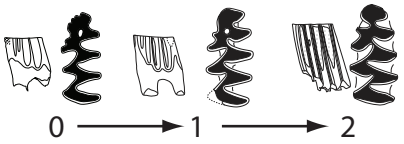
2 enamel band differentiation	**0** (nearly) uniform thickness [95≤SDQ≤105] **1** *Mimomys*-type (negative type) [SDQ>105] **2** *Microtus*-type (positive type) [SDQ<95]	0 → 1 → 2
3 sinuous line	**0** nearly flat **1** typical *Mimomys*-type (Hsd and Asd rise high in M_1) **2** all rise high	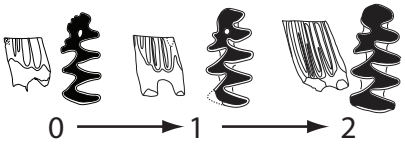
4 outline of triangles	**0** both walls go straight **1** both walls curve	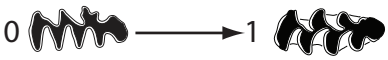
5 *Lagurus*-angle	**0** absent **1** present	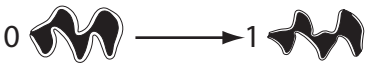
6 root number pattern of all molars (in order of M^1, M^2, M^3, Lower molars)	**0** 3 or 4, 3, 3, 2 **1** 3, 3, 2, 2 **2** 3, 2, 2, 2 **3** 2 or 3, 2, 2, 2 **4** rootless	0 → 1 → 2 → 3 →4
7 enamel islet on ACC of M_1	**0** present **1** absent	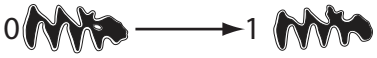
8 *Mimoms*-angle	**0** present, but weak **1** strong and close to BSA3 **2** strong but far from BSA3 like a independent salient angle **3** absent	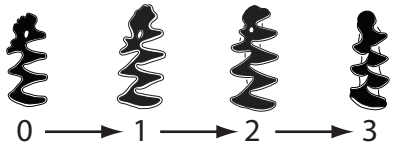
9 anterior cap (AC) of M_1	**0** wide open to the other part of ACC with BRA3 absent **1** open with BRA3 obtuse and not opposite to LRA4 **2** open with BRA3 obtuse and opposite to LRA4 **3** isolated from the other part of ACC with BRA3 acute and opposite to LRA4	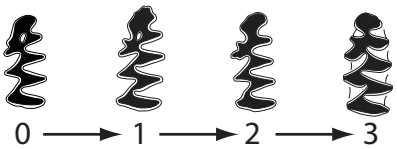
10 closeness of BRA3 and LRA3 on M_1	**0** open **1** closed	
11 relative position of the apexes of LRA3 and BRA2 on M_1	**0** obliquely opposite to each other **1** that of LRA3 extends anteriorly and in front of that of BRA2	

Characters	Coding	Illustration etc.
12 T4 on M_3	**0** present **1** weak **2** absent	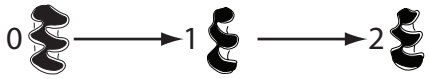
13 dentine field division of M^3	**0** two-fielded **1** normal	
14 relative position of apexes of LRA2 and BRA2 on M^3	**0** opposite to each other **1** that of BRA2 extends posterior to the back of that of LRA2	
15 anterior enamel islet on M^3	**0** present **1** absent	
16 posterior enamel islet on M^3	**0** present **1** absent	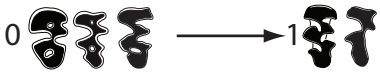
17 LRA3 on M^3	**0** absent **1** present **2** strong	
18 BSA3 on M^3	**0** present **1** strong **2** absent	

1. Dental cementum Dental cementum, in fact, exists in nearly all mammal species. Usually, it is thought to be a connective tissue that anchors tooth roots to the gum (periodontal ligament), maintaining the crown in position for effective occlusion. And it is usually continuously deposited throughout the life of a tooth and rarely remodeled or resorbed, grows in incremental bands, which can record the age and season of death of mammals. Usually, cementum is divided into two histological categories, cellular and acellular cementum (LIEBERMAN, 1994). The filling dental cementum deposited in the reentrant angles of arvicolids molars is mainly, in fact, a kind of cellular osseous cementum, which makes contributions to the development and the consolidation of the molars themselves (MATSUMOTO, 1997). Here, the gradual increase of dental cementum in the reentrant angles of arvicolids' molars is considered as a result of the gradual increase of the crown height, because the root development will become later and later with the process of crown height increase, so the filling dental cementum is helpful to anchor the molars in the alveolus. But, for the group or groups that don't have filling cementum deposited in the reentrant angles of the molars, another kind of cementum, pericoronal cementum, covering the dentine at dentin free area will take the same effect. Hence, dental cementum, in fact, exists in the molars of all arvicolid species, but here, the cementum just refers to the filling dental

cementum deposited in the reentrant angles of the molars.

2. Enamel band differentiation See the part of "Calculating method for quantified characters".

3. Sinuous line Similar with the development of the dental cementum, the increasing undulation of the sinuous line is another expression of the increasing crown height and delay of root development for fossil arvicolids. Where the sinuid or sinus becomes very high, the pericoronal cementum covering the dentine free area can help to anchor the molar into the alveolus. So, basically, the sinuous line tends to undulate increasingly with the process of evolution, or the process of crown height increase. But the evolution of this character is also parallel in different lineages. (For more detailed information about this character, please see the part of "Calculating method for quantified characters".)

4. Outline of triangles There are two states for this character. State 0 stands for that both walls of the triangles on all molars go straight, but don't curve. This state can be observed on some early forms and some cementless forms. State 1 stands for that both walls of the triangles on the lower molars are posteriorly curved, while the contrary on upper molars. This state can be observed on all the advanced cemented forms, and one cementless form, *Borsodia chinensis*. This character can probably be used to make distinctions between early cemented and cementless forms analyzed here.

5. *Lagurus*-angle *Langurus*-angle is a structure that can be observed on the M^1 and M^2 of *Borsodia chinensis* (PLATE 27, Figs 5~6), it looks like that LRA2 of $M^{1\sim2}$ is becoming flat-headed or concave-headed. This character can only be observed on this species among all the species being analyzed and can be thought as a autamorphy.

6. Root number Increase of crown height and loss of roots are two general evolutionary trends of fossil arvicolids, because they have adapt their molars to the grass diet. For the lower molars, they all have two roots at the most, even in the most ancient form, *Mimomys bilikeensis*. The lower molars seem lose the two roots simultaneously in advanced forms without a transition from two roots to one root. As for the upper molars, all have three roots, and sometimes M^1 has four roots like in *Mimomys bilikeensis*. The loss of roots from three roots to two roots for upper molars occurs one by one in the order of $M^{3\sim1}$. Finally, all upper molars lose all the roots directly form the two-root state, and

become rootless at the same time with the lower molars. But, apparently, the increase of crown height and loss of roots happened independently in different lineages.

7. Enamel islet on ACC of M_1 There are two states for this character. The evolution of this character, from state 0, present, to the state 1, absent, probably independently evolved twice in the early cementless forms and the advanced cemented forms, respectively.

8. *Mimomys*-angle Together with Character 7, *Mimomys*-angle is a very important character to diagnose the genus *Mimomys*. But, the same as Character 7, it seems that the disappear of *Mimomys*-angle also independently happened at least twice in one of the cemented lineages and the cementless lineage.

9. Anterior cap (AC) of M_1 In general, the outline of ACC tends to become more and more complicated. At he same time, changes will also happen to the anterior cap. When BRA3 is not developed, it will wide open to the other part of ACC as represented by the state 0. After the development of BRA3, its connectivity to the other part of ACC relies on the outline and relative position of BRA3 and LRA4. As represented by state 1, it can still keep open to the other part of ACC without a neck, and it can also be open to the other part of ACC with a neck formed by the oblique oppositeness of BRA3 and LRA4 as represented by state 2. It can also be nearly closed and separated from the other part of ACC by the close oppositeness of BRA3 and LRA4 as represented by state 3.

10. Closeness of BRA3 and LRA3 on M_1 This character is usually used as one of the diagnoses of the extant monotypic genus *Proedromys* THOMAS, 1911. On the M_1 of the monotypic species, *Proedromys bedfordi*, of this genus, BRA3 and LRA3 are closely opposite to each other, and separate T4 from the other part of ACC. This character is a autamorphy of this monotypic genus, not observable in all the other species studied here.

11. Relative position of the apexes of LRA3 and BRA2 on M_1 This character has two states. It seems that in the ancient forms and all cementless forms LRA3 and BRA2 are obliquely opposite to each other, but in advanced cemented forms the apex of LRA3 will extend anteriorly to the front of that of BRA2.

12. T4 on M_3 This is another character that is usually used to diagnose the

monotypic genus *Proedromys* Thomas, 1911. The M_3 of the monotypic species *Proedromys bedfordi* does not have T4 developed. For the species *Allophaiomys deucalion*, T4 on M_3 is comparatively weak. All the other species have a normal T4 developed on M_3.

13. Dentine field division of M^3 State 1 of this character, the two-fielded dentine field division, means that when there are two enamel islets developed, there will be simplification of BRA1 after the formation of the anterior islet, and the dentine will be separated only at is3, and divided into two parts. But in the case of *Borsodia chinensis*, there is no enamel islet developed at all, and the dentine field is just separated at isd and divided into two parts. The normal dentine field division means that there is only a posterior enamel islet developed, and the dentine field is divided into at least three parts by the closenesses of is2 and is3.

14. relative position of apexes of LRA2 and BRA2 on M^3 In the ancient forms and all the species with a two-fielded type of M^3, the apexes of LRA2 and BRA2 on M^3 are all opposite to each other. In the advanced forms with a normal dentine division type of M^3, the apex of BRA2 usually extends posteriorly to the back of that of LRA2.

15&16. Anterior and posterior enamel islet on M^3 Both anterior and posterior enamel islets are developed on ancient forms. The anterior enamel islet disappears first in advanced cemented forms, and the posterior one disappears later. In advanced cementless forms, it seems that both islets disappears simultaneously.

17. LRA3 on M^3 LRA3 is not developed in ancient forms, it becomes increasingly stronger in both cemented forms and cementless forms.

18. BSA3 on M^3 BSA3 present in ancient forms, it becomes stronger in the cement forms, and probably tend to be degenerate in cementless forms.

The character matrix is as follows:

Table 3. Character matrix of all the species analyzed

Species\Characters	1	2	3	4	5	6	7	8	9	10	11	12	13	14	15	16	17	18
Villanyia fanchangensis	0	1	1	0	0	3	1	3	2	0	0	0	0	0	0	0	1	0
Mimomys gansunicus	2	1	1	1	0	3	0	2	1	0	1	0	1	1	1	0	1	0
O. parallelus gen. et sp. nov.	2	1	2	1	0	4	1	1	3	0	1	0	1	1	1	0	1	0
Mimomys bilikeensis	0	0	0	0	0	0	0	0	0	0	0	0	0	0	0	0	0	0
Mimomys teilhardi	0	1	1	0	0	1	0	1	1	0	0	0	0	0	0	0	0	0
Villanyia sp. nov.	0	1	1	0	0	1	1	1	2	0	0	0	0	0	0	0	0	0

Species\Characters	1	2	3	4	5	6	7	8	9	10	11	12	13	14	15	16	17	18
Mimomys cf. *M. orientalis*	1	1	1	0	0	2	0	1	1	0	1	0	1	0	1	0	1	0
Villanyia sp. 1	0	1	1	0	0	2	1	1	2	0	0	0	0	0	?	?	1	0
Villanyia sp. 2	0	1	1	0	0	2	1	3	2	0	0	0	0	0	1	1	0	2
Allophaiomys deucalion	2	1	1	1	0	4	0	3	1	0	1	1	1	1	1	1	2	1
Proedromys bedfordi	2	1	1	1	0	4	1	3	1	1	1	2	1	1	1	1	0	1
Bosodia sp.	0	2	1	0	?	3	1	1	2	0	0	0	0	0	1	1	0	2
Villanyia cf. *V. fanchangensis*	0	1	1	0	0	3	1	3	2	0	0	0	0	0	0	0	1	0
Borsodia chinensis	0	2	1	0	1	3	1	3	2	0	0	0	0	0	1	1	0	2
O. peii	2	1	2	1	0	3	1	1	3	0	1	0	1	1	1	0	1	0

B. One intuitively acceptable phylogenetic hypothesis

As stated before, it seems that parallel evolutions of different morphological characters on molars of the arvicolids analyzed here are very common. Therefore, it appears too difficult to find out a real acceptable phylogenetic tree according to the maximus parsimony principle, or the so-called Occam's razor. Consequently, a intuitively acceptable phylogenetic tree will be proposed (Figure 7, plotted by Macclade 4, MADDISON AND MADDISON, 2003), and base all the other analysis on this hypothesis. By the way our hypothesis shows that the genera *Mimomys*, *Villanyia* in China don't make up monophyletic, but polyphyletic groups.

1. Character evolution reconstruction

[1]The evolutionary trends for all the characters selected here are illustrated in Table 1. According to our phylogenetic hypothesis, among the 18 characters selected here, parallel evolutions or ambiguous changes happened to seven of them, character 5, 6, 7, 8, 15, 16 and 17. Most of these characters are very important characters to diagnose some species of some genera. The reason that ambiguous change happened to the character 5, *Lagurus*-angle, is because the state of this character for *Borsodia* sp. from 93001 section, Lingtai is unknown, but it is believed here that this is a autamorphy for the genus *Borsoida*. As for the character 6, root number pattern of all molars, it sounds reasonable to consider it as a character of parallel evolution. As stated by FEJFAR AND HEINRICH (1989), the loss of roots is a general evolutionary trend for arvicolids, but it apparently happened independently in different groups. For example, the change from state 3 to state 4 of character 6, that is from rooted molars to rootless molars, happened independently twice both in the

Figure 7. An intuitively acceptable hypothesis about the phylogenetics of the arvicolid taxa studied here →

* produced by MacClade Version 4.08

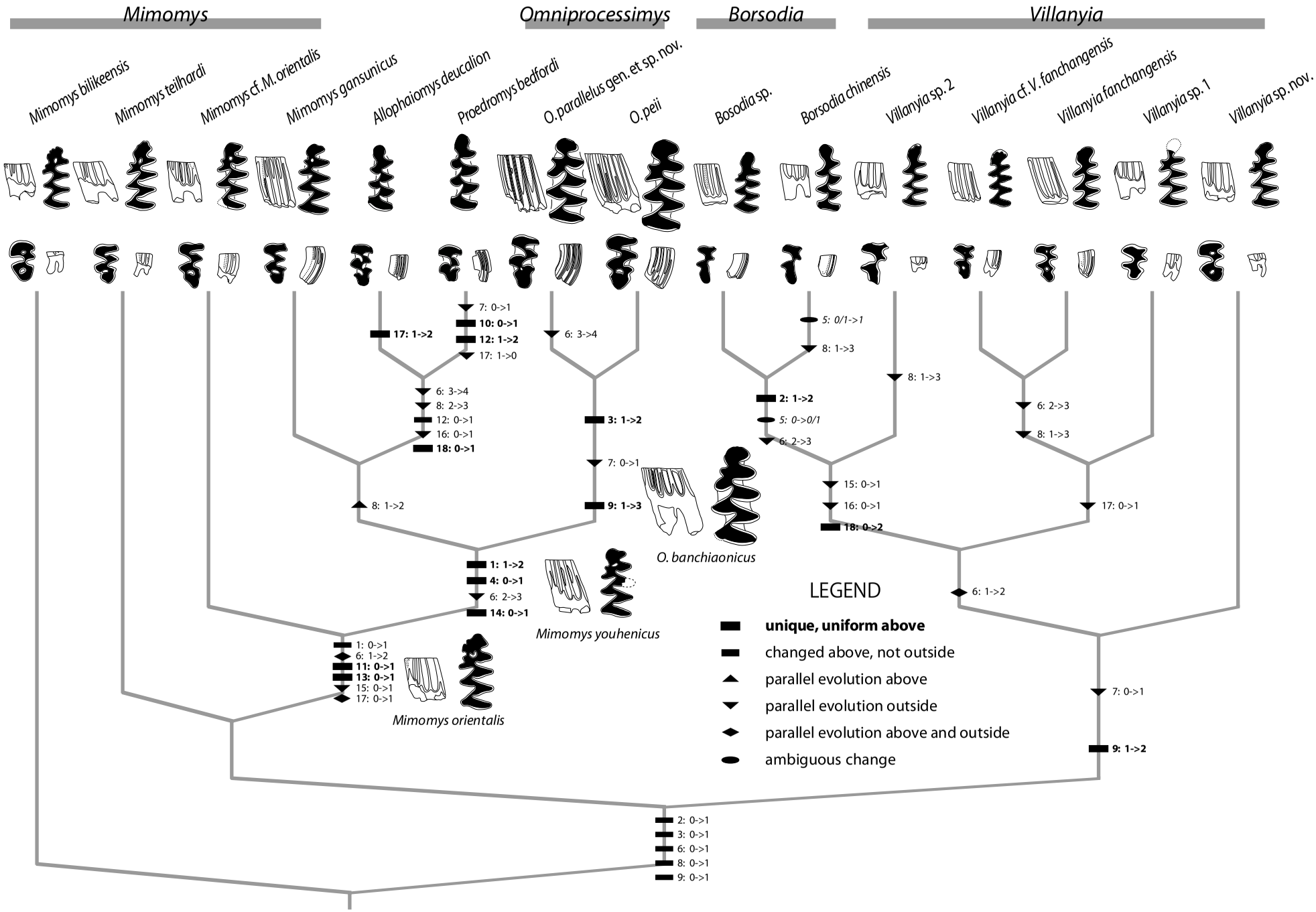
Mimomys
Omniprocessimys
Borsodia
Villanyia
Mimomys bilikeensis
Mimomys teilhardi
Mimomys cf. M. orientalis
Mimomys gansunicus
Allophaiomys deucalion
Proedromys bedfordi
O. parallelus gen. et sp. nov.
O. peii
Bosodia sp.
Borsodia chinensis
Villanyia sp. 2
Villanyia cf. V. fanchangensis
Villanyia fanchangensis
Villanyia sp. 1
Villanyia sp. nov.
17: 1->2
7: 0->1
10: 0->1
12: 1->2
17: 1->0
6: 3->4
6: 3->4
8: 2->3
12: 0->1
16: 0->1
18: 0->1
3: 1->2
7: 0->1
9: 1->3
8: 1->2
1: 1->2
4: 0->1
6: 2->3
14: 0->1
1: 0->1
6: 1->2
11: 0->1
13: 0->1
15: 0->1
17: 0->1
5: 0/1->1
8: 1->3
2: 1->2
5: 0->0/1
6: 2->3
8: 1->3
15: 0->1
16: 0->1
18: 0->2
6: 2->3
8: 1->3
17: 0->1
6: 1->2
7: 0->1
9: 1->2
2: 0->1
3: 0->1
6: 0->1
8: 0->1
9: 0->1
O. banchiaonicus
Mimomys youhenicus
Mimomys orientalis
LEGEND
unique, uniform above
changed above, not outside
parallel evolution above
parallel evolution outside
parallel evolution above and outside
ambiguous change

Omniprocessimys group, and the *Allophaioms-Proedromys* group; and the change from state 1 to state 2 also happened independently twice in both the cemented group with enamel islet on M_1 and the cementless group without enamel islet on M_1; and so on. The disappearance of the enamel islet on ACC of M_1, character 7, also independently evolved twice. The most ancient form that lost the enamel islet first if *Villanyia* sp. nov. from Gaotege, Inner Mongolia. But the loss of this enamel islet also happened in the cemented group in *Omniprocessimys parallelus*. The *Mimomys*-angle, character 8, is another character of parallel evolution. The ancient forms all have *Mimomys*-angle developed. But the loss of this angle happened independently twice both in the cemented group and the cementless group, like from *Mimomys gansunicus* to *Allophaiomys deucalion* and *Proedromys beddfordi*, and from *Villanyia* sp. 1 to *Villanyia fanchangensis*, and so on. With regard to the both enamel islets on M^3, another two parallel evolution characters 15 and 16, the anterior one disappeared first in *Mimomys gansunicus* of the *Mimomys* group, and the posterior one disappeared in *Allophiomys deucalion* and *Proedromys bedfordi* of this group; in the *Villanyia-Borsodia* group, it seems that the two islets disappeared simultaneously in *Borsoida*.

For all the other characters, no homoplasies can be found on the tree proposed here. Their evolutionary trends are just as illustrated in Table 2.

2. Representative arvicolid lineages

Based on the hypothesis suggested here, several arvicolid lineages from North China during Pliocene~Early Pleistocene can be established. But if supposing the confidence is determined by that the less parallel evolutions there are, the more reliable they are, then the two *Mimoms*-lineages are more reliable, because there are more homologies, but the other two *Villanyia-Borsoida* lineage, are not so reliable, because there are too many uncertainties.

1. *Mimomys bilikeensis-M. teilhardi-M. orientalis-M. youhenicus-M. gansunicus-Allophaiomys deucalion* lineage This is probably the arvicolid lineage that lasts the longest, spanning Pliocene~Early Pleistocene. Among all the species of this lineage, *Mimomys orientalis* is thought to be in the similar stage of evolution with *Mimomys* cf. *M. orientalis* from Gaotege, Inner Mongolia, because they have similar HH-index and resemble each other for all the other characters. The reason *Mimomys youhenicus* is put in the middle of *Mimomys orientalis* and *M. gansunicus* is also mainly based on the greater HH-index of *Mimomys youhenicus* than *M. orientalis*, and stronger *Mimomys*-angle than *Mimomys gansunicus*. The main evolutionary trends of this lineage is as follows:

1. Dental cementum increases with time. *Mimomys bilikeensis* and *M. teilhardi* don't have dental cementum at all. From *Mimomys orientalis* on, dental cementum starts to deposit in the reentrant angles of the molars. *Mimomys gansunicus* and *Allopahiomys deucalion* all have plenty of cementum deposited in the reentrant angles of the molars.

2. The undulation of the sinuous line increases with time. This trend can be reflected by the HH-indexes of all the sepcies in this lineage: *M. bilikeensis*(0.20)-*M. teilhardi*(0.39)-*M.orientalis*(1.29 or 1.05)-*M. youhenicus*(3.07). From *Mimomys gansunicus* on, the sinuses becomes too high to be measured.

3. Root number reduces with time. The root number pattern of all molars in the order of M^1, M^2, M^3, lower molar are as follows: *M. bilikeensis*(3/4, 3, 3, 2)-*M. teilhardi*(3, 3, 2, 2)-*M. orientalis*(3, 2, 2, 2)-*M. youhenicus*(?)-*M. gansunicus*(2/3, 2, 2, 2)-*A. deucalion*(rootless).

4. *Mimomys*-angle of *Mimomys bilikeensis* is weak, than it becomes very strong and located closely to BSA3 in *Mimomys teilhardi*, *M. orientalis* and *M. youhenicus*. It becomes weak again in *Mimomys gansunicus* and located far away from BSA3 like a independent salient angle. Finally it disappears in *Allophaiomys deucalion*.

5. In ancient forms, like *Mimomys bilikeensis*, *M. teilhardi*, and probably *Mimomys orientalis*, there are two enamel islets developed, both anterior and posterior, on M^3. The anterior one disappear disappears in *Mimomys gansunicus*, or maybe even earlier in *Mimomys youhenicus*. Finally, the posterior one also disappears in *Allophaiomys deucalion*.

2. *Omniprocessimys peii-O. parallelus* lineage This lineage probably stems from the former lineage somewhere around *Mimomys youhenicus*. The most conspicuous characteristic feature of this lineage is indicated by their special sinuous line. Take M_1 of *O. peii* for example, all the sinuses rise very high. The evolutionary trend of this lineage is as follows:

1. Loss of roots. The root number pattern of *O. peii* is 2 or 3, 2, 2, 2, while *O. parallelus* is totally rootless.

2. Increasing high position of sinuses and sinuids. In *O. peii*, take M_1 for example, the Prsd, Pmsd, and Misd don't not penetrate the crown height even in young individuals, but for the rootless *O. parallelus*, all these sinuses penetrate the crown height even in young individuals.

3. *Villanyia* sp. nov.-*Villanyia* sp. 1-*V. fanchangensis* lineage This is one of our less confident lineages because of insufficient materials. It represents one of the two cementless lineages during the Pliocene-Early Pleistocene in North China. *Villanyia* sp. nov. from Gaotege probably stemmed out of the *Mimomys-Allopahiomys* lineage directly from *Mimomys bilikeensis*. Due to the scarce materials of *Villanyia* sp. 1 from the newer layer of Gaotege section, what can be concluded is that it is more advanced than *Villanyia* sp. nov. on the basis of the greater HH-index. Based on the present knowledge, this lineage lasts until Late Pliocene. But the phylogenetic route after that is still not clear. The general evolutionary trends in this lineage are as follows:

1. Loss of roots. The root number pattern of *Villanyia* sp. nov. is 3, 3, 2, 2; that of *Villanyia* sp. 1 is 3, 2, 2, 2; that of Villanyia fanchangensis is 2 or 3, 2, 2, 2.
2. *Mimomys*-angle tends to disappear since *Villanyia* sp. 1.
3. The two enamel islets on M^3 probably lasts throughout the lineage. The reason why the two enamel islets on M^3 of *Villanyia* sp. 1 can not be observed is considered as scarce materials.

4. *Villanyia* sp. 2-*Borsodia chinensis* lineage This is the other cementless lineage and also one of our less confident lineages. It is believed that this is a lineage independent of the one above. It is probably an immigrant lineage or it probably stemmed out of the above lineage from *Villanyia* sp. nov.. Our uncertainty also comes from the scarcity of the materials of *Villanyia* sp. 2 from the newer layer of Gaotege section and *Borsodia* sp. from 93001 section of Lingtai. It is believed that the most conspicuous diferences between this lineage and the above one are that the loss of *Mimomys*-angle on M_1, two enamel islets and BSA3 on M^3. But on the only complete M_1 of *Borsodia* sp., a weak *Mimomys*-angle can be observed, which further amplifies our uncertainty. More new materials are necessary to make this lineage more acceptable. The only one conspicuous evolutionary trend of this lineage is the alteration of enamel band differentiation type form *Mimomys*-type (negative type) to *Microtus*-type (positive type) since *Villanyia* sp. 2.

In brief, four lineages of arvicolids that ever existed during Pliocene~Early Pleistocene in North China are preliminarily proposed. Among them, the *Mimomys-Allophaiomys* lineage is the longest one and lasts throughout the period of Pliocene~Early Pleistocene. This lineage clearly and plentifully demonstrates the evolutionary gradualism of fossil arvicolids frequently mentioned by other researchers. The *Omniprocessimys* lineage is probably a domestic one. Because no form as special as the species of this genus has been reported anywhere else all over the world. It is also believed that the two less confident cementless lineages are independent of each other, from which what can possibly be

inferred is that the genus *Villanyia* and *Borsodia* are not ancestral-descendant related, but concurrent during Pliocene~Early Pleistocene.

VIII. Pliocene ~ Early Pleistocene Arvicolid Biochronology of North China

The preliminary framework of Chinese Neogene mammal biochronology has been established by a series of studies (CHIU ET AL., 1979; LI ET AL., 1984; QIU, 1989, QIU AND QIU, 1990, 1995; TONG ET AL., 1995; QIU ET AL., 1999; DENG, 2006). Even though ZHENG AND LI (1986) and ZHENG AND LI (1990) made reviews on Chinese arvicolid biochronology, there has not been noticeable effects reflected in the Chinese Neogene mammal biochronology framework.

In the review of ZHENG AND LI (1986), four arvicolid ages were proposed: the Xicunian age characterized by *Mimomys* sp.; the Youhean age characterized by *Mimomys youhenicus*, *M. orientalis*, *Omniprocessimys banchiaonicus*; the Dachaian age characterized by *Mimomys peii*; and the Nihewanian age (strict sense) characterized by *Borsodia chinensis*, *Mimomys gansunicus*. Each of these ages was also correlated to a MN zone of Europe. The Xicunian age was correlated to MN15; the Youhean age was correlated to MN16; the Dacaian age was correlated to MN17; and the Nihewanian age (Strict sense) was correlated to MN18 (or MQ1). In the contribution to the "INTERNATIONAL SYMPOSIUM EVOLUTION, PHYLOGENY AND BIOSTRATIGRAPHY OF ARVICOLIDS (Rodentia, Mammalia)" by ZHENG AND LI (1990), instead of arvicolid ages, eight arvicolid zones were proposed, with each zone having one or more type localities and several typical arvicolid species. These zones include: Zone III characterized by *Mimomys youhenicus*, *M. orientalis*, and *Omniprocessimys banchiaonicus* from Youhe; Zone IV characterized by *Allophaiomys "terrae-rubrae"*, *Villanyia henduanshanensis*, *Hyperacrius yenshanensis*, and *Mimomys peii* from Dachai; Zone V characterized by *Allophaiomys* cf. *deucalion*, *Borsodia chinensis*, *Mimomys gansunicus*, *Hexianomys complicidens*, *Eothenomys melanogaster*, and *Eothenomys prochinensis* from Nihewan; Zone VI characterized by *Allophaiomys* cf. *pliocaeniucs*, *Proedromys* cf. *bedfordi*, *Lasiopodomys brandtiolides*, *Hexianomys complicides*, and *Eothenomys melanogaster*, *Eothenomys olitoroides* from Gongwangling, and so on. Essentially, the ages and the zones within these two reviews on Chinese arvicolid biochronology made by ZHENG AND LI (1986, 1990) were, in fact, only loosely defined, because there were no boundary restrictions for each of these ages or zones. Like the original framework of Mammal Neogene (MN) zones, they are, in fact, barely sequencing systems of different

arvicolid faunas occupying discrete geological time intervals on the basis of stage of evolution. Since these two contributions, a lot of arvicolid-bearing fossil sites of Pliocene~Early Pleistocene age has been newly discovered, which makes it possible to to provide a further update of the Chinese arvicolid biochronology framework. Even so, owing to the fact that few of these fossil sites have external age control, it is still impossible to improve it to a perfect stage. On the contrary, this framework is still in its preliminary stage even after the update proposed here.

A. The age of Renzidong from the "stage of evolution" view on fossil arvicolids

JIN ET AL. (2000) assigned the time interval between 2.0 and 2.4 Ma to the Renzidong fauna mainly based on the faunal comparions. As described in the Systematic Description part, there are three arvicolid forms unearthed from the cave sediments of the site. They are *Mimomys gansunicus*, *Villanyia fanchangensis*, and *Omniprocessimys parallelus*. *O. parallelus* is a new form and first described here, so there are no references for this form to compare with. As for the combination of the other two forms, even though there has been no report from other sites, FLYNN ET AL. (1997) listed three arvicolid forms discovered form the Haiyan Formation: *Borsodia chinensis*, *Mimomys orientalis*, *M. gansunicus*. After observing the arvicolid specimens from localities YS109, YS6, and YS120 of Haiyan Formation, Yushe, the author found that there was indeed one cementless form *Borsodia chinensis*, and one cemented form *Mimomys gansunicus*. It seemed that there was not any form as primitive as *Mimomys orientalis*, but another cementless form closely resembling *Villanyia fanchangensis* was obviously observed. *Mimomys gansunicus* and *Villanyia fanchangensis* from Renzidong are at the similar stage of evolution with *Mimomys gansunicus* and the cemetless form resembling *Villania fanchangensis* from Haiyan Formation, Yushe. FLYNN ET AL. (1997) correlated the Haiyan Formation to earlier Matuyama subchron. According to the personal communication with the chief researcher of Yushe Basin, Zhangxiang Qiu (Academician, IVPP, CAS), by the present author in Jun, 2007, the Haiyan Formation should be correlated to earlier Matuyama subchron at 2.3~2.14 Ma based on the recent calibration. Hence, the age assigned by JIN ET AL. (2000) to the Renzidong fauna is in agreement with the age of the Haiyan Formation based on fossil arvicolids and should be thought as acceptable.

B. The age of 93001 section, Lingtai from the "stage of evolution" view on fossil arvicolids

ZHENG AND ZHANG (2000, 2001), ZHANG AND ZHENG (2000, 2001) carried out a comprehensive biostratigraphic study on three sections from Lingtai, Gansu: 93001 and 93002 in Wenwanggou, and 72074(4) in Xiaoshugou. All these works were summarized in ZHENG AND ZHANG (2001). They combined the three sections based on the biostratigraphic zonation of small mammal fossils discovered from them and established six Bio zones persisting through from Late Miocene to Early Pleistocene. Among these zones, Zone III and Zone IV were correlated to the ELMA Ruscinian age, Zone V and a part of Zone VI were correlated to the ELMA Villanyian age. The Zone III, IV and V were correlated to the Yushean age, and the Zone VI was correlated to the Nihewanian age. The external age control for these Biozones relied upon the magnetostratigraphic work done by WEI ET AL. (1993) with some modification. The fossil arvicolids discovered from 93001 and 72074(4) are studied in this dissertation. Consequent upon the present study, and from the "stage of evolution" view of fossil arvicolids, it seems that the biozones, from Zone III to Zone V, on 93001 section perhaps do not persist that long as they were correlated in Fig. 2 by ZHENG AND ZHANG (2001). On the 93001 section, *Mimomys gansunicus* occurred from WL15 to WL8; *Villanyia* cf. *V. fanchangensis* occurred from WL11 to WL7. The lowest stratigraphic datum (LSD) for *Mimomys gansunicus* is WL15-2. Even though there is only one left M_3 and three blank layers, WL14~12, after that, the high-positioned Hsd and Hsld penetrating the crown height already around the commencement of root formation displays nearly the same stage of evolution as *Mimomys gansunicus* from Renzidong. On the other hand, the diference on M_1 that most specimens of *Mimomys gansunicus* from Renzidong have a "so-called" *Mimomys*-angle seemly indicates that the Renzidong form is a little more primitive than the form from 93001 section. *Villanyia* cf. *V. fanchangensis* is also somewhat a little more advanced than *Villanyia fanchangensis*, such as less developed anterior islet on M^3. In addition, it seems unconvincing to drag *Mimomys gansunicus* down to the same age as its ancestor based on the *Mimomys belikeensis - M. teilhardi - M. orientalis - M. youhenicus - M. gansunicus - Allophaiomys deucalion* lineage established here. The rather that there are no distinct changes through time observed on all the specimens referred to these species. As a compromise, the age of the biozones from Zone III to Zone V on 93001 section is temporarily assigned to the time interval around 2.5~0.7 Ma. This is just a unsettled comprise co²nsequent upon the "stage of evolution" of the

---

Figure 8. Pliocene~Early Pleisotcene arvicolid biochronology of North China →

* The magnetostratigraphic correlations of the lithostratigraphic units of Yushe and the stratigraphic position of arvicolid species are based on the personal communication with ZHANGXIANG QIU (IVPP, Academician of CAS, chief researcher of Yushe Basin) in Jun, 2007

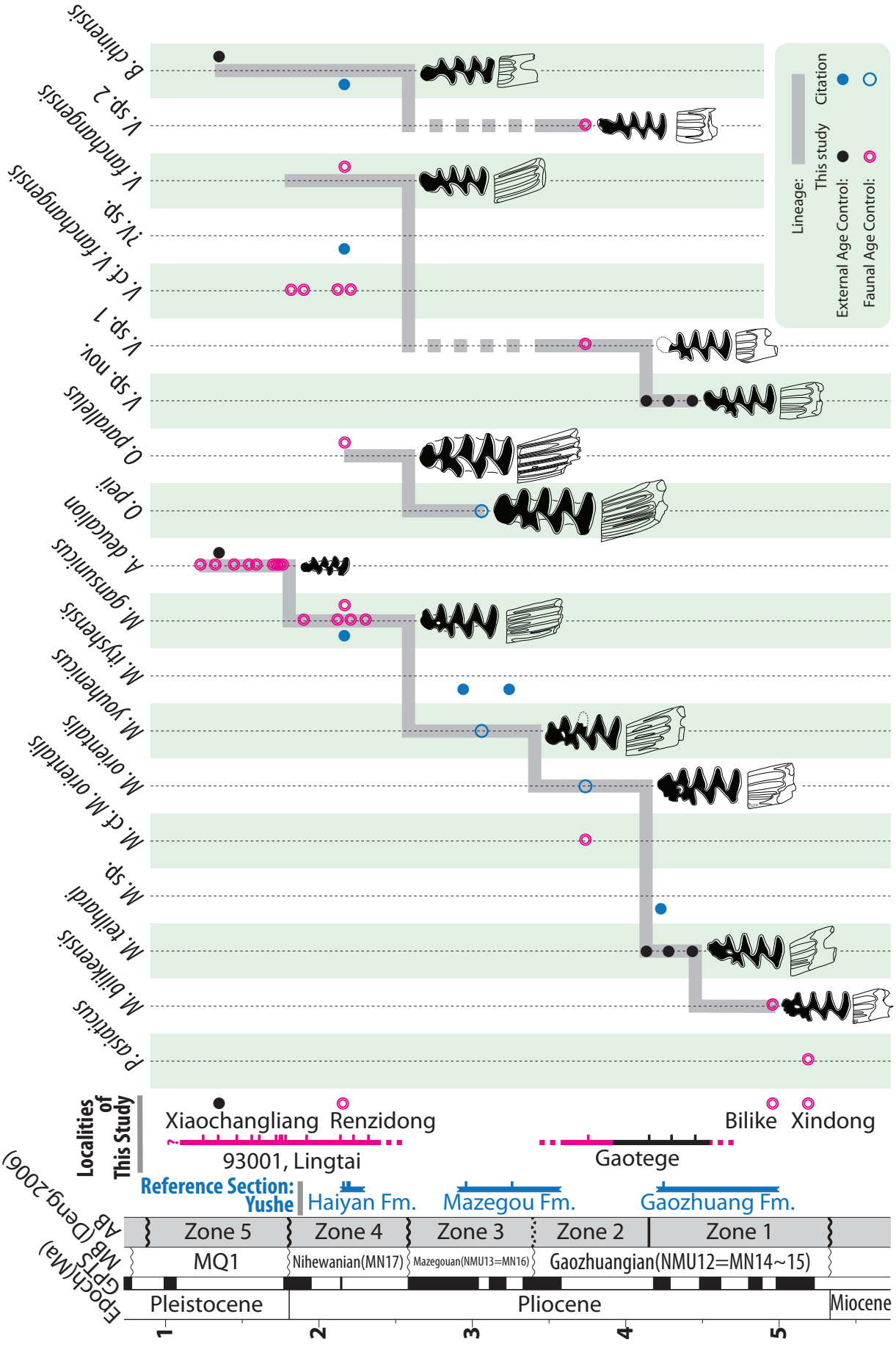
B. chinensis
V. sp. 2
V. fanchangensis
?V. sp.
V. cf. V. fanchangensis
V. sp. 1
V. sp. nov.
O. parallelus
O. petii
A. deucalion
M. gansuensis
M. tchyshensis
M. youlchenicus
M. orientalis
M. cf. M. orientalis
M. sp.
M. teilhardi
M. billikeensis
P. asiaticus
Lineage: This study Citation
External Age Control:
Faunal Age Control:
Localities of This Study
Xiaochangliang
Renzidong
93001, Lingtai
Bilike
Xindong
Gaotege
Reference Section: Yushe
Haiyan Fm.
Mazegou Fm.
Gaozhuang Fm.
Zone 5
Zone 4
Zone 3
Zone 2
Zone 1
MQ1
Nihewanian(MN17)
Mazegouan(NMU13=MN16)
Gaozhuangian(NMU12=MN14~15)
Pleistocene
Pliocene
Miocene
Epoch(Ma)
GPTS
MB (Deng,2006)
AB
1
2
3
4
5

arvicolid lineage preliminarily established here and it is still open to discussion.

C. Pliocene ~ Early Pleistocene Arvicolid Biochronology of North China

As stated before, by reason of lack of sufficient external age controls, at present, it is still unachievable to bring out a satisfying arvicolid biochronology framework in the strict sense of LINDSAY (2003). As a result, five loosely defined arvicolid biochronological zones are proposed. By loosely defined, it means that the boundaries for these zones still can not be defined on the basis of the present knowledge. Thus, for each zone, it can barely come up with the assigned typical arvicolid species. The assignments of the typical arvicolid species to each of these zones are mainly derived from the "stage of evolution", or the arvicolid lineages established here, where no external age controls are available, but derived from both the "stage of evolution" and the external age control (magnetostratigraphic data) where external age control is available. For the typical arvicolid species of each zone, if they are concurrent, they will be connected by a hyphen "-"; if they are supposed to be one after another in succession, they will be connected by a hyphen followed by a greater than mark ">". There are supposed to be no overlaps and gaps between the adjacent zones. That is to say, all the typical species are supposed to exist or last within the zone they are assigned to, but not to exceed the range of the zone, which is no other than the essence of biochronology, the organization of geologic time according to the irreversible process of evolution in the organic continuum.

1. *Promimomys asiaticus*-?>*Mimomys bilikeensis*->*M. teilhardi* Zone This zone is represented by *Promimomys asiaticus* from Huainan, Anhui, *Mimomys bilikeensis* from Bilike, Inner Mongolia, *Mimomys teilhardi*, and *Villnayia* sp. nov. from Gaotege, Inner Mongolia. *Promimomys asiaticus* was proposed by JIN AND ZHANG (2005) based on a left mandible with $M_{1\sim2}$ (V14006) discovered from the cave sediments of Dajushan, Huainan, Anhui. They thought the age of this fauna should be early Early Pliocene (equivalent to European Mammal Neogene zone MN14a). The age of Bilike fauna that *Mimomys bilikeensis* came from was thought to be Early Pliocene (equivalent of MN14). *Mimomys teilhardi* is from DB02-5~6, DB02-1~4, and DB03-1 layers of Gaotege section (Fig. 4). The magnetostratigraphic study result of XU ET AL. (2007) shows that DB02-5~6 and DB02-1~4 fall into the C3n.1n~C3n.1r chron, and DB03-1 is located slightly above C3n.1n (Fig. 4). According to their result, the absolute ages of these three layers are around 4.40~4.35 Ma, 4.20 Ma, and 4.15 Ma, respectively. It has been generally accepted that the genus *Promimomys* evolved from a cricetid form of the genus *Microtodon*, and the ancestor-descendant relation between the genus *Promimomys* and the genus *Mimomys* has also

been widely acknowledged. European researchers usually used the FAD of *Promimomys* to indicate the beginning of the European Mammal Neogene zone MN14 (e.g. AGUSTÍ ET AL., 2001). But here some morphological conflicts are met between the only *Promimomys* species, *P. aisaticus*, and the most primitive *Mimomys* species of China, *M. bilikeensis*. As mentioned by LI (2006) in his doctoral thesis, *Promimomys aisaticus* does have some primitive character, like no trace of *Mimomys*-angle observed on it ACC of M_1, but, on the other hand, the HH-index of *Promimomys aisaticus* is indeed higher (0.51 mm, LI, 2006) than that of *Mimomys bilikeensis* (0.20). Now that *Promimomys* has occured in East China, it is reasonable to believe that it should also occur in North China, especially in Inner Mongolia, where the ancestral form *Microtodon atavus* has been discovered in large quantities (FAHLBUSCH AND MOSER, 2004). So the relationship between *Promimomys aisaticus* and *Mimomys bilikeensis* is left open to discussion until more materials become available. At present, *Promimomys aisaticus* is doubtfully thought to be more ancient in time, and use it to mark the commencement of this zone, but the exact age of this boundary is still not clear. *Mimomys bilikeensis - Mimomys teilhardi* is, in fact, a gradually transforming series, so it will be impractical if a zone boundary is defined somewhere between the two species. The gradualism is reflected by: the HH-index increased from 0.20 mm to 0.39 mm; SDQ increased from 102 to 111; the *Mimomys*-angle increasingly became stronger; root number of M^3 decreased form three to two; and so on. The upper boundary of this zone is defined by the highest stratigraphic datum, DB03-1, of *Mimomys teilhardi* on Gaotege section, the age of which is around 4.15 Ma. After that, it seems that conspicuous changes happened in the DB03-2 arvicolid fauna of Gaotege section (discussed in the next zone). The author also observed the *Mimomys* sp. from YS4 of Nanzhuanggou Member, Gaozhuang Formation, Yushe, Shanxi, reported by FLYNN ET AL. (1997). Even though there are only two specimens, one nearly worn-out left M_1 of an aged individual and one right M^3 of a juvenile individual, and the nearly worn-out left M_1 doesn't provide much useful information, the juvenile M^3 does show some similar characters with *Mimomys teilhardi* from Gaotege section, such as two enamel islets, both posterior and anterior; nearly flat sinuous line, and so on. As a consequence, this zone can be correlated to the early Gaozhuangian (NMU12) in DENG (2006).

2. *Mimomys orientalis* Zone This zone is represented by *Mimomys* cf. *M. orientalis*, *Villanyia* sp. 1, and *Villanyia* sp. 2 from DB03-2 of Gaotege, Inner Mongolia, and *Mimomys orientalis* from Youhe, Weinan, Shaanxi. Because of sampling problem, the magnetostratigraphic work of XU ET AL. (2007) didn't cover the DB03-2 layer of Gaotege section. They just concluded a later than 4.072 Ma age for the DB03-2 layer. First the

succession of this zone following the zone 1 above is mainly based on the datum of appearances on Gaotege section, and the "stage of evolution" of the *Mimomys* lineage well established here. The upper boundary of zone 1 can be regarded as the lower boundary of this zone. Upper boundary can not be designated at present. For that reason, this zone can only be defined by typical species. The most conspicuous changes of *Mimomys* cf. *M. orientalis* compared with its ancestral form *Mimomys teilhardi* are occurrence of cementum in the reentrant angles of molars, and dramatically increased HH-index (1.29 mm). The reason that *Mimomys orientalis* is assigned to represent this zone is that it is apparently in the similar stage of evolution with *Mimomys* cf. *M. orientalis* from Gaotege because of comparable HH-index, and all other similar characters. This zone can be probably correlated to the late Gaozhuangian (NMU12) of DENG (2006).

3. *Mimomys youhenicus->Omniprocessimys peii* Zone This zone is represented by *Mimomys youhenicus* from Youhe, Weinan, Shaanxi and *Mimomys peii* from Dachai, Xiangfen, Shanxi. No species studied or restudied in this thesis can be assigned to this zone. The assignment of *Mimomys youhenicus* and *Mimomys peii* to represent this zone is totally based on the "stage of evolution". In this case, the two *Mimomys* lineages established here. The considerablely greater HH-index (3.07 mm) of *Mimomys youhenicus* than its ancestral forms *M. orientalis* (1.05 mm) and *Mimomys* cf. *M. orientalis* (1.29 mm) and the stronger *Mimomys*-angle close to BSA3 and so on than its descendant form *Mimomys gansunicus* are indicative of the suitability to seriate this zone after the *Mimomys orientalis* zone and before the next zone with the typical species, *Mimomys gansunicus*. Moreover, the other form *Omniprocessimys peii* is apparently more primitive than its descendant form *Omniprocessimys parallelus*, another typical species of the next zone that will be discussed next, on account of having roots on all molars, and weaker undulation of sinuous line. Within this zone, *Mimomys youhenicus* is thought to precede *Omniprocessimys peii* in time owing to the fact that the former one has a lower HH-index, while the later one's Hsd and Hsld are so high that they penetrated the crown height even in young individuals. The *Mimomys irtyshensis* from YS99 and YS105 of Mazegou Formation, Yushe, Shanxi reported by FLYNN EA AL. (1997) is indeed a form more primitive than *Mimomys gansunicus*, and probably represents the similar "stage of evolution" with *Mimomys youhenicus*. Consequently, this zone can supposably be compared with Mazegouan (NMU13) of DENG (2006). But both the lower boundary and the upper can not be decided based on the present knowledge, so this zone are just characterized by the appearance or existence of these two species.

4. *Mimomys gansunicus-Villanyia fanchangensis-Omniprocessimys parallelus* Zone

This zone is characterized by the co-occurrence of *Mimomy gansunicus*, *Villanyia* and *Borsodia* in North China, e.g. *Mimomys gansunicus*, *Villanyia* cf. *V. fanchangensis* and *Borsoida* sp. on 93001 section, Lingtai, Gansu, and by the co-occurrence of *Mimomys gansunicus*, *Omniprocessimys parallelus* and *Villanyia fanchangensis* in East China, e.g. Renzidong, Anhui. As mentioned before, the 2.4~2.0 Ma age assigned to Renzidong fauna by JIN ET AL. (2000) is acceptable, but the Renzidong arvicolid fauna can not represent a very long geological time interval, because they are all discovered from the cave-fissure sediments. While on 93001 section of Lingtai, *Mimomys gansunicus* is recorded from WL15 to WL8, and then a descendant form of it, *Allophaiomys deucalion*, appeared for the first time at WL6 of 93001 section. *Villanyia* cf. *V. fanchangensis* is recorded from WL11 to WL6. So it seems that the last appearances of *Mimomys gansunicus* and *Villanyia* cf. *V. fanchangensis* are recorded at WL8 and WL7, respectively. In this case, the geological time representing the boundary between WL7 and WL6 is preferred to define the upper boundary of this zone, and the lower boundary of the next zone at the same time, because the first appearance of *Allophaiomys deucalion*, the dsecendant of *Mimomys gansunicus* appeared from WL6. But because of the age problem of 93001 section discussed before, the exact age will be left undetermined until sufficient knowledge is accumulated. As for the lowest stratigraphic datum (LSD), WL15-2, of *Mimomys gansunicus*, that it can really represent the real first appearance of this species or not is still a question open to discussion, because *Mimomys gansunicus* from Lingtai is probably not so primitive as *Mimomys gansunicus* from Renzidong as discussed before. On the other section of Lingtai, the arvicolid materials from which are studied here, 72074(4) section, *Mimomys gansunicus* is recorded in L1-1, but there is only one specimen, a left mandible with $M_{1\sim2}$, and no *Mimomys gansunicus* is recorded in lower layers of this section. *Mimomys gansunicus* of L1-1 on 72074(4) section does not show more primitive characters than *Mimomys gansunicus* from Renzidong fauna. At present, the first appearance of *Mimomys gansunicus* will be used to define the lower boundary of this zone, but here it will be left undetermined until the discovery of a suitable section where the first appearance of *Mimomys gansunicus* is recorded. This zone can be correlated to the Nihewanian in the sense of FLYNN ET AL. (1997), because *Mimomys gansunicus*, *Borsoida chinensis* were discovered from YS109, YS6, YS120 of the Haiyan Formation, Yushe, Shanxi. Besides, another arvicolid form closely resembling *Villanyia fanchangensis* were observed by the present author.

5. *Allophaiomys deucalion-Borsodia chinensis* Zone This zone is characterized by the co-occurrence of *Allophaiomys deucalion* and *Borsodia chinensis*. According to the

magnetostratigraphic study result by ZHU ET AL. (2001), the culture layer of Xiaochangliang Paleolithic site was dated at 1.36 Ma. The author sampled the culture layer of this site, and obtained 10 forms of small mammals (ZHANG ET AL., in press) using screen-washing method. *Allophaiomys deucalion* and *Borsodia chinensis* were also included in them. This is the only well-dated layer within this zone. Besides *Allophaiomys deucalion* is also recorded at WL6~WL2+ on 93001 section, Lingtai, Gansu. As discussed in the former zone, the lower boundary of this zone is determined by the first apparence of *Allophaiomys deucalion* recorded at WL6 of 93001 section. What can be concluded now is that this boundary should at least be older than the culture layer of Xiaochangliang site. As for the upper boundary, at present, it will be left undetermined, but, at least, it should be younger than the culture layer of Xiaochangliang site, and should be defined by the last appearance of *Allophaiomys deucalion* or *Borsodia chinensis*, or both of them.

Acknowledgements

Among all studied or re-studied localities, the author only did the field work of Xiaochangliang site by himself. As for the fossil materials from all the other localities, the author is overwhelmed by the generosity of the chief researchers of these localities who or whose team worked hard in the field to collect the fossils and granted the author the opportunities to study or restudy all the fossil materials. These kind chief researchers are Prof. SHAOHUA ZHENG, Prof. ZHAOQUN ZHANG (IVPP, CAS) of Lingtai, Prof. CHANGZHU JIN (IVPP, CAS) of Renzidong, Prof. ZHUDING QIU (IVPP, CAS) of Bilike, and Dr. QIANG LI (IVPP, CAS) of Gaogete. The author is extremely grateful to all the chief researchers. The author is also grateful to Academician ZHANXIANG QIU (IVPP, CAS) for the valuable discussion about the works done in Yushe Basin, Shanxi. I am also thankful for the kindness of Prof. XING XU (IVPP, CAS) who allowed me to photograph specimens I observed during my stays at IVPP.

During my study life of these three and a half years in Japan, Prof. YOSHINARI KAWAMURA of Aichi University of Education and Curator HIROYUKI TARUNO of Osaka Museum of Natural History not only directed my study, but also helped me a lot to get used to Japan. I gratefully acknowledge them. I am also grateful to Prof. SHUSAKU YOSHIKAWA, Prof. HISAO KUMAI, Prof. MUNEKI, MITAMURA, Dr. KOTARO, HIROSE, Dr. JUN INOUE, Dr. AKIKO MURAKAMI, Dr. AKIRA TSUJIMOTO and others of my lab, Natural History of Anthropogene Lab., Department of Biology & Geosciences / Graduate School of Science, Osaka City University, who helped me a lot on both my daily life and my research.

I greatly appreciate their help and give my grateful thanks to them for all the good memories they brought to me.

I also want to express my gratitude to my wife SHUXIAN GUAN and my parents. Without their support, I can not finish my doctoral thesis.

References

AGUSTÍ, J., CABRERA, L., GARCES, M., KRIJGSMAN, W., OMS, O., AND PARES, J. M. (2001). A calibrated mammal scale for Neogene of Western Europe-State of the art. *Earth-Science Reviews* **52,** 247-260.

BELL, C. J., LUNDELIUS JR., E. L., BARNOSKY, A. D., GRAHAM, R. W., LINDSAY, E. H., RUEZ JR., D. R., SEMKEN JR., H. A., WEBB, S. D., AND ZAKRZEWSKI, R. J. (2004). The Blancan, Irvingtonian, and Rancholabrean Mammal Ages. *In* "Late Cretaceous and Cenozoic Mammals of North America." (M. O. WOODBURNE, Ed.). Columbia University Press, New York.

CAI, B. Q., ZHANG, Z. Q., ZHENG, S. H., QIU, Z. D., LI, Q., AND LI, Q. (2004). New advances in the stratigraphic study on representative sections in the Nihewan Basin, Hebei. *Professional Papers of Stratigraphy and Paleontology* **28,** 267-285.

CARLS, N., AND RABEDER, G. (1988). Arvicolids (Rodentia, Mammalia) from the Earliest Pleistocene of Schernfeld (Bavaria). *Beitrage zur Palaontologie von Osterreich* **14,** 123-238.

CHIU, C. S., LI, C. K., AND CHIU, C. T. (1979). The Chinese Neogene: a preliminary review of the mammalian localities and faunas. *Ann. Geol. Pays. Hell., Hors. Ser.* **1,** 263-272.

CRUSAFONT-PAIRO, M. (1950). La euestion del llamado Meotico espanol. *Arrahona* **1,** 25-36.

CRUSAFONT-PAIRO, M. (1951). El sistema Miocénico en la depresion Española del Vallés-Penedés. *In* "Int. Geol. Congr. Rep. XVIII Session." pp. 33-43, Great Britain.

CRUSAFONT-PAIRO, M. (1965). Observations à un travail de M. Freudenthal et P. Y. Sondaar sur des nouveaux gisements à *Hipparion* d'Espagne. *Koninkl Nederl Akademie van Wetenschappen. Amsterdam, Proc., B* **68,** 121-126.

DENG, T. (2006). Chinese Neogene mammal biochronology. *Vertebrata PalAsiatica* **44,** 143-163.

ERBAJEVA, M. A. (1998). Late Pliocene Itantsinian faunas in Western Transbaikalia. *The Dawn of the Quaternary* **60,** 417-429.

ERBAJEVA, M. A. (1998). *Allophaiomys* in the Baikalian region. *Paludicola* **2,** 20-27.

FAHLBUSCH, V. (1976). Report on the International Symposium on Mammalian Stratigraphy of the European Tertiary. *Newsletter Stratigraphy* **5,** 160-167.

FAHLBUSCH, V., AND MOSER, M. (2004). The Neogene mammalian faunas of Ertemte and Harr Obo in Inner Mongolia (Nei Mongol), China. - 13. The genera *Microtodon* and *Anatolomys* (Rodentia, Cricetidae). *Senckenbergiana lethaea* **84,** 323-349.

FEJFAR, O., HEINRICH, W.-D., PEVZNER, M. A., AND VANGENGEIM, E. A. (1997). Late Cenozoic sequences of mammalian sites in Eurasia: an updated correlation. *Palaeogeography, Palaeoclimatology, Palaeoecology* **133,** 259-288.

FEJFAR, O., AND REPENNING, C. A. (1998). The ancestors of the lemmings (Lemmini, Arvicolinae, Cricetidae, Rodentia) in the Early Pliocene of Woelfersheim near Frankfure am Mainz, Germany. *Senckenbergiana lethaea* **77,** 161-193.

FLYNN, L. J., WU, W. Y., AND DOWNS, W. R. (1997). Dating vertebrate microfaunas in the late Neogene record of Northern China. *Palaeogeography, Palaeoclimatology, Palaeoecology* **133,** 227-242.

FORSYTH-MAJOR, C. I. (1902). Exhibition of, and remarks upon some jaws and teeth of Pliocene voles (*Mimomys* gen. nov.). *Zoological Society of London Proceedings* **1,** 102-107.

GROMOV, I. M., AND POLYAKOV, I. Y. (1977). "Voles (Microtinae)." E. J. Brill Publishing Co., New Delhi.

HEINRICH, W.-D. (1978). Zur biomertrischen Efassung eines Evolutionstrends bei *Arvicola* (Rodentia, Mammalia) aus dem Pleistozän Thüringens. *Säugetierkdl. Inform.* **2,** 3-21.

HINTON, M. A. C. (1926). "Monograph of the Voles & Lemmings (Microtinae). Living and Extinct." The British Museum (Natural History), London.

JIN, C. Z., AND ZHANG, Y. Q. (2005). First discovery of *Promimomys* (Arvicolidae) in East Asia. *Chinese Science Bulletin* **50,** 327-332.

JIN, C. Z., ZHENG, L. T., DONG, W., LIU, J. Y., XU, Q. Q., HAN, L. G., ZHENG, J. J., WEI, G. B., AND WANG, F. Z. (2000). The Early Pleistocene deposits and mammalian fauna from Renzidong, Fanchang, Anhui Province, China. *Acta Anthropologica Sinica* **19,** 184-198.

KAWAMURA, Y. (1988). Quaternary Rodent Faunas in the Japanese Islands (Part I&II). *Memoirs of the Faculty of Science, Kyoto University, Series of Geology and Mineralogy* **53,** 31-348.

KOWALSKI, K. (1960). Pliocene Insectivores and Rodents from Rebielice Krolewskie (Poland). *Acta Zoologica Cracoviensia* **5,** 155-192.

KOWALSKI, K. (2001). Pleistocene Rodents of Europe. *Folia Quaternaria* **72,** 3-389.

KRETZOI, M. (1990). History of research of fossil arvicolids. *In* "International symposium: Evolution, Phylogeny and Biostratigraphy of Arvicolids (Rodentia, Mammalia)." (O. FEJFAR, AND W.-D. HEINRICH, Eds.), pp. 305-312. Geological Survey, Prague, Rohanov (Czechoslovakia).

LI, C. K., WU, W. Y., AND QIU, Z. D. (1984). Chinese Neogene: subdivision and correlation. *Vertebrata PalAsiatica* **22,** 163-178.

LI, Q. (2006). Pliocene Rodents from the Gaotege Fauna, Nei Mongol (Inner Mongolia). *PH. D. Dissertation of The Chinese Academy of Sciences*.

LI, Q., WANG, X. M., AND QIU, Z.-D. (2003). Pliocene Mammalian Fauna of Gaotege in Nei Mongol (Inner Mongolia), China. *Vertebrata PalAsiatica* **41,** 104-114.

LIEBERMAN, D. E. (1994). The Biological Basis for Seasonal Increments in Dental Cementum and Their Application to Archaeological Research. *Journal of Archaeological Science* **21,** 525-539.

LINDSAY, E. H. (2003). Chronostratigraphy, Biochonology, Datum Events, Land Mammal Ages, Stage of Evolution, and Appearance Event Ordination. *In* "Vertebrate Fossils and Their context." (L. J. FLYNN, Ed.), pp. 212-230. American Museum of Natural History.

LINDSAY, E. H. (1990). The setting. *In* "European Neogene Mammal Chronology." (E. H. LINDSAY, V. FAHLBUSCH, AND P. MEIN, Eds.), pp. 1-14. Plenum Press, Schloss Reisensburg, Germany.

MADDISON, D. R., AND MADDISON, W. P. (2003). MacClade 4: Analysis of phylogeny and character evolution. Version 4.08. Sinauer Associates, Sunderland, Massachusetts.

MARKS, P. (1971). Turolian. *G. Geol. Bologna* **37,** 209-213.

MATSUMOTO, T. (1997). Histological Study of Lower Molar Teeth in Japanese Field Voles, *Microtus montebelli*. *Journal of Kyushu Dental Society* **51,** 639-649.

MCKENNA, M. C., AND BELL, S. K. (1997). "Classification of mammals above species level." Columbia University Press, New York.

MEIN, P. (1975). Résultats de groupe de travail des vertébrés: Biozonation du Néogène méditerranéen àpartir des mammifères. *In* "Report on Activity of the RCNMS Working Groups (1971-1975)." (J. SENES, Ed.), pp. 78-81, Bratislava.

MEIN, P. (1979). Rapport d'activité de travail vertebres mise à jour de la biostratigraphie du Néogene basée sur les mammifères. *Ann. Géol. Pays Hellén., Tome hors serie 1979***,** 1367-1372.

MEIN, P. (1990). Updating of MN Zones. *In* "European Neogene Mammal Chronology." (E. H. LINDSAY, V. FAHLBUSCH, AND P. MEIN, Eds.), pp. 73-90. Plenum Press, New York, Schloss Reisensburg, Germany.

OMS, O., DINARES-TURELL, J., AGUSTI, J., AND PARES, J. M. (1999). Refinements of the European Mammal Biochronology from the Magnetic Polarity Record of the Plio-Pleistocene Zujar Section, Guadix-Baza Basin, SE Spain. *Quaternary Research* **51,** 94-103.

PEI, W. C. (1939). New fossil material and artifacts collected from the Choukoutien region during the years 1937~39. *Bull. Geol. Soc. China* **19,** 207-234.

QIU, Z. D. (1988). Neogene micromammals of China. *In* "The palaeoenvironment of East Asia from the Mid-Tertiary." (P. WHYTE, Ed.), pp. 834-848, Hong Kong.

QIU, Z. D., AND STORCH, G. (2000). The early Pliocene Micromammalian Fauna of Bilike, Inner Mongolia, China (Mammalia: Lipotyphla, Chiroptera, Rodentia, Lagomorpha). *Senckenbergiana lethaea* **80,** 173-229.

QIU, Z. X. (1990). The Chinese Neogene Mammalian Biochronology - Its Correlation with the European Neogene Mammalian Zonation. *In* "European Neogene Mammal Chronology." (E. H. LINDSAY, V. FAHLBUSCH, AND P. MEIN, Eds.), pp. 527-556. Plenum Press, New York, Schloss Reisensburg, Germany.

QIU, Z. X., AND QIU, Z. D. (1995). Chronological sequence and subdivision of Chinese Neogene mammalian faunas. *Palaeogeography, Palaeoclimatology, Palaeoecology* **116,** 41-70.

QIU, Z. X., WU, W. Y., AND QIU, Z. D. (1999). Miocene Mammal Faunal Sequence of China: Palaeozoogeography and Eurasian Relations. *In* "The Miocene Land Mammals of Europe." (G. E. RÖSSNER, AND K. HEISSIG, Eds.), pp. 443-455. Verlag Dr. Friedrich Pfeil, München.

RABEDER, G. (1981). Die Arvicoliden (Rodentia, Mammalia) aus dem Pliozän und dem alteren Pleistozän von Niederösterreich. *Beiträge zur Paläontologie von Österreich* **8,** 1-373.

REPENNING, C. A. (1987). Biochronology of the Microtine Rodents of the United States. *In* "Cenozoic mammals of North America: geochronology and biostratigraphy." (M. O. WOODBURNE, Ed.), pp. 236-268. University of California Press, Berkeley.

REPENNING, C. A. (1992). *Allophaiomys* and the Age of the Olyor Suite, Krestovka Sections, Yakutia. *U.S. Geological Survey Bulletin* **2037,** 1-95.

REPENNING, C. A. (2003). *Mimomys* in North America. *Bulletin of the American Museum of Natural History* **279,** 469-512.

REPENNING, C. A., FEJFAR, O., AND HEINRICH, W.-D. (1990). Arvicolid rodent biochronology of the Nothern Hemisphere. *In* "International symposium: Evolution, Phylogeny and Biostratigraphy of Arvicolids (Rodentia, Mammalia)." (O. FEJFAR, AND W.-D. HEINRICH, Eds.), pp. 385-418. Geological Survey, Prague, Rohanov (Czechoslovakia).

REPENNING, C. A., AND GRADY, F. (1988). The microtine rodents of the Cheetah Room fauna, Hamilton Cave, West Virginia, and the spontaneous origin of *Synaptomys*. *U.S. Geological Survey Bulletin* **1853,** 1-32.

ROSE, K. D. (1981). The Clarkforkian land-mammal age and mammalian faunal composition across the Paleocene-Eocene boundary. *Univ. Michigan Papers in Paleontology* **26,** 1-197.

SALVADOR, A. (1994). "International stratigraphic guide." Boulder, CO: Geological Society of America, Inc.

SAVAGE, D. E. (1977). Aspects of vertebrate paleontological stratigraphy and geochronology. *In* "Concepts and Methods in Biostratigraphy." (E. G. KAUFFMAN, AND J. E. HAZEL, Eds.), pp. 427-442.

STEININGER, F. F., BERNOR, R. L., AND FAHLBUSCH, V. (1990). European Neogene Marine/ Continental Chronologic Correlations. *In* "European Neogene Mammal Chronology." (E. H. LINDSAY, V. FAHLBUSCH, AND P. MEIN, Eds.), pp. 15-46. Plenum Press, New York, Schloss Reisensburg, Germany.

TANG, Y. J., LI, Y., AND CHEN, W. Y. (1995). Mammalian fossils and the Age of Xiaochangliang Paleolithic Site of Yangyuan, Hebei. *Vertebrata PalAsiatica* **33,** 74-83.

TEDFORD, R. H. (1970). Principles and practices of mammalian geochronology in North America. *In* "North American Paleontological Convention, 1969." pp. 666-703.

TEDFORD, R. H., FLYNN, L. J., QIU, Z. X., OPDYKE, N. D., AND DOWNS, W. R. (1991). Yushe Basin, China; Paleomagnetically calibrated mammalian biostratigraphic standard for the Late Neogene of Eastern Asia. *Journal of Vertebrate Paleontology* **11,** 519-526.

TEILHARD DE CHARDIN, P. (1926). Étude géologique sur la région du Dalai-Noor. *Mém. Soc. Géol France* **7,** 1-56.

TEILHARD DE CHARDIN, P., AND PIVETEAU, J. (1930). Les mammifères fossilles de Nihowan (Chine). *Ann. Pal.* **19,** 1-134.

TONG, Y. S., ZHENG, S. H., AND QIU, Z. D. (1995). Cenozoic Mammal Ages of China. *Vertebrata PalAsiatica* **33,** 290-314.

VAN DER MEULEN, A. J. (1973). Middle Pleistocene smaller mammals from the Monte Peglia (Orvieto, Italy) with special reference ot the phylogeny of *Microtus* (Arvicolidae, Rodentia). *Quaternaria* **17,** 1-144.

WEI, L. Y., CHEN, M. Y., ZHAO, H. M., AND SUN, J. M. (1993). Magnetostratigraphic study on the Late Miocene-Pliocene Lacustrine sediments near Leijiahe. *In* "Monograph of the meeting in hornor of Prof. YUAN FULI on the Hundredth Anniversary of his Birth. Beijing." pp. 63-69. Geological Publishing House, Beijing.

WEI, Q. (1999). The framework of archaeological geology of the Nihewan Basin. *In* "Evidence for evolution - Essays in honor of Prof. CHUNCHIEN YOUNG on the hundredth anniversary of his birht." pp. 193-207. Ocean Press.

WILSON, D. E., AND REEDER, D. M. (1993). "Mammal species of the world - A taxonomic and Geographic Reference." Smithsonian Institution Press, Washington and London.

WOOD, H. E., CHANEY, R. W., CLARK, J., COLBERT, E. H., JEPSEN, G. L., REESIDE, J. B., AND STOCK, C. (1941). Nomenclature and correlation of the North American continental Tertiary. *Geological Society of America Bulletin* **52,** 1-48.

WOODBURNE, M. O. (1987). "Cenozoic Mammals of North America." University California Press, Berkeley.

WOODBURNE, M. O. (2004). " Late Cretaceous and Cenozoic Mammals of North America. " Columbia University Press, New York.

XU, Y. L., TONG, Y. B., LI, Q., SUN, Z. M., PEI, J. L., AND YANG, Z. Y. (2007). Magnetostratigraphic Dating on the Pliocene Mammalian Fauna of the Gaotege Section, Central Inner Mongolia. *Geological Review* **53,** 250-261.

XUE, X. X. (1981). An Early Pleistocene Mammalian Fauna and its Stratigraphy of the River You, Weinan, Shensi. *Vertebrata PalAsiatica* **19,** 35-44.

YANG, Z. G., LIN, H. M., ZHANG, G. W., AND WANG, S. J. (1996). Lower Pleistocene in the Nihewan Basin. *In* "Quaternary stratigraphy in China and its international correlation." (Z. G. YANG, AND H. M. LIN, Eds.), pp. 109-130. Geological Publishing House.

YOUNG, C. C. (1935). Miscellaneous Mammalian Fossils from Shansi and Honan. *Palaeotologia Sinica* **9**.

ZAZHIGIN, V. S. (1980). Late Pliocene and Anthropogene Rodents of the South of Western Siberia. *Academy of Sciences of the USSR. Transactions* **339,** 1-156.

ZHANG, Z. Q., AND ZHENG, S. H. (2000). Late Miocene-Early Pliocene Biostratigraphy of Loc. 93002 Section, Lingtai, Gansu. *Vertebrata PalAsiatica* **38,** 274-286.

ZHANG, Z. Q., AND ZHENG, S. H. (2001). Late Miocene-Pliocene Biostratigraphy of Xiaoshigou section, Lingtai, Gansu. *Vertebrata PalAsiatica* **39,** 54-66.

ZHENG, S. H. (1976). A Middle Pleiostocene Micromammal Fauna from Heshui, Gansu. *Vertebrata Palasiatica* **14,** 112-119.

ZHENG, S. H. (1994). Preliminary report on the late Miocene-Early Pleistocene micromammals collected from Lingtai of Gansu, China in 1992 and 1993. *Northern Hemisphere Geo-Bio Travers* **2,** 44~56.

ZHENG, S. H., AND LI, C. K. (1986). A review of Chinese *Mimomys* (Arvicolidae, Rodentia). *Vertebrata PalAsiatica* **24,** 81-109.

ZHENG, S. H., AND LI, C. K. (1990). Comments on fossil arvicolids of China. *In* "International symposium: Evolution, Phylogeny and Biostratigraphy of Arvicolids (Rodentia, Mammalia)." (O. FEJFAR, AND W.-D. HEINRICH, Eds.), pp. 431-442. Geological Survey, Prague, Rohanov (Czechoslovakia).

ZHENG, S. H., WU, W. Y., LI, Y., AND WANG, G. D. (1985). Late Cenozoic Mammalian Faunas of Guide and Gonghe Basin, Qinghai Province. *Vertebrata PalAsiatica* **23,** 89-134.

ZHENG, S. H., AND ZHANG, Z. Q. (2000). Late Miocene-Early Pleistocene Micromammals from Wenwanggou of Lingtai, Ganus, China. *Vertebrata PalAsiatica* **38,** 58~71.

ZHENG, S. H., AND ZHANG, Z. Q. (2001). Late Miocene-Early Pleistocene Biostratigraphy of the Leijiahe Area, Lingtai, Gansu. *Vertebrata PalAsiatica* **39,** 215-228.

ZHU, R., HOFFMAN, K. A., POTTS, R., DENG, C. L., Y, X. P., GUO, B., SHI, C. D., GUO, Z. T., YUAN, B. Y., HOU, Y. M., AND HUANG, W. W. (2001). Earliest presence of humans in northeast Asia. *Nature* **413,** 413-417.

ZONG, G. F. (1987). Note on Some Mammalian Fossils from the Early Pleistocene of Di-Qing County, Yunnan. *Vertebrata PalAsiatica* **25,** 69-76.

ZONG, G. F., TANG, Y. J., XU, Q. Q., AND YU, Z. Q. (1982). The Early Pleistocene in Tunliu, Shanxi. *Vertebrata PalAsiatica* **20,** 236-247.

PLATES

PLATE 1

(Scale bar = 1 mm for occlusal view, and 2.5 mm for lateral view)

Mimomys bilikeensis (QIU AND STORCH, 2000)

Bilike, Huade County, Inner Mongolia

Figs. 1~16—M_1

1, V11909.1069	2, V11909.1084	3, V11909.1087	4, V11909.1089
5, V11909.1099	6, V11909.1104	7, V11909.1114	8, V11909.1124
9, V11909.1137	10, V11909.1143	11, V11909.1155	12, V11909.1309
13, V11909.1166	14, V11909.1190	15, V11909.1201	16, V11909.1202

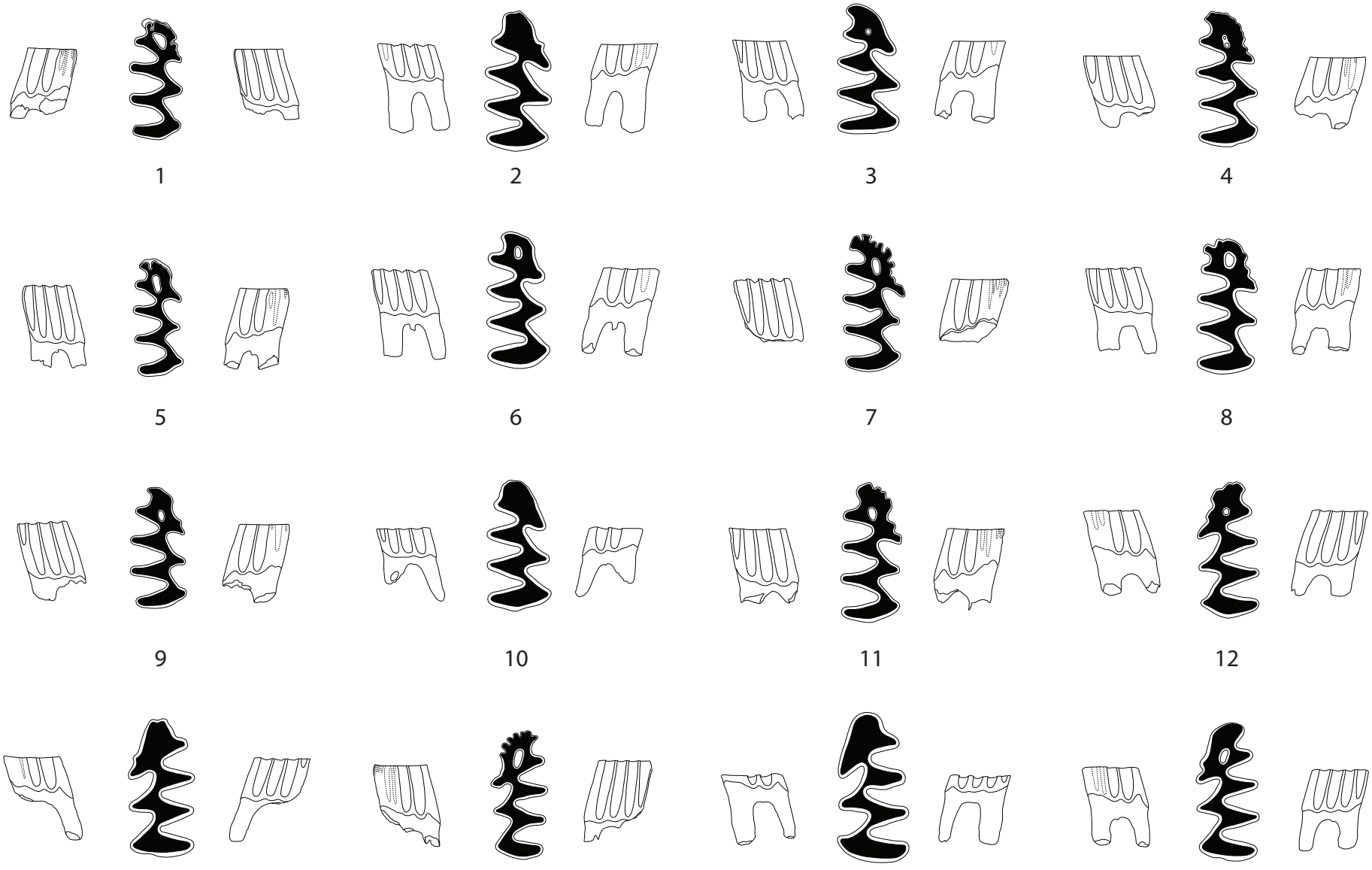

PLATE 1

PLATE 2

(Scale bar = 1 mm for occlusal view, and 2.5 mm for lateral view)

Mimomys bilikeensis (QIU AND STORCH, 2000)

Bilike, Huade County, Inner Mongolia

Figs. 1~4 — M_2

1, V11909.1518 2, V11909.1520 3, V11909.1526 4, V11909.1568

Figs. 5~8 — M_3

5, V11909.1861 6, V11909.1862 7, V11909.1864 8, V11909.1887

Figs. 9~12 — M^1

9, V11909.60 10, V11909.65 11, V11909.143 12, V11909.226

Figs. 13~16 — M^2

13, V11909.538 14, V11909.556 15, V11909.559 16, V11909.583

1

2

3

4

5

6

7

8

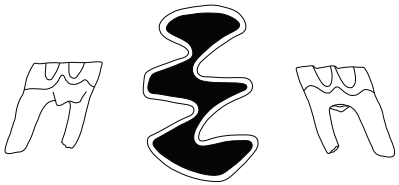

9

10

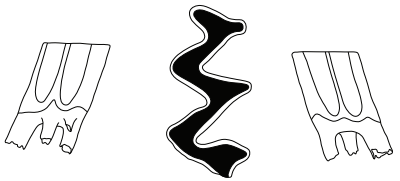

11

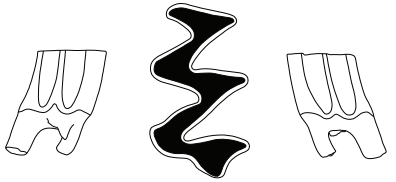

12

13

14

15

16

PLATE 2

PLATE 3

(Scale bar = 1 mm for occlusal view, and 2.5 mm for lateral view)

Mimomys bilikeensis (QIU AND STORCH, 2000)

Bilike, Huade County, Inner Mongolia

Figs. 1~4 — M^3

1, V11909.720	2, V11909.722	3, V11909.726	4, V11909.737
5, V11909.751	6, V11909.769	7, V11909.781	8, V11909.821
9, V11909.830	10, V11909.835	11, V11909.870	12, V11909.895
13, V11909.904	14, V11909.931	15, V11909.946	16, V11909.1000

1

2

3

4

5

6

7

8

9

10

11

12

13

14

15

16

PLATE 3

PLATE 4

(Scale bar = 1 mm for occlusal view, and 2.5 mm for lateral view)

Mimomys teilhardi LI, 2006

Gaotege, Inner Mongolia

Figs. 1~16 M_1

1, VXXX19.171	2, VXXX19.172	3, VXXX19.199	4, VXXX19. 154
5, VXXX19.400	6, VXXX19.545	7, VXXX19.547	8, VXXX19.548
9, VXXX19.550	10, VXXX19.551	11, VXXX19.656	12, VXXX19.657
13, VXXX19.661	14, VXXX19.689	15, VXXX19.690	16, VXXX19.694

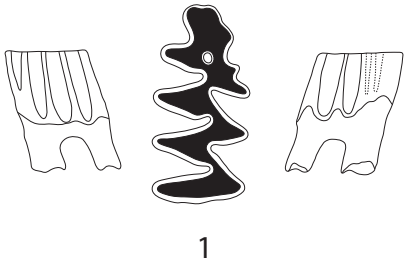

1

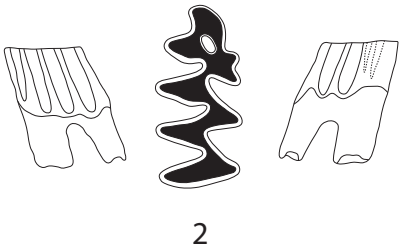

2

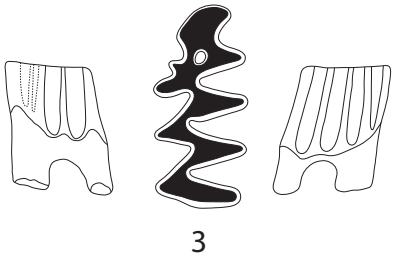

3

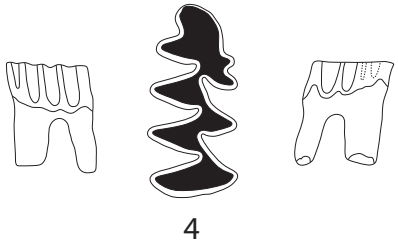

4

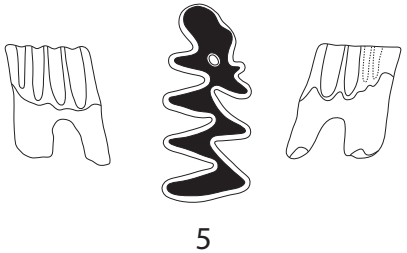

5

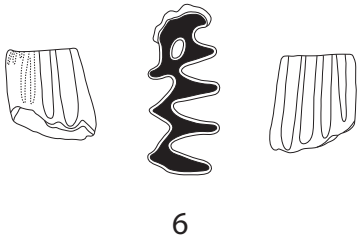

6

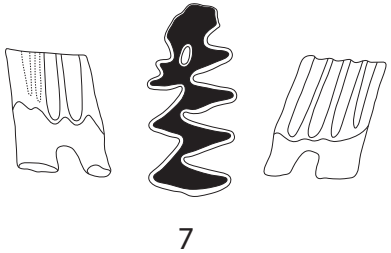

7

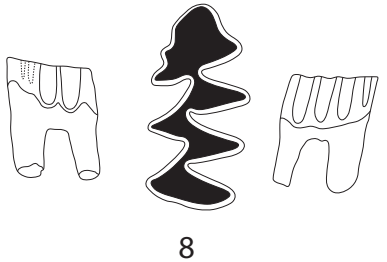

8

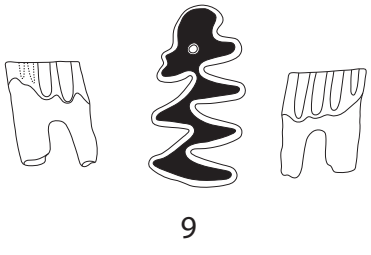

9

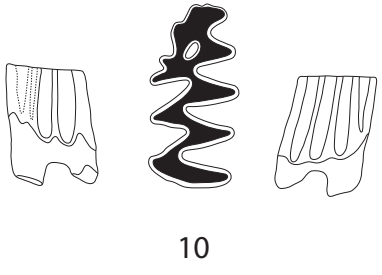

10

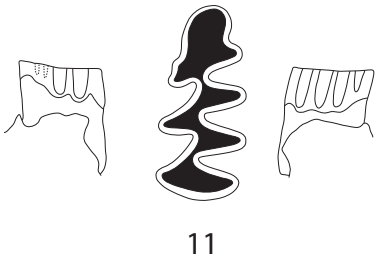

11

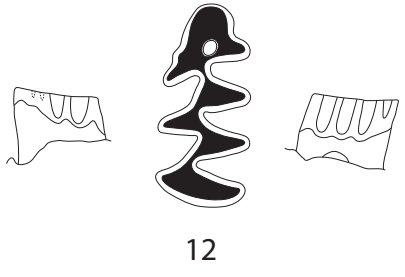

12

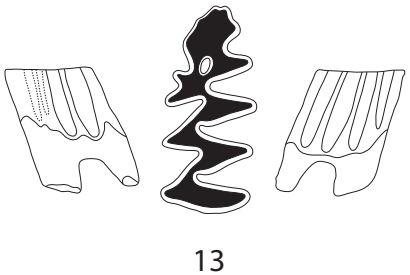

13

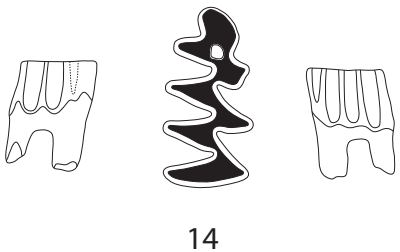

14

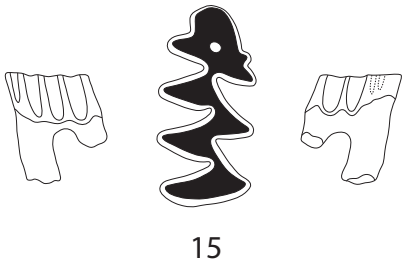

15

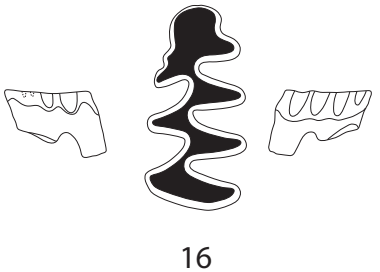

16

PLATE 4

PLATE 5

(Scale bar = 1 mm for occlusal view, and 2.5 mm for lateral view)

Mimomys teilhardi - *Villanyia* sp. nov. COMPLEX

Gaotege, Inner Mongolia

Figs. 1~4 — M_2

1, VXXX19.218 2, VXXX19.420 3, VXXX19.564 4, VXXX19.698

Figs. 5~8 — M_3

5, VXXX19.294 6, VXXX19.446 7, VXXX19.583 8, VXXX19.705

Figs. 9~12 — M^1

9, VXXX19.26 10, VXXX19.332 11, VXXX19.454 12, VXXX19.670

Figs. 13~16 — M^2

13, VXXX19.65 14, VXXX19.356 15, VXXX19.488 16, VXXX19.673

1

2

3

4

5

6

7

8

9

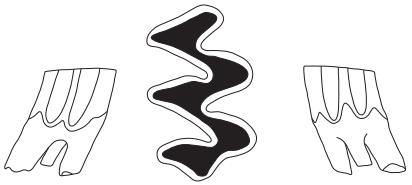

10

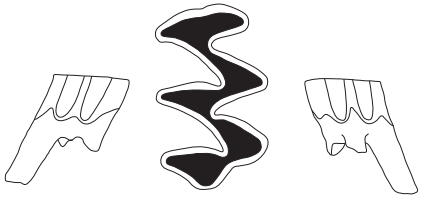

11

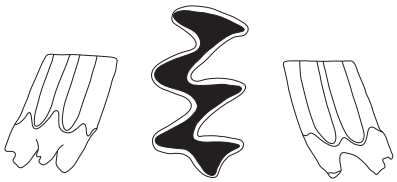

12

13

14

15

16

PLATE 5

PLATE 6

(Scale bar = 1 mm for occlusal view, and 2.5 mm for lateral view)

Mimomys teilhardi - *Villanyia* sp. nov. COMPLEX

Gaotege, Inner Mongolia

Figs. 1~16 — M^3

1, VXXX19.122	2, VXXX19.128	3, VXXX19.130	4, VXXX19.148
5, VXXX19.376	6, VXXX19.379	7, VXXX19.380	8, VXXX19.382
9, VXXX19.511	10, VXXX19.513	11, VXXX19.520	12, VXXX19.528
13, VXXX19.626	14, VXXX19.627	15, VXXX19.684	16, VXXX19.687

1

2

3

4

5

6

7

8

9

10

11

12

13

14

15

16

PLATE 6

PLATE 7

(Scale bar = 1 mm for occlusal view, and 2.5 mm for lateral view)

Mimomys cf. *M. orientalis* YOUNG, 1935

Gaotege, Inner Mongolia

Figs. 1~10 — M_1

1, DB03-2-019	2, DB03-2-023	3, Li200705-02	4, Li200705-03
5, Li200705-04	6, Li200705-05	7, Li200705-07	8, Li200705-08
9, Li200705-10	10, Li200705-12		

Fig. 11 — M_2

11, DB03-2-030

Fig. 12 — M^1

12, DB03-2-008

Fig. 13 — M^2

13, DB03-2-013

Figs. 14~16 — M^3

14, DB03-2-016	15, DB03-2-017	16, DB03-2-018

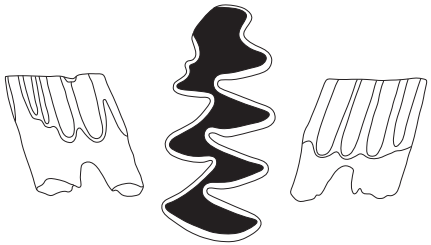

1

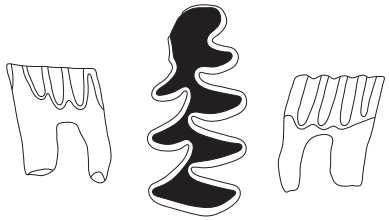

2

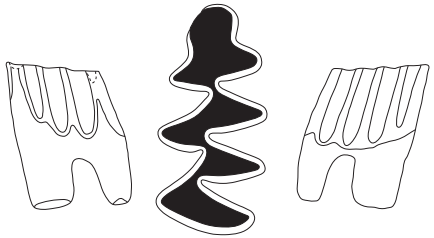

3

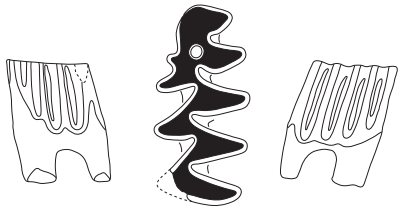

4

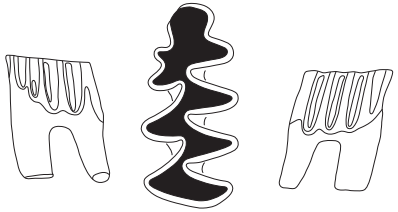

5

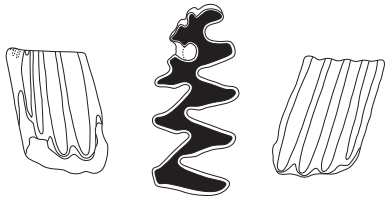

6

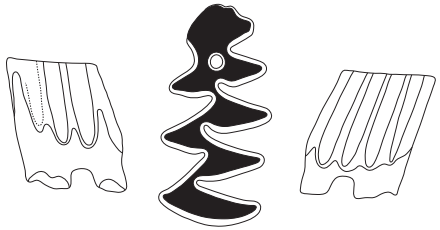

7

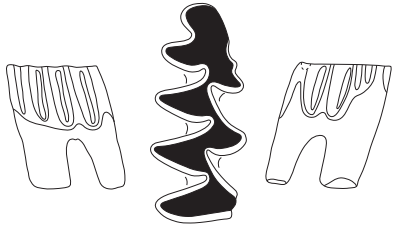

8

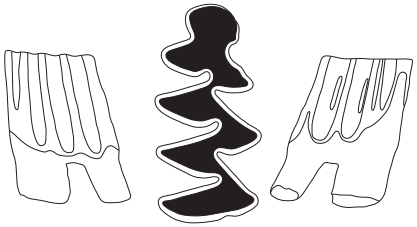

9

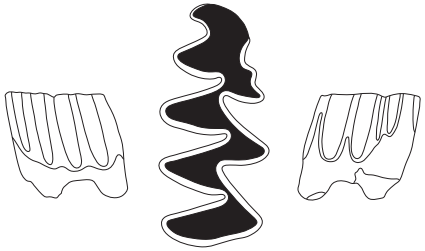

10

11

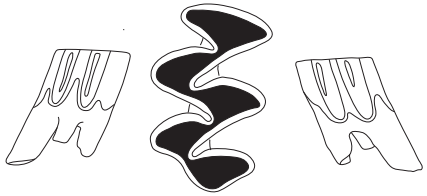

12

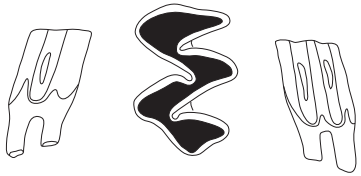

13

14

15

16

PLATE 7

PLATE 8

(Scale bar = 1 mm for occlusal view, and 2.5 mm for lateral view)

Mimomys gansunicus ZHENG, 1976

Renzidong, Fanchang, Anhui

Figs. 1~16—M_1

1, V13990.016	2, V13990.031	3, V13990.038	4, V13990.039
5, V13990.044	6, V13990.048	7, V13990.049	8, V13990.060
9, V13990.065	10, V13990.068	11, V13990.070	12, V13990.092
13, V13990.097	14, V13990.103	15, V13990.106	16, V13990.111

1

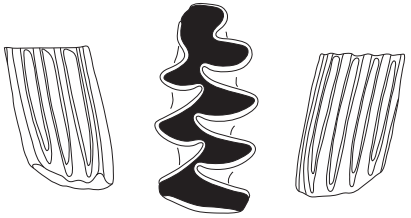

2

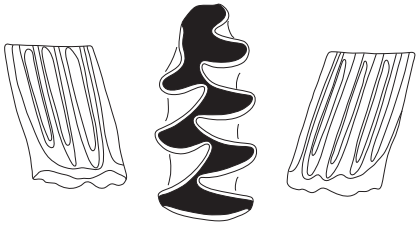

3

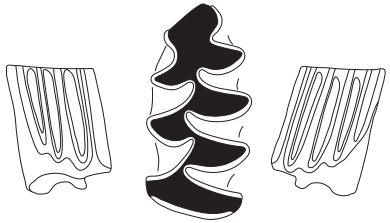

4

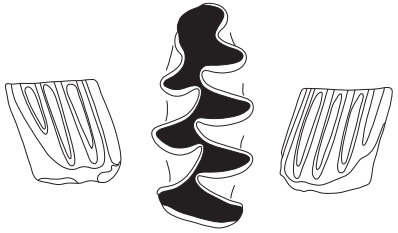

5

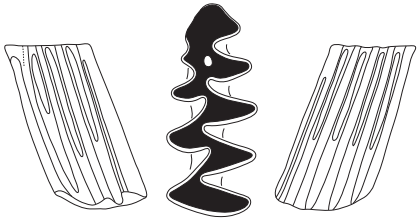

6

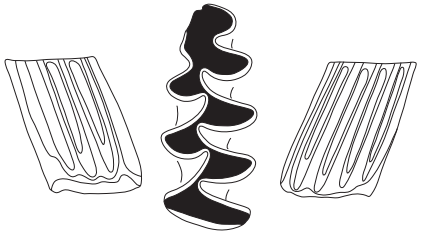

7

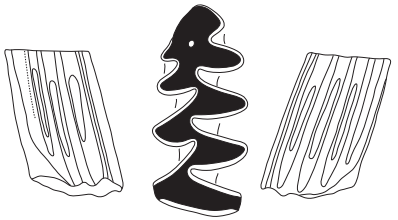

8

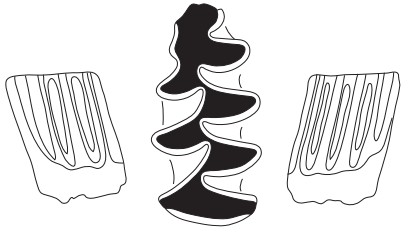

9

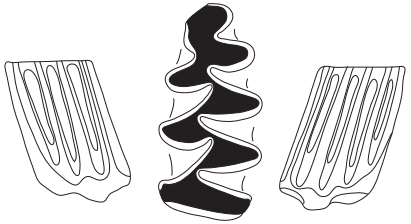

10

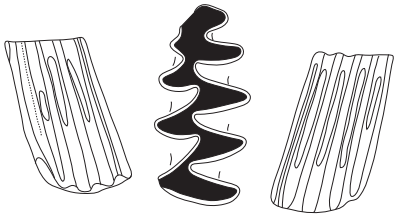

11

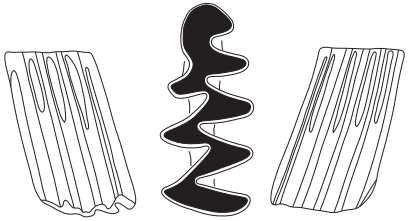

12

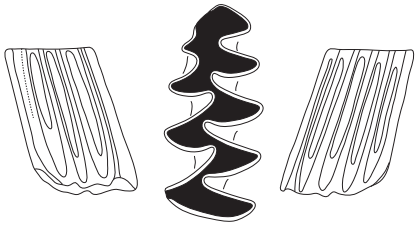

13

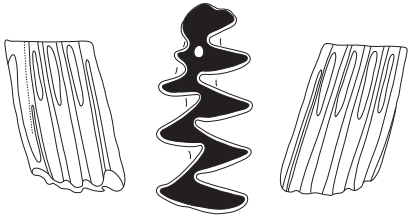

14

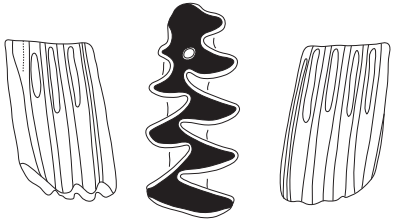

15

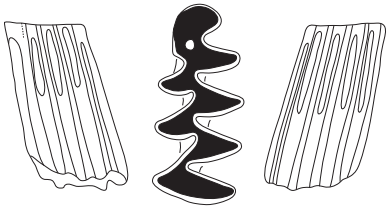

16

PLATE 8

PLATE 9

(Scale bar = 1 mm for occlusal view, and 2.5 mm for lateral view)

Mimomys gansunicus ZHENG, 1976

Renzidong, Fanchang, Anhui

Figs. 1~4 — M_2

1, V13990.211 2, V13990. 213 3, V13990. 218 4, V13990.220

Figs. 5~8 — M_3

5, V13990. 367 6, V13990. 368 7, V13990. 372 8, V13990. 373

Figs. 9~12 — M^1

9, V13990. 458 10, V13990. 454 11, V13990. 459 12, V13990. 463

Figs. 13~16 — M^2

13, V13990. 652 14, V13990. 655 15, V13990. 663 16, V13990. 664

1

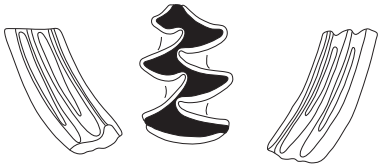

2

3

4

5

6

7

8

9

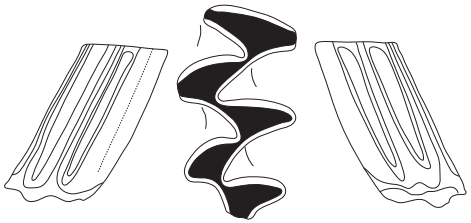

10

11

12

13

14

15

16

PLATE 9

PLATE 10

(Scale bar = 1 mm for occlusal view, and 2.5 mm for lateral view)

Mimomys gansunicus ZHENG, 1976

Renzidong, Fanchang, Anhui

Figs. 1~16 — M^3

1, V13990. 780	2, V13990. 781	3, V13990. 783	4, V13990. 787
5, V13990. 788	6, V13990. 791	7, V13990. 792	8, V13990. 800
9, V13990. 802	10, V13990. 803	11, V13990. 804	12, V13990. 805
13, V13990. 809	14, V13990. 810	15, V13990. 812	16, V13990. 814

1

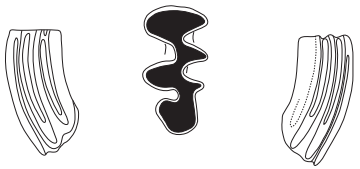

2

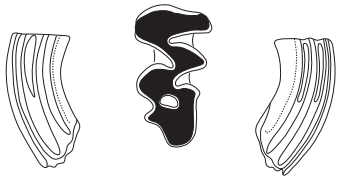

3

4

5

6

7

8

9

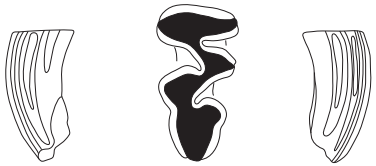

10

11

12

13

14

15

16

PLATE 10

PLATE 11

(Scale bar = 1 mm for occlusal view, and 2.5 mm for lateral view)

Mimomys gansunicus ZHENG, 1976

93001, Lingtai, Gansu

Figs. 1~15 — M_1

1, WL11-7-01	2, WL11-6-05	3, WL11-5-10	4, WL11-3-11
5, WL11-1-01	6, WL10-11-07	7, WL10-11-08	8, WL10-8-12
9, WL10-7-01	10, WL10-5-01	11, WL10-11	12, WL8-37;
13, WL8-38	14, WL8-39	15, WL8-34	

72074(4), Lingtai, Gansu

Fig. 16 — M_1

16, L1-1-01

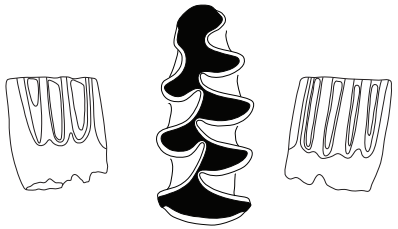

1

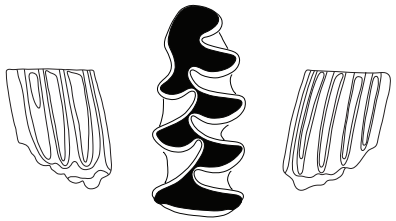

2

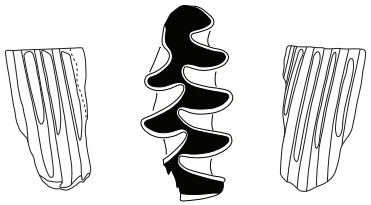

3

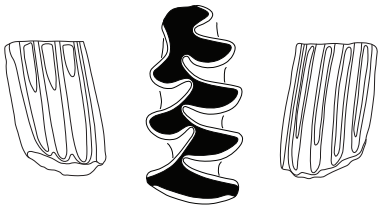

4

5

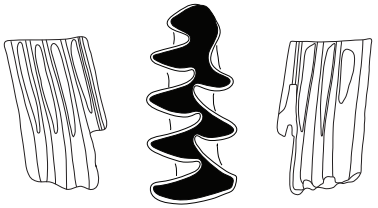

6

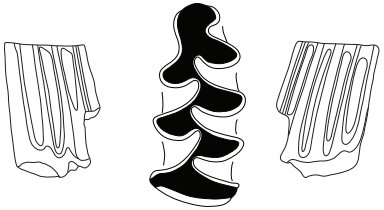

7

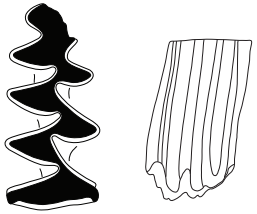

8

9

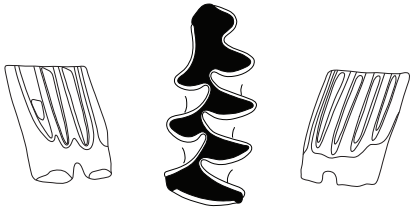

10

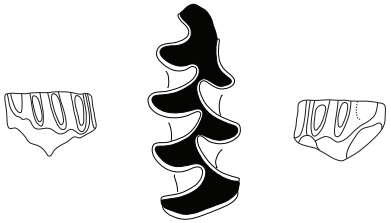

11

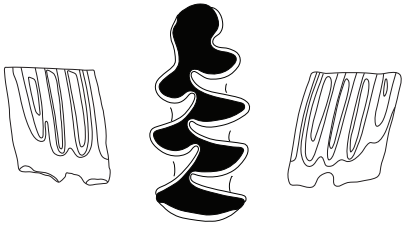

12

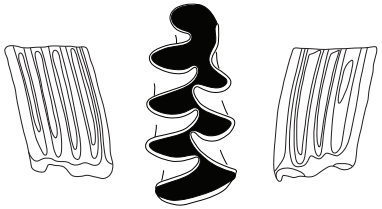

13

14

15

16

PLATE 11

PLATE 12

(Scale bar = 1 mm for occlusal view, and 2.5 mm for lateral view)

Mimomys gansunicus ZHENG, 1976

93001, Lingtai, Gansu

Figs. 1~4 — M_2

1, WL11-6-01 2, WL11-3-09 3, WL10-7-01-1 4, WL8_1-20

Figs. 5~8 — M_3

5, WL15-2-01 6, WL11-3-05 7, WL10-8-07 8, WL8_1-23

Figs. 9~12 — M^1

9, WL11-6-04 10, WL10-8-01 11, WL10-2-05 12, WL8_1-14

Figs. 13~16 — M^2

13, WL11-6-03 14, WL11-5-03 15, WL10-10-02 16, WL8_1-02

1

2

3

4

5

6

7

8

9

10

11

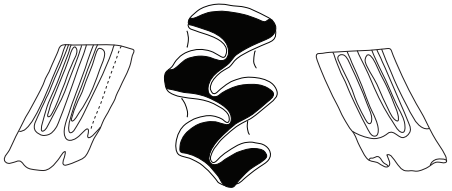

12

13

14

15

16

PLATE 12

PLATE 13

(Scale bar = 1 mm for occlusal view, and 2.5 mm for lateral view)

Mimomys gansunicus ZHENG, 1976

93001, Lingtai, Gansu

Figs. 1~16 — M^3

1, WL11-7-03	2, WL11-7-04	3, WL11-7- 05	4, WL11-5-06
5, WL11-4-01	6, WL11-3-04	7, WL10-10-03	8, WL10-10-04
9, WL10-10-05	10, WL10-8-09	11, WL10-7-03	12, WL10-2-02
13, WL8_1-31	14, WL8_1- 32	15, WL8_1-33	16, WL8-03

1

2

3

4

5

6

7

8

9

10

11

12

13

14

15

16

PLATE 13

PLATE 14

(Scale bar = 1 mm for occlusal view, and 2.5 mm for lateral view)

Omniprocessimys parallelus gen. et sp. nov.

Renzidong, Fanchang, Anhui

Figs. 1~16 — M_1

1, VXXXXX.005	2, VXXXXX.008	3, VXXXXX.009	4, VXXXXX.010
5, VXXXXX.011	6, VXXXXX.012	7, VXXXXX.013	8, VXXXXX.015
9, VXXXXX.023	10, VXXXXX.030	11, VXXXXX.055	12, VXXXXX.057
13, VXXXXX.061	14, VXXXXX.064	15, VXXXXX.066	16, VXXXXX.067

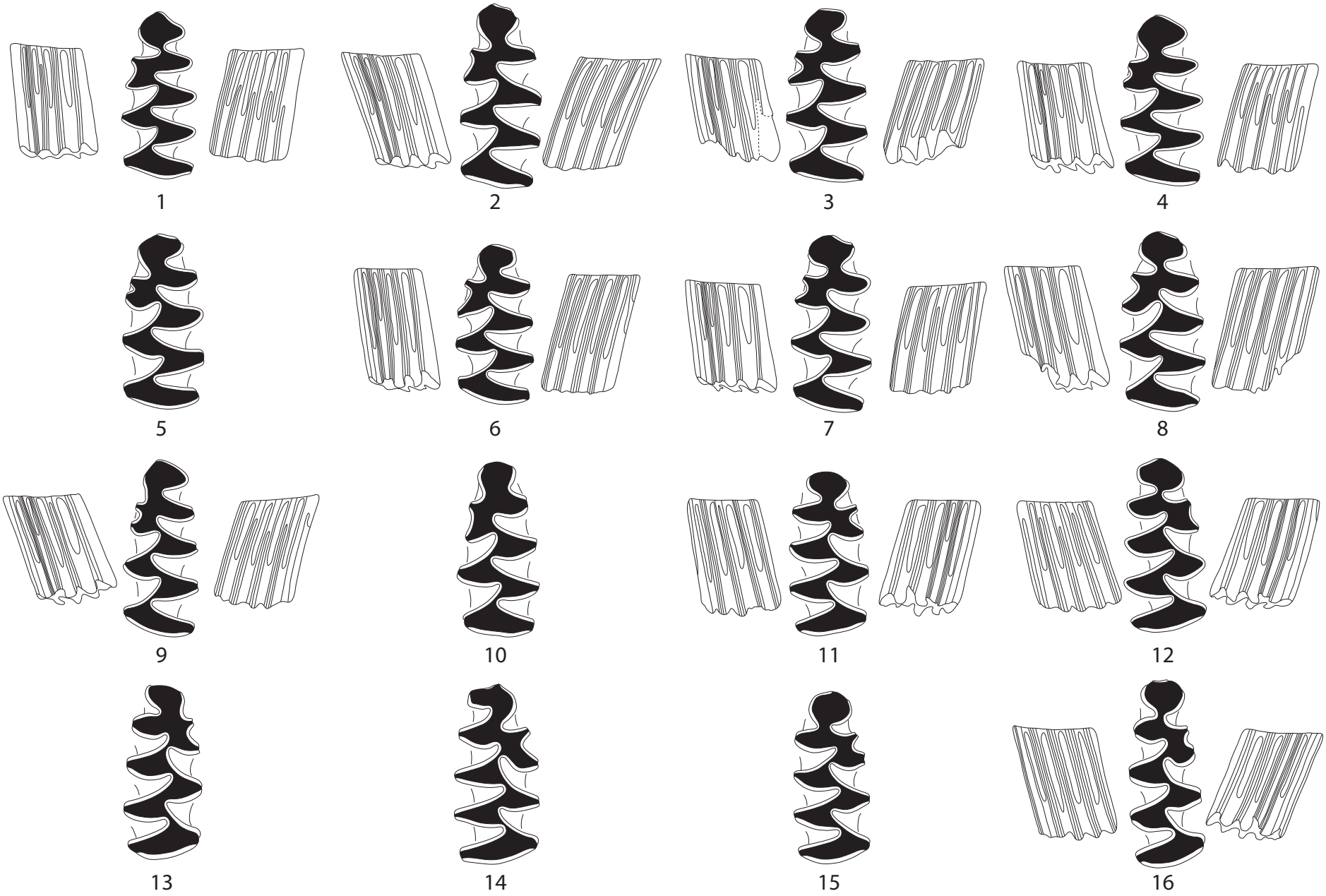

PLATE 14

PLATE 15

(Scale bar = 1 mm for occlusal view, and 2.5 mm for lateral view)

Omniprocessimys parallelus gen. et sp. nov.

Renzidong, Fanchang, Anhui

Figs. 1~4 — M_2

1, VXXXXX.080 2, VXXXXX.081 3, VXXXXX.084 4, VXXXXX.090

Figs. 5~8 — M_3

5, VXXXXX.123 6, VXXXXX.131 7, VXXXXX.139 8, VXXXXX.141

Figs. 9~12 — M^1

9, VXXXXX.166 10, VXXXXX.168 11, VXXXXX.169 12, VXXXXX.170

Figs. 13~16 — M^2

13, VXXXXX.228 14, VXXXXX.230 15, VXXXXX.231 16, VXXXXX.238

1

2

3

4

5

6

7

8

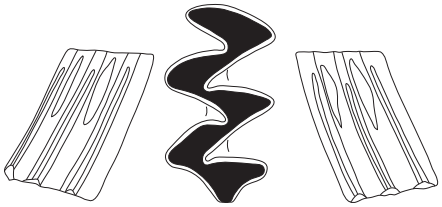

9

10

11

12

13

14

15

16

PLATE 15

PLATE 16

(Scale bar = 1 mm for occlusal view, and 2.5 mm for lateral view)

Omniprocessimys parallelus gen. et sp. nov.

Renzidong, Fanchang, Anhui

Figs. 1~16 — M^3

1, VXXXXX.289	2, VXXXXX.290	3, VXXXXX.291	4, VXXXXX.295
5, VXXXXX.296	6, VXXXXX.297	7, VXXXXX.299	8, VXXXXX.300
9, VXXXXX.303	10, VXXXXX.307	11, VXXXXX.308	12, VXXXXX.312
13, VXXXXX.313	14, VXXXXX.314	15, VXXXXX315	16, VXXXXX.316

1

2

3

4

5

6

7

8

9

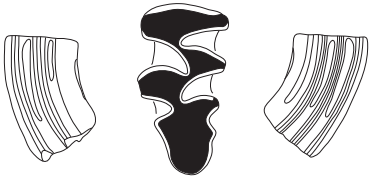

10

11

12

13

14

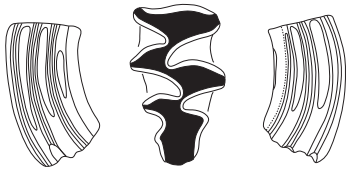

15

16

PLATE 16

PLATE 17

(Scale bar = 1 mm for occlusal view, and 2.5 mm for lateral view)

Villanyia sp. nov.

Gaotege, Inner Mongolia

Figs. 1~16 — M_1

1, VXXX19.163	2, VXXX19.168	3, VXXX19.170	4, VXXX19.175
5, VXXX19.185	6, VXXX19.186	7, VXXX19.198	8, VXXX19.202
9, VXXX19. 153	10, VXXX19.391	11, VXXX19.398	12, VXXX19.542
13, VXXX19.544	14, VXXX19.546	15, VXXX19.635	16, VXXX19.693

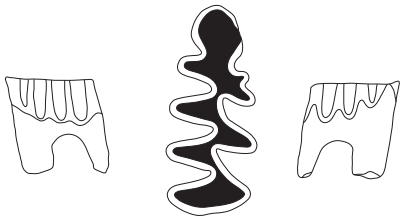

1

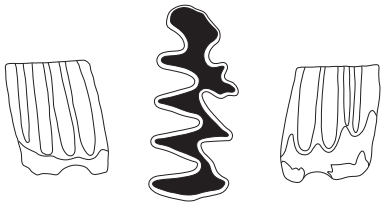

2

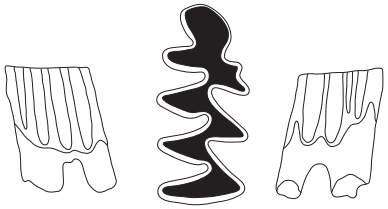

3

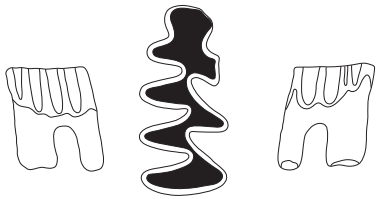

4

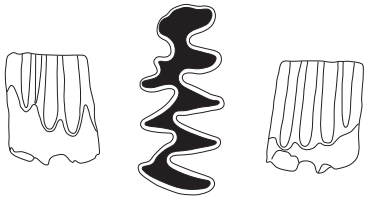

5

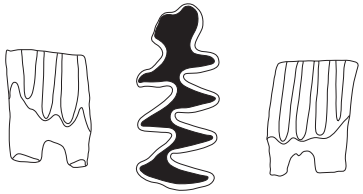

6

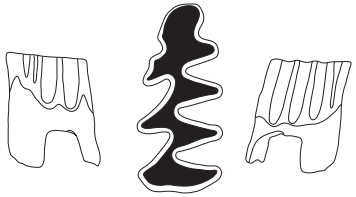

7

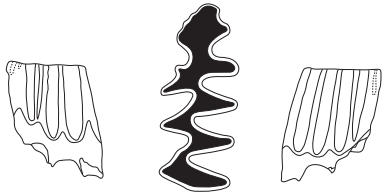

8

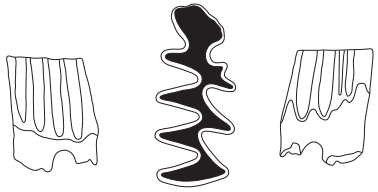

9

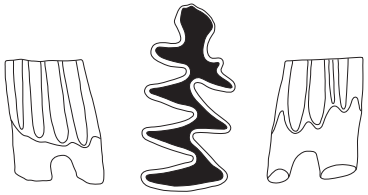

10

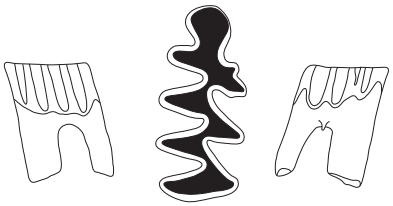

11

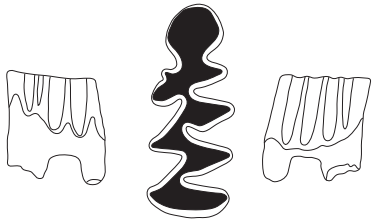

12

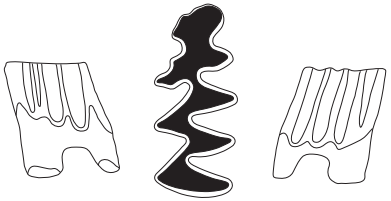

13

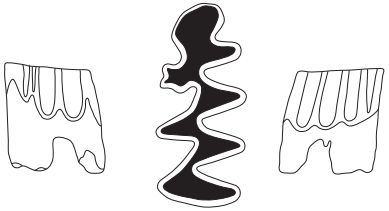

14

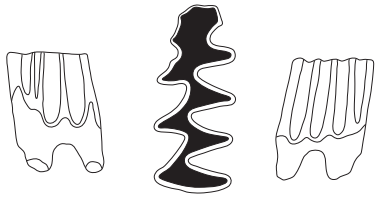

15

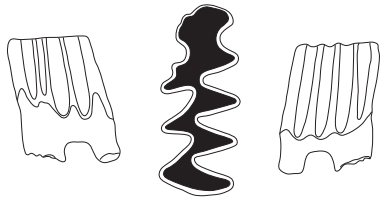

16

PLATE 17

PLATE 18

(Scale bar = 1 mm for occlusal view, and 2.5 mm for lateral view)

Villanyia fanchangensis ZHANG ET AL., in press

Renzidong, Fanchang, Anhui

Figs. 1~16 — M_1

1, V13991.9	2, V13991.17	3, V13991.28	4, V13991.50
5, V13991.52	6, V13991.56	7, V13991.131	8, V13991.196
9, V13991.199	10, V13991.200	11, V13991.249	12, V13991.287
13, V13991.289	14, V13991.291	15, V13991.297	16, V13991.458

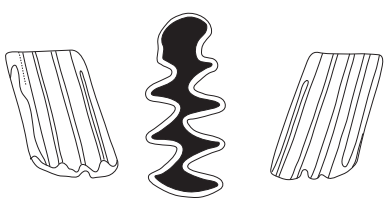

1

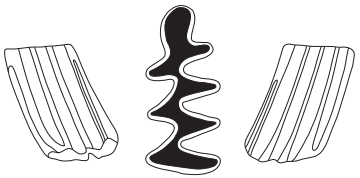

2

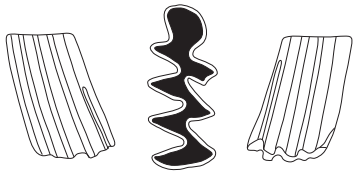

3

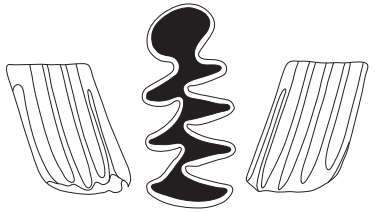

4

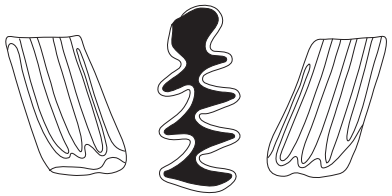

5

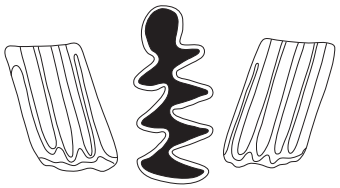

6

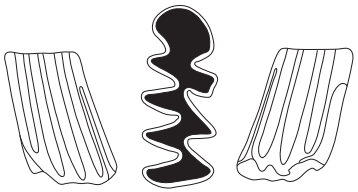

7

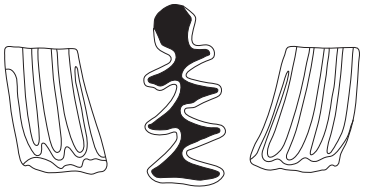

8

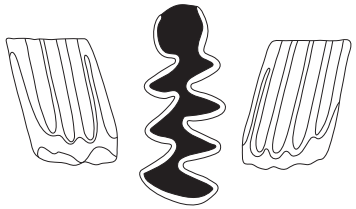

9

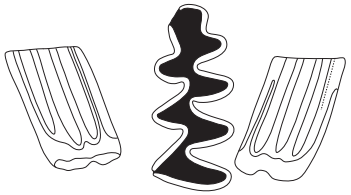

10

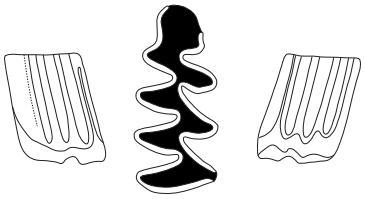

11

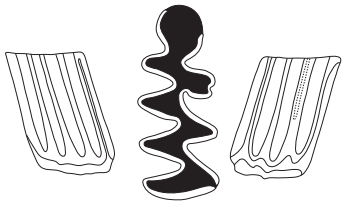

12

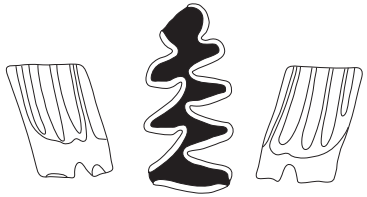

13

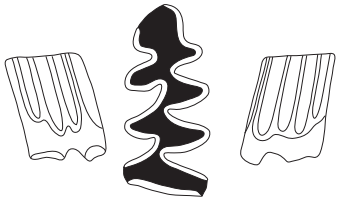

14

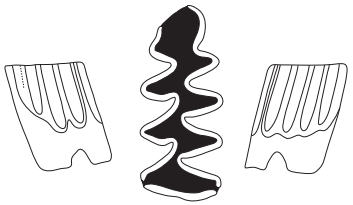

15

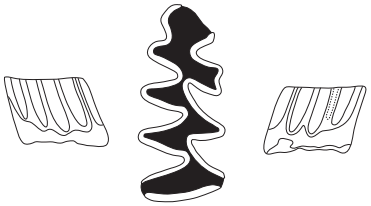

16

PLATE 18

PLATE 19

(Scale bar = 1 mm for occlusal view, and 2.5 mm for lateral view)

Villanyia fanchangensis ZHANG ET AL., in press

Renzidong, Fanchang, Anhui

Figs. 1~4 — M_2

1, V13991.479 2, V13991.520 3, V13991.589 4, V13991.632

Figs. 5~7 — M_3

5, V13991.744 6, V13991.754 7, V13991.824

Figs. 8~12 — M^1

8, V13991.861 9, V13991.876 10, V13991.903 11, V13991.971

12, V13991.1036

Figs. 13~16 — M^2

13, V13991.1039 14, V13991.1086 15, V13991.1122 16, V13991.1158

1

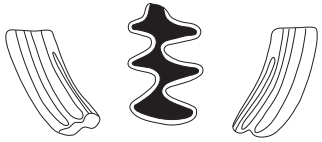

2

3

4

5

6

7

8

9

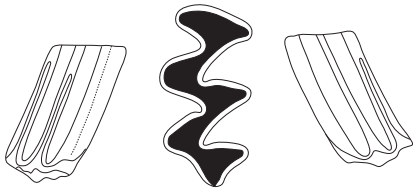

10

11

12

13

14

15

16

PLATE 19

PLATE 20

(Scale bar = 1 mm for occlusal view, and 2.5 mm for lateral view)

Villanyia fanchangensis ZHANG ET AL., in press

Renzidong, Fanchang, Anhui

Figs. 1~16 — M^3

1, V13991.1234	2, V13991.1245	3, V13991.1264	4, V13991.1274
5, V13991.1284	6, V13991.1285	7, V13991.1299	8, V13991.1302
9, V13991.1304	10, V13991.1321	11, V13991.1330	12, V13991.1332
13, V13991.1336	14, V13991.1337	15, V13991.1342	16, V13991.1351

1

2

3

4

5

6

7

8

9

10

11

12

13

14

15

16

PLATE 20

PLATE 21

(Scale bar = 1 mm for occlusal view, and 2.5 mm for lateral view)

Villanyia cf. *V. fanchangensis* ZHANG ET AL., in press

93001, Lingtai, Gansu

Figs. 1~8 — M_1

1, WL11-7-05	2, WL11-3-07	3, WL10-8-10	4, WL10-7-01
5, WL10-4-01	6, WL10-2-03	7, WL10-2-04	8, WL8-08

Figs. 9~16 — M^3

9, WL11-5-04	10, WL10-11-04	11, WL10-10-02	12, WL10-8-03
13, WL10-02	14, WL8-01	15, WL8-02	16, WL8-04

1

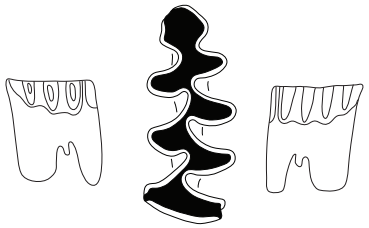

2

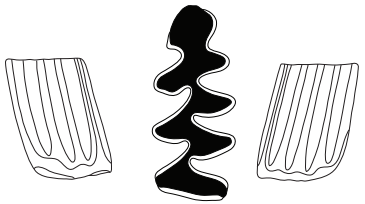

3

4

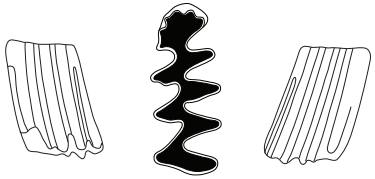

5

6

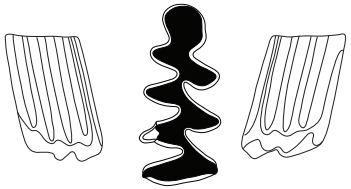

7

8

9

10

11

12

13

14

15

16

PLATE 21

PLATE 22

(Scale bar = 1 mm for occlusal view, and 2.5 mm for lateral view)

Villanyia cf. *V. fanchangensis* ZHANG ET AL., (in press)

93001, Lingtai, Gansu

Figs. 1~4 — M_2

1, WL11-7-09 2, WL11-5-07 3, WL10-2-01 4, WL8-12

Figs. 5~8 — M_3

5, WL11-7-06 6, WL11-3-11 7, WL10-8-06 8, WL10-2-02

Figs. 9~12 — M^1

9, WL11-6-01 10, WL11-5-02 11, WL10-03 12, WL8-07

Figs. 13~16 — M^2

13, WL11-7-10 14, WL11-3-03 15, WL10-06 16, WL8-06

1

2

3

4

5

6

7

8

9

10

11

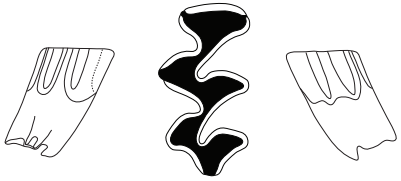

12

13

14

15

16

PLATE 22

PLATE 23

(Scale bar = 1 mm for occlusal view, and 2.5 mm for lateral view)

Villanyia sp. 1

Gaotege, Inner Mongolia

Figs. 1~2 — M_1

1, Li200705-01 2, Li200705-13

Figs. 3~5 — M^2

3, DB03-2-14 4, DB03-2-15 5, DB03-2-43

Figs. 6~7 — M^3

6, DB03-2-44 7, DB03-2-47

Mimomys cf. *M. orientalis* - *Villanyia* sp. 1 COMPLEX

Gaotege, Inner Mongolia

Figs. 8~10 — M_2

8, DB03-2-32 9, DB03-2-34 10, DB03-2-36

Figs. 11~12 — M_3

11, DB03-2-41 12, DB03-2-42

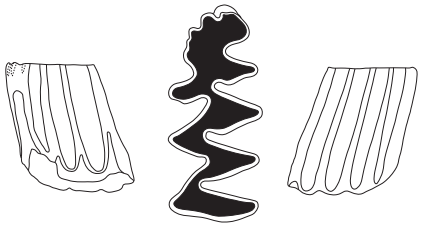

1

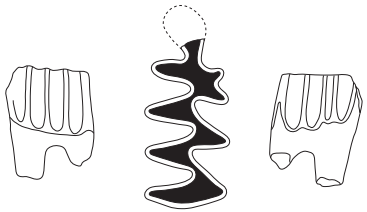

2

3

4

5

6

7

8

9

10

11

12

PLATE 23

PLATE 24

(Scale bar = 1 mm for occlusal view, and 2.5 mm for lateral view)

Villanyia sp. 2

Gaotege, Inner Mongolia

Figs. 1~3 — M_1

1, DB03-2-21 2, DB03-2-25 3, Li200705-11

Figs. 4~5 — M^1

4, DB03-2-45 5, DB03-2-48

Figs. 6~7 — M^2

6, DB03-2-46 7, DB03-2-49

Fig. 8 — M^3

8, DB03-2-50

Mimomys cf. *M. bilikeensis* (QIU AND STORCH, 2000)

72074(4), Lingtai, Gansu

Fig. 9 — M_1

9, L5-3-03

Figs. 10~11 — M_2

10, L5-3-02 11, L5-2-04

Figs. 12~13 — M_3

12, L5-3-01 13, L5-2-01

Figs. 14~15 — M^2

14, L5-2-03 15, L5-2-02

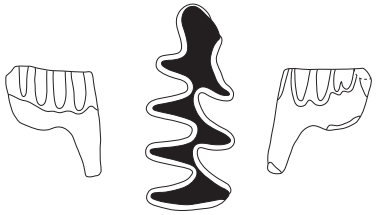

1

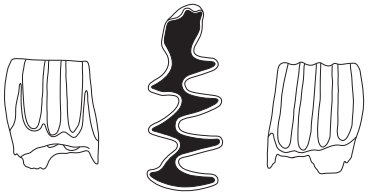

2

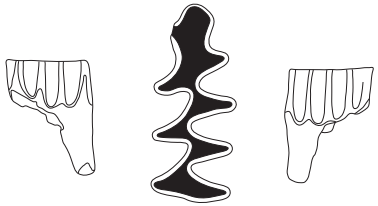

3

4

5

6

7

8

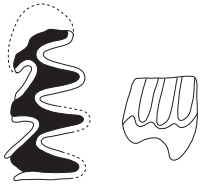

9

10

11

12

13

14

15

PLATE 24

PLATE 25

(Scale bar = 1 mm for occlusal view, and 2.5 mm for lateral view)

Allophaiomys deucalion KRETZOI, 1969

Xiaochangliang, Nihewan

Figs. 1~9 — M_1

1, V15325.28 2, V15325.37 3, V15325.36 4, V15325.30
5, V15325.29 6, V15325.33 7, V15325.34 8, V15325.35
9, V15325.31

Fig. 10 — M_2

10, V15325.52

Fig. 11 — M_3

11, V15325.58

Fig. 12 — M^1

12, V15325.4

Fig. 13 — M^2

13, V15325.9

Figs. 14~16 — M^3

14, V15325.23 15, V15325.21 16, V15325.22

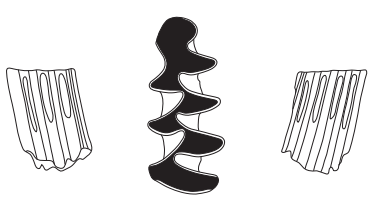

1

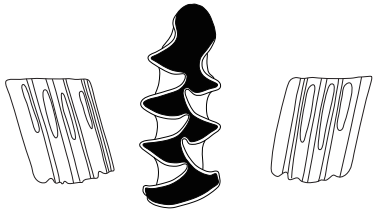

2

3

4

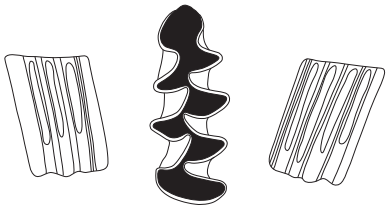

5

6

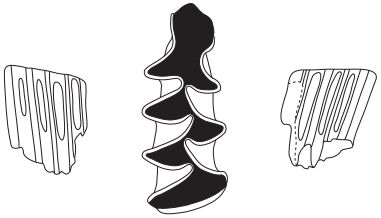

7

8

9

10

11

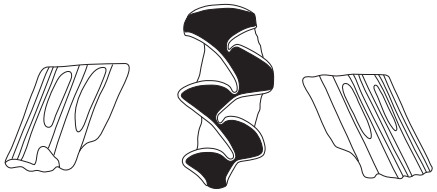

12

13

14

15

16

PLATE 25

PLATE 26

(Scale bar = 1 mm for occlusal view, and 2.5 mm for lateral view)

Allophaiomys deucalion KRETZOI, 1969

93001, Lingtai, Gansu

Figs. 1~9 — M_1

1, WL6-03 2, WL5-08 3, WL4-05 4, WL4-06
5, WL3-08 6, WL5+-14 7, WL5+-15 8, WL5+-16
9, WL2+-03

Fig. 10 — M_2

10, WL5-08

Fig. 11 — M_3

11, WL6-01

Fig. 12 — M^1

12, WL5-05

Figs. 13~15 — M^3

13, WL5-03 14, WL5+-13 15, WL2+-02

1

2

3

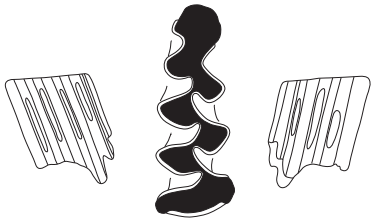

4

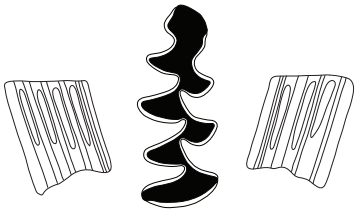

5

6

7

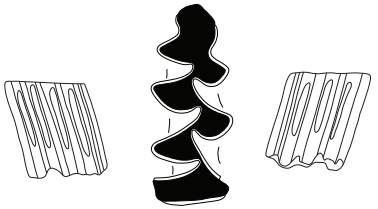

8

9

10

11

12

13

14

15

PLATE 26

PLATE 27

(Scale bar = 1 mm for occlusal view, and 2.5 mm for lateral view)

Borsodia chinensis (KORMOS, 1934)

Xiaochangliang, Nihewan

Figs. 1~2 — M_1

1, V15323.36 2, V15323.41

Fig. 3 — M_2

3, V15323.45

Fig. 4 — M_3

4, V15323.68

Fig. 5 — M^1

5, V15323.6

Fig. 6 — M^2

6, V15323.17

Figs. 7~13 — M^3

7, V15323.26 8, V15323.25 9, V15323.24 10, V15323.27

11, V15323.28 12, V15323.31 13, V15323.32

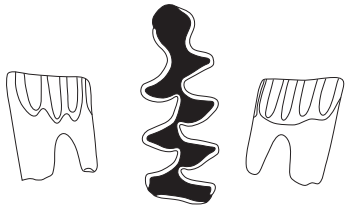

1

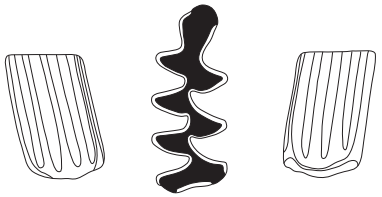

2

3

4

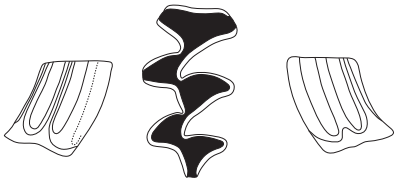

5

6

7

8

9

10

11

12

13

PLATE 27

PLATE 28

(Scale bar = 1 mm for occlusal view, and 2.5 mm for lateral view)

Borsodia sp.

93001, Lingtai, Gansu

Figs. 1~2 — M_1

1, WL11-5-01 2, WL8-10

Figs. 3~5 — M_2

3, WL10-10 4, WL10-11 5, WL3-01

Figs. 6~8 — M_3

6, WL11-1-01 7, WL10-12 8, WL8-13

Figs. 1~16 — M^3

9, WL11-7-11 10, WL11-3-01 11, WL10-11-03 12, WL10-10-03

13, WL10-8-04 14, WL10-07 15, WL10-09 16, WL8-03

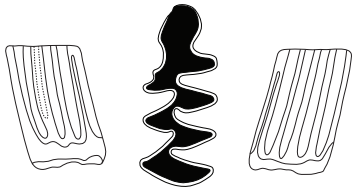

1

2

3

4

5

6

7

8

9

10

11

12

13

14

15

16

PLATE 28

PLATE 29

(Scale bar = 1 mm for occlusal view, and 2.5 mm for lateral view)

Proedromys bedfordi Thomas, 1911

93001, Lingtai, Gansu

Figs. 1~3 — M_1

1, WL2-04 2, WL7+-04 3, WL5+-19

Figs. 4 — M_3

4, WL5+-04

Figs. 5~6 — M^3

5, WL1-01 6, WL4+-02

Proedromys bedfordi and *Allophaiomys deucalion* COMPLEX

93001, Lingtai, Gansu

Figs. 7~9 — M_2

7, WL1-03 8, WL1-04 9, WL5+-07

Figs. 10 — M^1

10, WL2-01

Figs. 11~13 — M^2

11, WL1-02 12, WL5+-17 13, WL4+-01

Arvicolinae gen. et sp. indet.

93001, Lingtai, Gansu

Figs. 14 — M_1

14, WL8-14

1

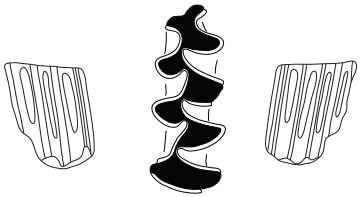

2

3

4

5

6

7

8

9

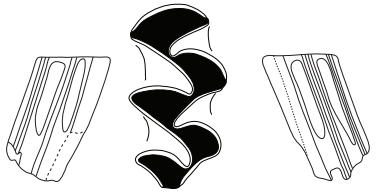

10

11

12

13

14

PLATE 29

PLATE 30

(Scale bar = 1 mm for occlusal view, and 2.5 mm for lateral view)

ZHENG AND LI, 1986

Mimomys orientalis YOUNG, 1935

Figs. 1~2 — M_1

1, 75渭①_1.2　　2, V8110

Mimomys youhenicus XUE, 1981

Figs. 3~4 — M_1

1, 75渭①_1.3　　2, 75渭①_1.4;

Borsodia chinensis (KORMOS, 1934)

Figs. 5~11

5~6, RV30011 (TYPE, $M_{1\sim2}$ on mandible)　　7~9, V8109 ($M_{1\sim3}$ on mandible)
10~11, V4766 ($M_{1\sim2}$ on mandible)

Mimomys gansunicus ZHENG, 1976

Figs. 12 — M_1

12, V4765 (TYPE)　　14, V XXX19.689　　15, V XXX19.690　　16, V XXX19.694

Mimomys cf. *M. intermedius* NEWTON, 1881

Figs. 13~14

13~14, V8111 ($M_{1\sim2}$ on mandible)

Omniprocessimys banchiaonicus (ZHENG ET AL., 1975)

Figs. 15 — M_1

15, V4755 (TYPE)

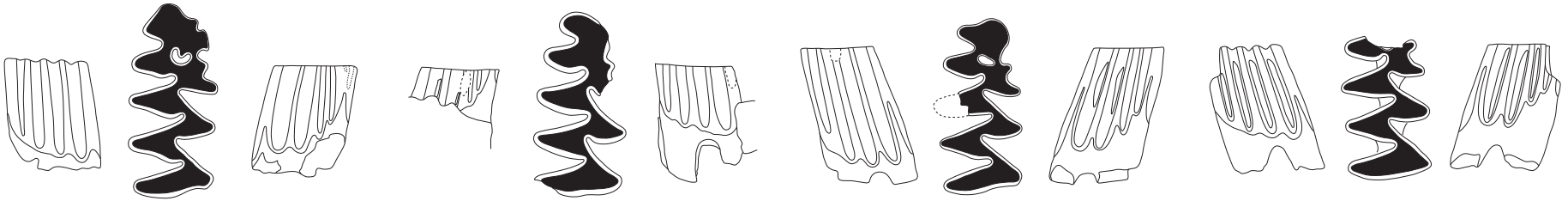

1 2 3 4

5 6 7 8

9 10 11 12

13 14 15

PLATE 30

PLATE 31

(Scale bar = 1 mm for occlusal view, and 2.5 mm for lateral view)

ZHENG AND LI, 1986

Omniprocessimys peii (ZHENG AND LI, 1986)

Figs. 1~6 — M_1

1, V8112 2, V8114.1 3, V8114.2 4, V8114.3
5, V8114.6 6, V8114.8

Figs. 7~8 — M_2

7, V8114.13 8, V8114.16

Figs. 9~10 — M_3

9, V8114.19 10, V8114.20

Figs. 11~12 — M^1

11, V8114.22 12, V8114.30

Figs. 13~14 — M^2

13, V8114.42 14, V8114.47

Figs. 15~16 — M^3

15, V8114.52 16, V8114.54

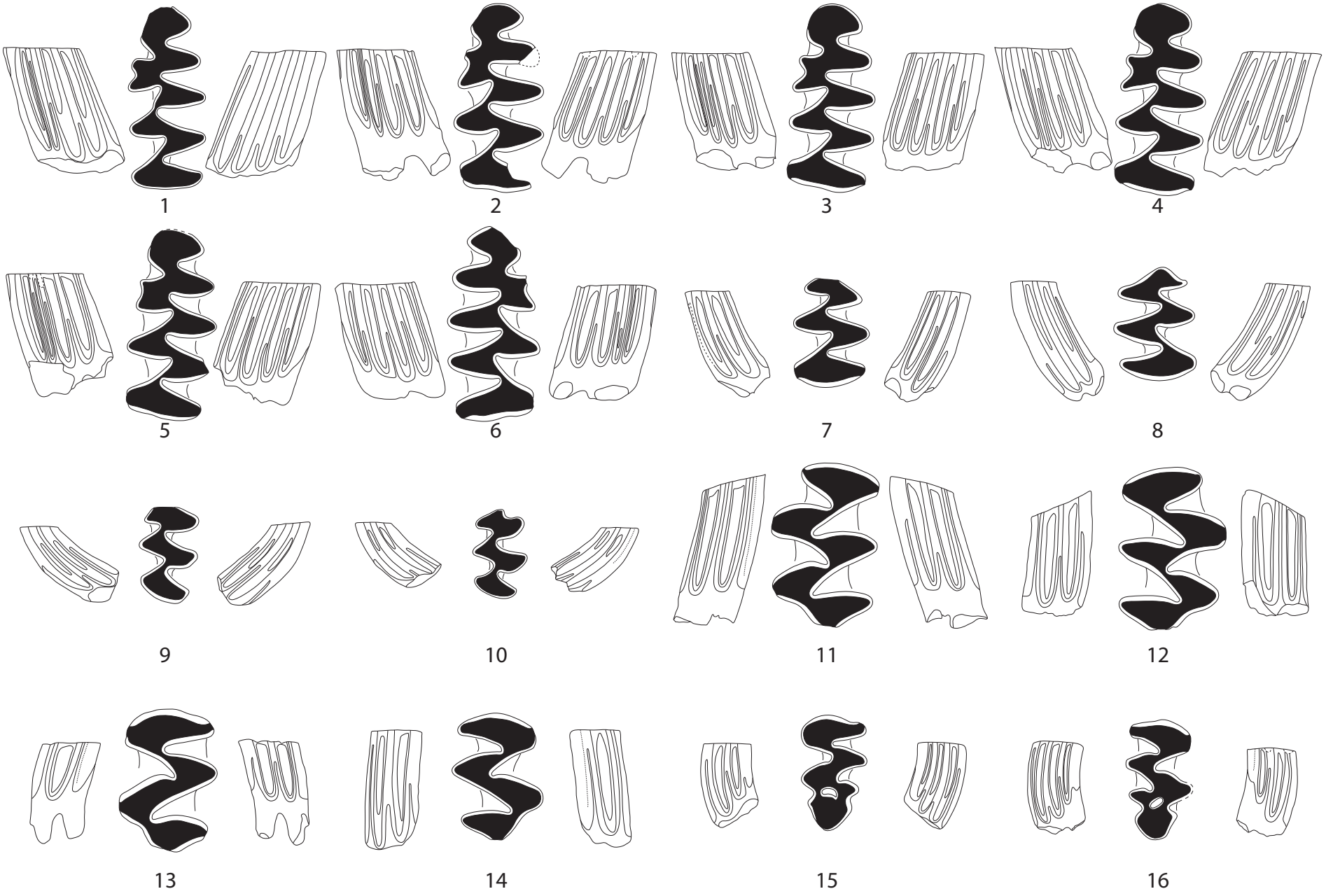

PLATE 31